"CUBOSOME BASED NANOFORMULATION OF RESVERATROL AND PIPERINE FOR TARGETING MELANOMA"

Thesis submitted to

KLE ACADEMY OF HIGHER EDUCATION AND RESEARCH (BELAGAVI)

(Deemed-to-be-University)

[Declared as Deemed-to-be-University u/s3 of the UGC Act, 1956 vide Govt. of India Notification No. F.9-19/2000-U.3(A)]

Accredited 'A' Grade by NAAC (2nd Cycle)

Placed in Category 'A' by MHRD (GoI)

For the award of the degree of

Doctor of Philosophy
In the Faculty of Pharmacy

By

Bhaskar Kallappa Kurangi M.Pharm.

(Registration No: KLEU/Ph.D./17-18/DO1217009)

Under the Guidance of

Prof. (Dr.) Sunil Satyappa Jalalpure Ph.D

Principal, KLE College of Pharmacy, Belagavi,
KLE Academy of Higher Education and Research, Belagavi - 590010, Karnataka, India

January - 2021

UNDERTAKING

I, Mr. **Bhaskar Kallappa Kurangi** hereby declare that the information and the data mentioned in my thesis entitled **"Cubosome based nanoformulation of resveratrol and piperine for targeting melanoma"** belongs to me and is original.

I am aware of definition of plagiarism as detailed below:

- An act or instance of using or closely imitating the language and thoughts of another author without authorization and the representation of that author's work as one's own, as by not crediting the original author.
- A piece of writing or other work reflecting such unauthorized use or imitation.
- The deliberate or reckless representation of another's words, thoughts or ideas as one's own without attribution in connection with submission of academic work, whether graded or otherwise.

I hereby declare that the thesis prepared by me is original-one and does not involve plagiarism anywhere. In case at a later stage it is found that I have indulged in plagiarism, then I am solely responsible for the same and the Institution is at liberty to take any disciplinary action against me including cancellation of dissertation or any other penalties imposed by the University.

Date:

Place: Belagavi

Mr. Bhaskar Kallappa Kurangi
Full time Ph. D Research Scholar
Reg.No:DO1217009
KAHER, Belagavi-590010.

PLAGIARISM REPORT

KLE ACADEMY OF HIGHER EDUCATION AND RESEARCH

(Formerly known as KLE University)

(Deemed-to-be-University established u/s 3 of the UGC Act, 1956)

Accredited 'A' Grade by NAAC (2nd Cycle) Placed in Category 'A' by MHRD (GoI)

JNMC Campus, Nehru Nagar, Belagavi-590 010, Karnataka State, India

☎: 0831-2444444 FAX: 0831-2493777 Web: http://www.kledeemeduniversity.edu.in E-mail: info@kledeemeduniversity.edu.in

Ref. No. KAHER/AA/20-21/D-05012100l

5th January 2020

Sir,

The soft copy of Ph.D. research thesis of **Mr. Bhaskar K. Kurangi, Faculty of Pharmacy** of KAHER, Belagavi has submitted thesis CD for anti-plagiarism check at the office of the undersigned through "Turn-it-in" package. The scan has been carried out and the scanned output reveals a match percentage of **5%** which is within the acceptable limit of 10%.

To obtain the comprehensive report of the plagiarism test, research scholar can send a mail to **diracademic@kledeemeduniversity.edu.in** along with the Registration Number, Name of the Scholar, Name of Guide/Co-guide and title of the thesis.

DIRECTOR Deemed-to-be University ACADEMIC AFFAIRS

Dr. (Mrs. Roopa M. Bellad
Director, Academic Affairs

To,

Mr. Bhaskar K. Kurangi
Full -Time Ph.D. Scholar,
2017-18 Batch, Faculty of Pharmacy,
College of Pharmacy, KAHER
Belagavi.

Cc to :

1. The Principal, College of Pharmacy, Belagavi.
2. Dr. Sunil Jalalpure, Prof.of Pharmacognosy & Phytochemistry, College of Pharmacy Belagavi – **Guide**

KLE ACADEMY OF HIGHER EDUCATION AND RESEARCH

(Deemed-to-be-University)

[Declared as Deemed-to-be-University u/s3 of the UGC Act, 1956 vide Govt. of India Notification No.F.9-19/2000-U.3 (A)]

Accredited 'A' Grade by NAAC (2nd Cycle)

Placed in Category 'A' by MHRD (GoI)

CopyrightDeclaration

We hereby declare that **KLE ACADEMY OF HIGHER EDUCATION AND RESEARCH, BELAGAVI, KARNATAKA,** *shall have the rights to preserve, use and disseminate this thesis in print or electronic format for academic/research purpose.*

Signature

Mr. Bhaskar Kurangi
Full time Ph.D Research Scholar
Reg.No:DO1217009
KAHER, Belagavi-590010.

Place: Belagavi

Date:

Signature Guide

Prof. (Dr.) Sunil Jalalpure
Principal, KLE College of Pharmacy, KAHER,
Belagavi-590010.

Place: Belagavi

Date:

KLE ACADEMY OF HIGHER EDUCATION AND RESEARCH

(Deemed-to-be-University)

[Declared as Deemed-to-be-University u/s3 of the UGC Act, 1956 vide Govt. of India Notification No.F.9-19/2000-U.3 (A)]

Accredited 'A' Grade by NAAC (2nd Cycle)

Placed in Category 'A' by MHRD (GoI)

Declaration

I hereby declare that the thesis entitled **"CUBOSOME BASED NANOFORMULATION OF RESVERATROL AND PIPERINE FOR TARGETING MELANOMA"** *is a bonafide and original research carried out by me under the guidance of* **Prof. (Dr.) Sunil Satyappa Jalalpure,** *Deputy Director, Dr. Prabhakar Kore Basic Science Research Center, Principal, KLE College of Pharmacy, Belagavi- 590010. The thesis or any part thereof has not formed the basis for the award of any degree/fellowship or similar title to any candidate of any University.*

Place: Belagavi

Date:

Signature

Mr. Bhaskar Kallappa Kurangi

Full time Ph.D. ResearchScholar

RegistrationNo:DO1217009

KLE ACADEMY OF HIGHER EDUCATION AND RESEARCH

(Deemed-to-be-University)

[Declared as Deemed-to-be-University u/s3 of the UGC Act, 1956 vide Govt. of India Notification No.F.9-19/2000-U.3 (A)]

Accredited 'A' Grade by NAAC (2nd Cycle)

Placed in Category 'A' by MHRD (GoI)

Certificate

This is to certify that the thesis entitled **"CUBOSOME BASED NANOFORMULATION OF RESVERATROL AND PIPERINE FOR TARGETING MELANOMA"** *is a bonafide record of original research carried out by* **Mr. Bhaskar Kallappa Kurangi** *under the guidance of* **Prof. (Dr.) Sunil Satyappa Jalalpure,** *Deputy Director, Dr. Prabhakar Kore Basic Science Research Center, Principal, KLE College of Pharmacy, Belagavi-590010.*

Place: Belagavi

Date:

Signature

Prof. (Dr.) M. S. Ganachari

Dean, Faculty of Pharmacy

KAHER, Belagavi– 590010.

KLE ACADEMY OF HIGHER EDUCATION AND RESEARCH

(Deemed-to-be-University)

[Declared as Deemed-to-be-University u/s3 of the UGC Act, 1956 vide Govt. of India Notification No.F.9-19/2000-U.3 (A)]

Accredited 'A' Grade by NAAC (2nd Cycle)

Placed in Category 'A' by MHRD (GoI)

Certificate

This is to certify that the thesis entitled **"CUBOSOME BASED NANOFORMULATION OF RESVERATROL AND PIPERINE FOR TARGETING MELANOMA"** *is a bonafide record of original research carried out by* **Mr. Bhaskar Kallappa Kurangi** *under the guidance of* **Prof. (Dr.) Sunil Satyappa Jalalpure,** *Deputy Director, Dr. Prabhakar Kore Basic Science Research Center, Principal, KLE College of Pharmacy, Belagavi-590010.*

Place: Belagavi

Date:

Signature

Prof. (Dr.) Sunil S. Jalalpure

Principal,

KLE College of Pharmacy

KAHER,Belagavi - 590010

KLE ACADEMY OF HIGHER EDUCATION AND RESEARCH

(Deemed-to-be-University)

[Declared as Deemed-to-be-University u/s3 of the UGC Act, 1956 vide Govt. of India Notification No.F.9-19/2000-U.3 (A)]

Accredited 'A' Grade by NAAC (2nd Cycle)

Placed in Category 'A' by MHRD (GoI)

KLE
EMPOWERING PROFESSIONALS

Certificate

This is to certify that the thesis entitled **"CUBOSOME BASED NANOFORMULATION OF RESVERATROL AND PIPERINE FOR TARGETING MELANOMA"** *is a bonafide record of original research carried out by* **Mr. Bhaskar Kallappa Kurangi** *for the award of degree of DOCTOR OF PHILOSOPHY IN FACULTY OF* ***Pharmacy*** *under my supervision and guidance.*

Place: Belagavi
Date:

Signature Guide
Prof. (Dr.) Sunil S. Jalalpure
Principal,
KLE College of Pharmacy, Belagavi,
KAHER, Belagavi-590010.

ACKNOWLEDGEMENT

I would like to thank great almighty and all those numerous individuals whose blessing, continuous support and enthusiasm kept my vision alive during this amazing journey of Ph.D.

Firstly, I would like to express my sincere gratitude and heartfelt thanks to my research guide, Respected Dr. Sunil S. Jalalpure, for his constant guidance and co-operation throughout my dissertation work.He gave constant encouragement and support in various ways. I shall forever remain indebted to him for having inculcated me in a zeal for research and a quest for knowledge. I could not have imagined having a better advisor and mentor for my Ph. D study.I am indebted to him, for his faith in me and providing the right direction whenever I needed it the most.

I am deeply indebted to our Honorable former Vice-Chancellor, Prof. (Dr.) C. K. Kokate and respected Vice-Chancellor Prof. (Dr.) Vivek A. Saoji for giving me an opportunity and providing state of art facilities to join and complete Ph. D. course as Full Time research scholar at Dr. Prabhakar Kore Basic Science Research Centre, Belagavi.

I appreciate the generous support from the KLE Academy of Higher Education and Research, Belagavi for funding my research and my deep sense of gratitude to entire staffs at KLE College of Pharmacy, Belagavi and Dr. Prabhakar Kore Basic Science Research Center for providing all necessary support required during the course of study.

I express my deep gratitude to former Director of Academic Affairs Dr. Daksha Dixit, respected Director of Academic Affairs Dr. Roopa Bellad, KLE Academy of Higher Education and Research for their support and co-operation.

I owe my special thanks to Prof. (Dr.) Ramesh Chavan, and Mr. Shivanand G. Hiremath, Junior Laboratory technician, Department of Pathology, J.N. Medical College, Belagavi, for helping me in histopathology studies. I am thankful to the authorities of Urinary Biomarkers

Research Center, KLEs Dr. Prabhakar Kore Hospital and Medical Research Centre, Belagavi, for providing the facility of fluorescence microscope.

I take this opportunity to genuinely acknowledge my seniors, colleagues, and juniors who guided and supported me from the early days of my research. Mr. Satveer Jagwani and Dr. Dinesh Dhamecha, Dr. Sanjay Mishra, Dr. Suneel Dodamani, Dr. Satish Hedge, Dr. Shabana Shaikh, Dr. Uday Kumar, Dr. Ritiha Patil, Ms. Dhanashree Patil, Ms. Geetanjali, Mrs. Priya Shetti, Ms. Nikita Patil, Ms. Supriya Chimagave for being a constant support during my research.

Special thanks to Sami Labs, Bangalore, India for providing the gift sample of Resveratrol and Piperine for my research work.

I express my immense gratitude and love to my greatest source of inspiration, my parents Mr. Kallappa Kurangi and Mrs. Basavva Kurangi, and my elder brother Dr. Anil and my beautiful wife Pooja for their endless encouragement, guidance and support through all these years.

Thanking you, one and all.

Date: **Mr. Bhaskar Kurangi**

Place: Belagavi

Table of contents

List of abbreviations

ANOVA: Analysis of variance

AO: Acridine orange

A375: Human melanoma cell line

A431: Human Squamous carcinoma cell line

Balb/c: albino laboratory –bred strain mice

BC: Blank cubosome

B16F10: Mouse melanoma cell line

B16/DOX: doxorubicin-resistant B16 melanoma cell subline

cm: Centimeter

CO_2: Carbon dioxide

cP: Centipoises

CPCSEA: Committee for the Purpose of Control and Supervision of Experiments on Animals

CYP 3A4: Cytochrome P450 3A4

C57BL/C: C57 Black 6

C6: Coumarin 6

C6-CUB: Coumarin-6 loaded cubosome

DAPI: 4', 6-diamidino-2-phenylindole

DLS: Dynamic Light Scattering

DMEM: Dulbecco's Modified Eagle's medium

DMSO: Dimethyl sulphoxide

DNA:Deoxyribonucleic acid

DSC: Differential scanning calorimetry

EE: Entrapment efficiency

EB: Ethidium bromide

FBS: Fetal bovine serum

FT-IR: Fourier Transform infrared spectroscopy

g: Gram

GMO: Glyceryl monooleate

h: Hour

HPLC: High Performance Liquid Chromatography

HR-TEM: High Resolution Transmission Electron Microscopy

IAEC: Institutional Animal Ethics Committee

IC_{50}: Half maximal inhibitory concentration

ICH: International Council for Harmonization

i.d.: internal diameter

kg: kilogram

KBr: Potassium bromide

LOD: Limit of detection

LOQ: Limit of quantification

L929: Normal mouse fibroblast

min: minute

mm: millimeter

mg: Milligram

ml: Milliliter

MTT: 3-(4,5-dimethylthiazol-2-yl)-2,5-diphenyltetrazolium bromide

N: Number of theoretical plates

nm: Nanometer

ns: No significant

P: Probability

PALS: Phase Analysis light Scattering

PB: Phosphate Buffer

PBS: Phosphate buffer saline

PDI: polydispersity index

PEG: Polyethylene glycol

PFA: Paraformaldehyde

PRESS: Predicted residual error sum of square

pH: power of hydrogen/ povouir hydrogen

PDA: Prominence diode array

PF-127: Pluronic F-127

PHYT: Phytantriol

PI: Piperine

PS: Particle size

PVDF: polyvinylidene difluoride

r^2: Correlation coefficient

ROS: Reactive oxygen species

RPC: Resveratrol and piperine loaded cubosome

RP: Resveratrol and piperine

rpm: Revolution per minute

RV: Resveratrol

RSD: Relative standard deviation

SAED: Selected area electron diffraction

SD: Standard deviation

SLN: Solid lipid nanoparticles

SLS: Sodium Lauryl Sulphate

SK MEL 28: Human melanoma cell line

TEM: Transmission electron microscopy

USA: United States of America

USFDA: United States Food and Drug Administration

USP: United States Pharmacopeia

UV: Ultraviolet

v/v: Volume by volume

w/v: Weight by volume

w/w: Weight by weight

XRD: X-Ray Diffraction

ZP: Zeta potential

2θ: Diffraction angle

2FI: Two factor interaction

µg: Microgram

µm: Micrometer

°C: Degree centigrade

%: Percentage

<: Less than

>: Greater than

List of tables

List of figures

	and marketed gel (D,F), Estimation of tumor volume and body weight (G and I) during 6 weeks treatment and post 6 weeks treatment (H and J) respectively. (n=6), (*** P<0.001, ** P<0.01, * P<0.05, NS- not significant) vs control group	
22	Representative Hematoxylin and eosin stained images of tumor tissues obtained from BALB/c mice melanoma model in different groups demonstrating change in epidermis thickness (I) and tumor necrosis (II). Different groups represents as Normal skin (A), Untreated tumor (control) (B,G), Prophylactically and therapeutically treated with RPC-gel (C,H and E,J) and marketed gel (D,I and F,K) respectively. (Magnification- 4X)	62

Abstract

Background

Melanoma is one of the most aggressive type of skin cancer, with high incidence rate and mortality, throughout the world. Despite of noteworthy development in melanoma treatment, the destructive nature of the disease makes it difficult for clinicians to manage the condition. Hence, there is need remains to achieve improved therapeutic activity and overall survival time using herbal constituents, which can offer improved efficacy over existing chemotherapy, in melanoma therapy. Resveratrol (RV) and piperine (PI) are the model drugs of choice for their potential antimelanoma activity. However, their clinical application is limited due to their poor pharmacokinetic properties.

Objectives

The current research work aims to investigate the effect of Cubosomal nanoformulation of RV and PI against Melanoma.Hence the objectives of thestudy are:

1. To formulate, evaluate and optimize RV and PI loaded cubosomal nanoformulation.
2. To study anticancer activity of optimized cubosomal nanoformulation against Melanoma.

Methodology

The RV and PIloaded cubosomes (RPC) were prepared by Fragmentation techniques using high-speed homogenization method followed by probe sonication. A 3^2 factorial design was used for the optimization of the RPC using Design-Expert® software. The prepared formulations were characterized for entrapment efficiency, particle size, shape and zeta potential. The optimized RPC5 formulation was subjected to *in vitro* release study, *in vitro* cell culture studies (cytocompatibility, cytotoxicity and cell uptake studies). Cubosomal gel (RPC-gel) was formulated from the optimized RPC5 and characterized for pH, viscosity and

ex vivo skin permeation and retention studies. *In vivo* skin toxicity and pharmacodynamic (prophylactic and therapeutic treatment modalities) studies of RPC-Gel was performed in B16F10 cells induced melanoma bearing BALB/c mice.

Results

The optimized cubosome formulation (RPC5) containsthe cubicshaped nanoparticles with a mean particle size and zeta potential of 110±3.30 nm and -34.3 ± 1.04 mV respectively. The entrapment efficiency of RV and PI entrapped inside the RPC was 88.12 ± 1.54 and 85.17 ± 0.25% respectively. *In vitro* drug release of optimized RPC demonstrated biphasic drug release with diffusion-controlled release of RV (92.7 ± 2.08%) and PI (72.48 ± 3.36%). Optimized RPC was further formulated into cubosomal gel (RPC-Gel) by using carbopol (1% w/v) and the prepared gel was evaluated for *ex vivo* permeation and deposition which shows better drug permeation and deposition in mice skin layers in comparison to RP-Gel. Cell compatibility studies of free RV and PI (RP) and RPC5 was evaluated against mouse fibroblast culture (L929) which showed no significant difference in cellviability, which confirms its cytocompatibility. *In vitro* cytotoxicity studies in A375 cells demonstrated an improved anticancer activity of RPC5 in comparison with free RP. These outcomes were supported by a cell uptake study in A375 cells, in which RPC5 exhibited a higher uptake than RP. Furthermore, images obtained from fluorescent microscopy forA375 cells after 3 and 5 h of incubation showed higher internalization of coumarin 6 (C6) loaded cubosome (C6-CUB) as compared to those of the free C6.Stability study showed the ability of RPC to maintain their stability at room temperature. Composition of RPC-Gel has been proved non-irritant to the mice skin. Apharmacodynamic investigation revealed a significant reduction in tumor growth and significant increase in the body weight in RPC-Gel treated melanoma-bearing BALB/c mice when compared to control (non-treated) melanoma-bearing BALB/c mice. These findings were supported by histopathological analysis, of tumor tissues of BALB/c mice demonstrated extensive tumor necrosis in the same mice on treatment with

RPC-Gel. The results of *in vitro* and *in vivo* studies thereby proposing, RPC-Gel to be a promising drug delivery system bytopical application for the melanoma treatment.

Conclusion

These results implied that delivery of RPC substantially controlled the melanoma condition, hence RPC can be considered as a promising nano drug delivery system in the management of melanoma skin cancer.

Keywords: Resveratrol; Piperine; cubosome; melanoma; cell uptake; pharmacodynamic

1. INTRODUCTION

1.1 BACKGROUND

Melanoma:

Melanoma is the most lethal kind of skin cancer and is a malignant type of tumor originating from uncontrolled proliferation of melanocytes. Ultraviolet (UV) irradiation from sunlight is the main environmental risk factor for melanoma skin cancer development. The occurrence of annual cases of melanoma has been increased by nearly 50% worldwide over the last decade, which predominates in United sates of America, New Zealand, Australia, and North European countries (1). According to Global Cancer Statistics, in 2018 about 2,87,723 new cases and 60,712 deaths were reported worldwide (2). Nowadays, the treatments recommended for melanoma are surgery, radiation therapy, chemotherapy, immunotherapy, and targeted therapy. Surgery is preferred in melanoma patients with early stages (I-IIIB), whereas radiotherapy is rarely used in primary tumor treatment of skin, bone, and brain metastases. In advanced and metastatic melanoma, chemotherapy is the first line treatment given either individually or in combinations with immunotherapy or targeted therapy. These therapies are either less effective enough or can cause severe adverse effects and assist in development of multi-drug resistance. After extensive clinical trial research, very few drugs like dacarbazine, Interferon-2b, Interleukin-2, Ipilimumab, Ontak, Dabrafenib have been approved by USFDA (3). Despite of this noteworthy development in melanoma treatment, patients with advanced-state metastatic melanoma revealed the median overall survival time, which is less than 6 months (1). Hence there is need remains to achieve improved therapeutic activity and overall survival time using herbal constituents, which can offer improved efficacy over existing chemotherapy, in melanoma therapy.

Resveratrol (RV) is a nutraceutical which have exciting pharmacological potential and attracted a lot of research attention in last decade owing to its demonstration of antioxidant, cardioprotective, neuroprotective, immunomodulatory, anti-inflammatory and anticancer properties (4). RV has been reported for various anti-cancer activities against thyroid cancer, breast cancer, leukemia, colon cancer, prostate cancer, ovarian cancer, melanoma, liver cancer and squamous cell cancer (5). Despite of its promising therapeutic effects, RV has got limited success due to its poor solubility, instability, and poor oral bioavailability resulting from its fast metabolism (6). In order to increase its therapeutic applicability and to overcome these issues, a transdermal approach has been selected. In addition to this, a combination strategy which may afford additive or synergistic effect along with bioavailability enhancement of RV in effective management of melanoma has been selected by using piperine. Piperine (PI) is a natural alkaloid found in *Piper nigrum* and *Piper longum* and has been used not only as food spices but also as potential therapeutic agent for various diseases including obesity, inflammation, arthritis, depression, and different types of cancers. Also, PI acts as a bioavailability enhancer for so many other drugs (7). The major obstacle in transdermal delivery of these phytoconstituents is the stratum corneum, a barrier in the penetration and diffusion through the skin. Hence, an approach is needed to develop a nanoparticulate drug delivery system which can overcome this barrier with effective delivery of these phytoconstituents at targeted melanocytes.

RESVERATROL

Resveratrol (RV) (3,4,5-trihydroxystilbene) is a naturally occurring phytoalexin and polyphenolic compound present in a numerous types of dietary sources including grapes, plums, peanuts and red wine.

Figure 1 shows the molecular structure of trans-RV. It is highly hydrophobic with a partition coefficient of 3.1 and an aqueous solubility of 0.03 g/L. Despites its poor aqueous solubility, it is expected to demonstrate high membrane permeability due to its lipophilicity. It is freely soluble in ethanol and dimethyl sulfoxide. RV exists in two geometric isomers, cis and trans. The trans-isomer is more abundant and biologically active than the cis-isomer. However, trans-isomer of RV can be easily isomerized to the cis-isomer when exposed to sunlight, or ultraviolet (UV) light at 360 and 254 nm (4).

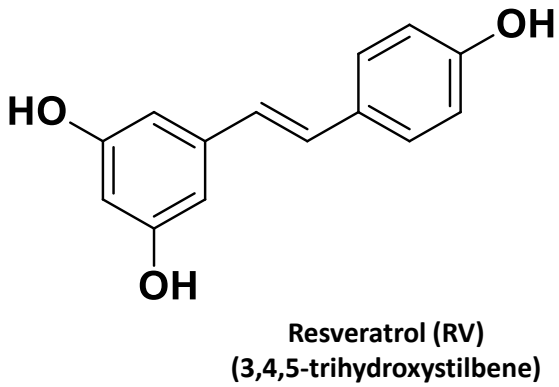

Figure 1: Chemical structure of Resveratrol (RV)

RV as therapeutic agent in treatment of different diseases:

RV has since received an increasing scientific attention, leading to investigation on its biological activity, and to numerous publications. RV was first isolated from white hellebore (*Veratrum grandiflorum*) plant. This natural polyphenol has been detected in more than 70 plant species, and is also found in discrete amounts in red wines and various food products. Today a number of therapeutic actions have been reported by RV viz. anti-carcinogenic, anti-inflammatory, anti-diabetic, anti-microbial, cardioprotective, neuroprotective, anti-ageing, anti-oxidant and anti-viral activities (8) (Figure 2).

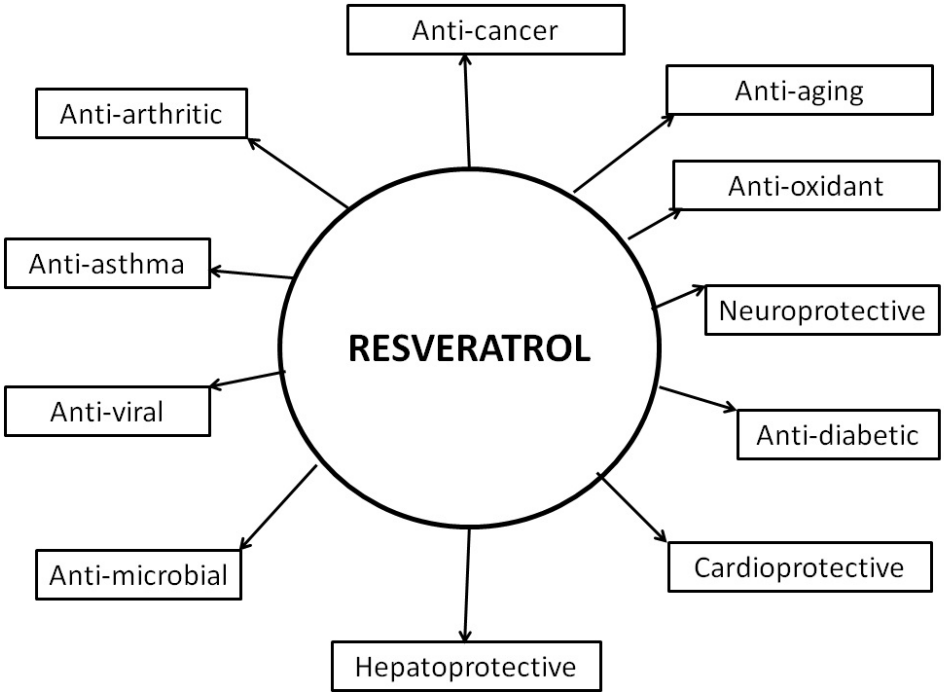

Figure 2: Biological activities of Resveratrol (RV)

However, because RV has been shown *in vitro* and *in vivo* to have chemopreventive and chemotherapeutic effects on cancers by targeting multiple pathways, it is a promising anticancer agent. Resveratrol affects all three stages of carcinogenesis: initiation, promotion, and progression (9).

Many studies of RV have been reported for anti-melanoma activity like, in doxorubicin resistant murine melanoma cells, the potency of RV has been demonstrated by inducing apoptosis and inhibiting the growth of melanoma tumors in mice (10), whereas in another study it was demonstrated that RV in combination with temozolomide acts as an effective cytotoxic agent against melanoma cells (11). In addition to this, RV also acts as a radiation sensitizer for melanoma treatment (12) and apoptosis inducer and growth inhibitor for human melanoma cells (13). Due to its poor bioavailability the *in vivo* anti-cancer effects of RV are strongly limited (14). Hence approach is to be done, to increase its bioavailability using either by bioenhancer or nanotechnology.

PIPERINE (PI)

Piperine (PI) is a natural alkaloid found in *Piper nigrum* and *Piper longum* belongs to Piperaceae family. Figure 3 shows PI molecular structure. PI has been used not only as food spices but also as potential therapeutic agent for various diseases including obesity, inflammation, arthritis, and different types of cancers (7) (Figure 4).

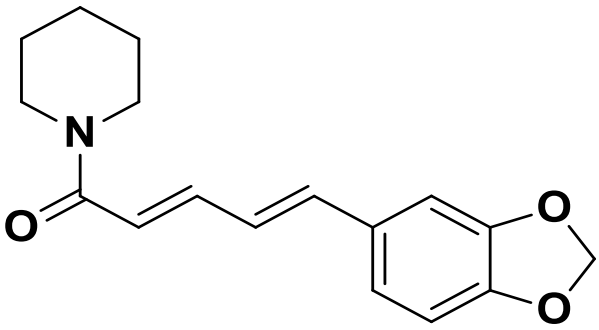

Figure 3: Chemical Structure of Piperine (PI)

Piperine as therapeutic agent in treatment of different diseases:

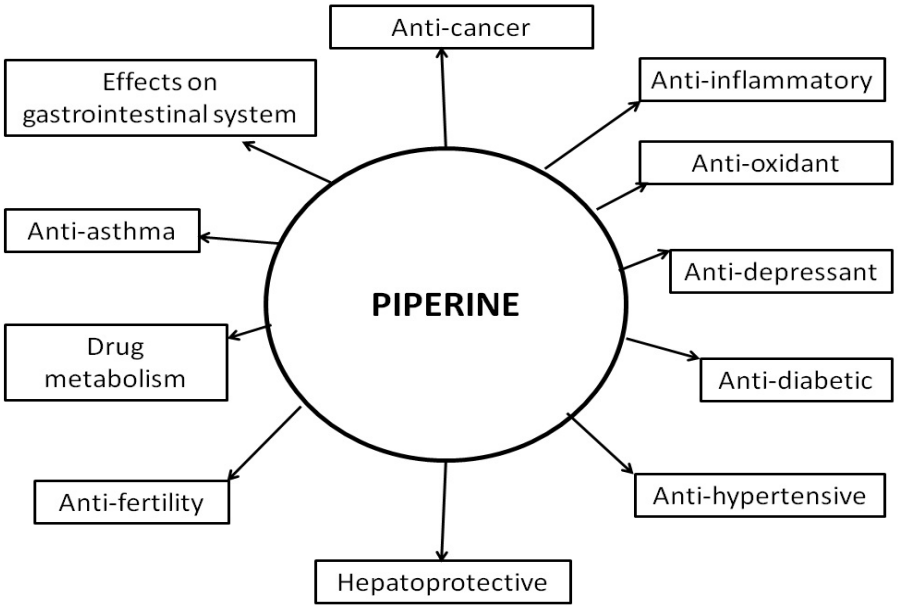

Figure 4: Biological activities of Piperine (PI)

PI has anticancer and antitumor activity which can be due to its immunomodulatory properties, including the activation of cellular and humoral immune responses (15). It inhibits cytochrome P450 3A4 (CYP3A4) and P-glycoprotein by which bioavailability of other drugs can be enhanced (16). Many studies have shown PI as a prominent phytoconstituent that can be used in the melanoma treatment. It was found that PI decreased lung metastasis induced by B16F10 melanoma cells by the activation of antioxidative protection enzymes and modulating lipid peroxidation (17). Clinical trials have been conducted to assess the efficacy of PI in a bioavailability enhancement of other phytoconstituents. The anti-proliferative effects of PI were observed in mouse and human melanoma cell lines, which demonstrated cytotoxic effects produced by apoptosis and cell cycle arrest at G1 phase in both SK MEL 28 and B16 F0 cell lines (18). But, due to intense first-pass metabolism, pH-mediated metabolism to piperidine and photoisomerization, leads to difficulty in the administration of PI (19,20). Many studies have been reported for PI combination with RV which has shown potential synergistic effect with enhanced bioavailability. This combination approach has been potentiated antidepressant, anticancer and other activities (21–24). A nanoparticulate approach needs to be taken to increase their effectiveness for better targeting to melanoma.

Transdermal drug delivery system

Transdermal delivery represents an attractive alternative to oral and parental delivery of drugs.

The major advantages include

- Bypass first pass metabolism in liver.
- Avoidance of gastrointestinal problems.
- Noninvasive and self administration.
- Controlled drug plasma level.

- Reduction in undesirable side effects.
- Reduced dosing frequency.
- Better for drugs with short half life.
- Easily terminate the treatment any time.
- Increased patient compliance.
- Inexpensive.

In transdermal delivery of drugs, the skin penetration of the drug is limited as a result of the barrier function of the highly organized structure of the stratum corneum, outermost layer of the skin. Several approaches have been presented to improve the skin permeation such as chemical modification of the active molecule, applying a skin permeation enhancer and iontophoresis that facilitates the breakthrough of the stratum corneum barrier. With the advancement of skin penetration strategies, various anticancer therapeutics ranging from lipophilic small-molecule drugs to hydrophilic biomacromolecules, can be administered transdermally, offering an optional regimen in the treatment of melanoma (25).

Transdermal deliveries have shown enormous therapeutic potential in the treatment of skin cancer with reduced adverse effects. Most of transdermal applications focus on the treatment of superficial skin cancer as the drugs can concentrate in the tumor tissue after overcoming the skin barrier (Figure 5). The crucial issue in topical formulations is to increase the thermodynamic activity of the active molecule in the vehicle while decreasing it in skin, which results in increasing the partition of the molecule from vehicle to skin and decreasing the barrier function of the skin (26). Hence there is need of novel nanotechnology which could effectively deliver the drug through the skin in targeting melanoma.

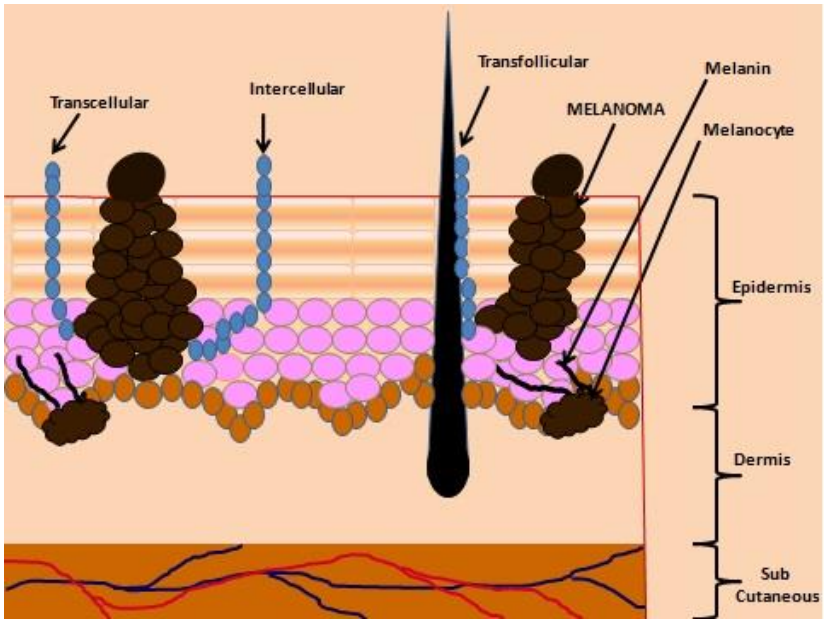

Figure 5: Schematic representation of melanoma development in the human skin and possible mechanism of drug loaded nanoparticles transport through the stratum corneum barrier

CUBOSOMES

As nanotechnology makes drug delivery systems much smaller, lighter, stronger, cleaner, more specific and more precise, there is enough evidence to believe that nanomedicine would bring hope for better management of melanoma. Polymeric nanoparticles, liposomes, dendrimers, cubosomes, polymersomes and niosomes are currently leading the research interest in targeting and curing skin cancers. From all these nanoparticles cubosome have somewhat more application for melanoma skin cancer.

Cubosome is bicontinuous cubic liquid crystalline structure formed as colloidal dispersion in water with the help of suitable surfactants can result into nanostructured systems. Generally cubosomes have particle size 100 to 300 nm. Cubosomes are the hydrated surfactant structures that can self- associate to form a bicontinuous liquid cubic crystal phase maintaining its thermodynamic stability (Figure 6). These are viscous isotropic binary systems, the highly

twisted lipid bilayer and high surface area (~400 m^2/g) of cubosomes results in higher adjuvant incorporation (26). The main structural components of cubosomes include first amphiphilic lipids such as Monoolein/ Glyceryl monooleate (GMO), or phytantriol (PHYT) and second stabilizer like Pluronic F-127. Oral, ophthalmic, mucosal, topical, parentral (intravenous) and intranasal etc. are preferred potential routes of delivery of cubosomes.

Structure of Cubosomes

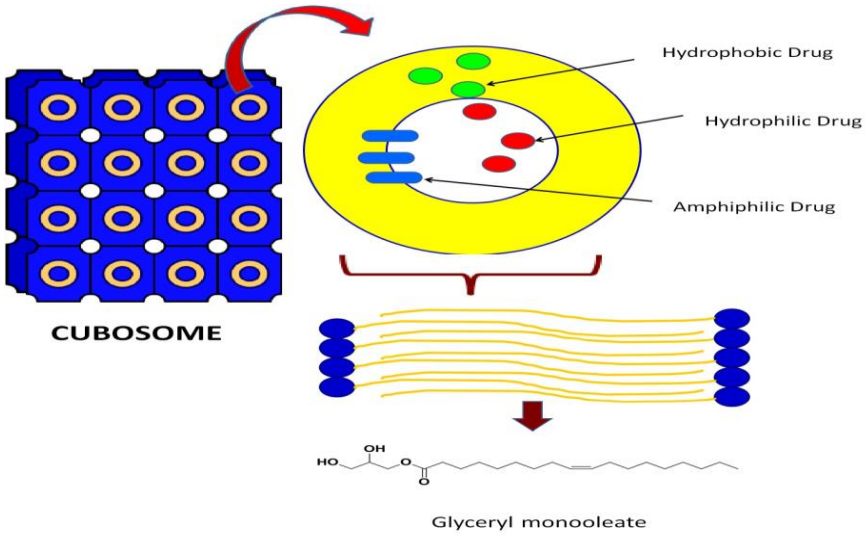

Figure 6: Schematic representation of Cubosome

Advantages of Cubosomes (27)

- Improved thermodynamic stability.
- Maximum drug loading capacity because of increased surface area.
- Encapsulate hydrophilic, lipophilic and amphiphilic drugs.
- Biodegradable lipid imparting bioadhesive and biocompatible properties.
- Administered by different ways of routes.
- Sustained, targeted and controlled drug release achieved.
- Very simple method of preparation.

- Bicontinuous cubic liquid crystalline phase of cubosomes even stable in excess water.
- These are an excellent vehicle to protect the sensitive drug such as peptides and proteins, from the enzymatic degradation and *in vivo* degradation.

Method of preparation (28)

There are two main approaches typically used to produce cubosome dispersions: (i) top-down and (ii) bottom-up approaches.

The top-down approach requires the dispersion of an extremely viscous lipid or bulk cubic phase into the aqueous solution using High-pressure homogenization and sonication techniques in which the high energy is created. The bottom-up approach is one in which a single phase liquid precursors is prepared using a hydrotrope (e.g., chloroform, ethanol), which is miscible with water insoluble lipids and finally diluted into a two phase regime of cubosomes coexisting with an excess aqueous phase.

Applications of cubosome

- Sustained drug release.
- Topical treatment of Burns.
- Melanoma therapy.
- Improved ophthalmic drug delivery.
- Carriers of cosmeceuticals actives.
- Theranostic applications.
- Delivery of protein vaccines.
- pH responsive drug delivery from cubic phase matrices.
- Protein entrapment and PEGylation of cubosomes.

1.2 REVIEW OF LITERATURE

Naves et al., (2017) extensively reviewed types of skin cancer with special emphasis on the melanoma, the targeting strategies, drugs used for chemotherapy treatment, nanotechnology approach to treat melanoma with some case studies. This review suggests that enhanced permeability and retention is the basis for using nanotechnology, aiming for topical drug delivery. Authors have reported a case study involving two different approaches for targeting melanoma skin cancer therapy, namely, magnetic-based core–shell particles and electrospun mats. The literature mentioned indicates the controlled delivery of drug-loaded nanofibers for melanoma skin cancer therapy. The details mentioned thus suggest that possibilities to enhance the topical drug delivery after massaging the skin, or pulling out the follicles may be an alternative route for the therapeutic absorption (29).

Kurangi et al., (2018) summarizes the research work in melanoma chemoprevention and treatment using the herbal phytoconstituents. Phytoconstituents like carotenoids, flavonoids, some polyphenols, piperine alkaloid, and sulforaphane have been mentioned for their high anticancer potential mostly which is being used for melanoma treatment or prevention. Relevant mechanisms involved in the pharmacological effects of these phytochemicals are also explained. Most of the phytoconstituents have been reported for both *in vitro* and *in vivo* antimelanoma activity (30).

Johnson et al., (2011) examined the activity of piperine in the enhancement of pharmacokinetic parameters of resveratrol via inhibiting its glucuronidation. The major problem in achieving desire activity of resveratrol is poor *in vivo* bioavailability due its fast metabolism. It was found from the *in vivo* study in C57BL/6 mice that piperine co-administration with resveratrol, have significantly increased the degree of exposure of resveratrol (229%) and the maximum serum

concentration (Cmax; 1544%). The results obtained thus demonstrated that piperine has significantly increased the bioavailability of resveratrol (24).

Carletto et al., (2016) formulated resveratrol-loaded poly(ε-caprolactone) nanocapsules and evaluated for its antimelanoma activity using *in vitro* and *in vivo* model. These developed nanocapsules were spherically-shaped and negative charged with size less than 150 nm, and high encapsulation efficiency. Resveratrol-loaded nanocapsules decreased cell viability and proliferation of melanoma cells (B16F10). *In vivo* results in subcutaneously induced C57BL/6J mice showed that resveratrol-loaded nanocapsules have decreased the tumor volume and increased the necrotic area and inflammatory infiltrate of melanoma as compared to free resveratrol. The metastasis and pulmonary hemorrhage was prevented by using developed nanocapsules. Therefore, the results obtained showed that resveratrol-loaded nanocapsules can effectively used in the treatment of melanoma progression and thus provides an improvement in the melanoma condition (31).

Fofaria et al., (2014) evaluated *in vitro* cytotoxic activity of piperine in B16 F0, SK MEL 28 and A375 melanoma cells. Piperine treatment inhibited the growth of all types of melanoma cells in concentration and time-dependent manner. The growth inhibitory effects of piperine were mediated by cell cycle arrest of melanoma cells in G1 phase and using apoptosis induction mediated through reactive oxygen species generation. The results obtained showed that ROS generated played an important role in inducing DNA damage and activation of checkpoint kinase 1 leading to G1 cell cycle arrest and apoptosis (18).

Nadia et al., (2014) developed and characterized silver sulfadiazine loaded cubosome nanoparticles for the topical treatment of burn infections. An emulsification process was used in the preparation of cubosome dispersion using different concentrations of a lipid, surfactant, and

stabilizer. The optimum formulae of cubosome dispersion (monoolein 82.5%, polyvinyl alcohol 2.5% and poloxamer 407 15%) were incorporated in a chitosan (1.5%), carbopol 940 (1%) or chitosan/carbopol mixture based hydrogels, to form cubosomal hydrogels (cubogels). The prepared cubosomes were nano sized with cubic shape structure. *In vivo* study in the male wister rats and histopathological results demonstrated that the prepared cubogels were successful in the treatment of deep second degree burn which showed excellent healing results with least side effects in comparison with the marketed product (32).

Sharma et al., (2015) formulated and evaluated fluconazole loaded cubosomal gel for the treatment of fungal infections. Different cubosomal formulations were prepared by top down technique (using sonication followed by homogenization) and optimized using central composite design. Different ratios of drug, lipid and polymer have been used to evaluate the effect on dependent variables like entrapment efficiency and permeability (6^{th} h). The formulated cubosomes were characterized for particle size, entrapment efficiency, drug permeability and surface morphology. Optimized cubosome formulation was found with cubic shaped nanoparticle with particle size, % entrapment efficiency and drug permeability was 171 nm, 83.3%, and 91.89 % respectively. The optimized cubosome dispersion was further converted to cubosomal gel by using 1% carbopol. *In vitro* antifungal study showed that cubosomal gel has enhanced antimicrobial effect on *Candida albicans* strain in comparison to marketed Flucose gel, which may be due to high drug loading and enhanced diffusion of the drug (33).

Tupal et al., (2016) investigated the effect of the formulated Doxorubicin loaded solid lipid nanoparticles for topical treatment of skin cancer. The prepared nanoparticles were characterized for particle size, entrapment efficiency, zeta potential and surface morphology. *In vitro* and *in vivo* cytotoxicity of optimized formulation were evaluated on murine melanoma (B16F10) cells by

MTT assay and melanoma induced Balb/C mice, respectively. Melanoma in Balb/C mice was induced by subcutaneous injection of B16F10 cells (2×10^6). *In vitro* study results revealed that Doxorubicin nanoparticles are more prone to cytotoxic in comparison with Doxorubicin solution. Animal study demonstrated that Doxorubicin nanoparticles (low and high dose) significantly reduced the tumor volume in comparison to free doxorubicin solution (34).

Khan et al., (2015) prepared 5- Fluorouracil loaded transfersomal system and evaluated for the skin cancer treatment. Transfersomal formulations were prepared using Span-80 and Tween-80, and evaluated for vesicle size, shape, deformability, entrapment efficiency, and *in vitro* skin permeation. Gel formulation was prepared by incorporating optimized transfersome into carbopol 940 gel (1%) and evaluated for its *in vivo* anticancer activity. The gel formulation showed better drug penetration and deposition through the skin as compared to marketed gel. *In vivo* study in swiss albino male mice showed that the transfersomal gel was non-irritant to the mice skin and reduced the tumor size maximally in comparison with marketed gel. The *in vivo*, histopathological and biochemical results suggested that 5- Fluorouracil loaded transfersomal gel is an effective carrier for topical delivery in the treatment for skin cancer (35).

Safwat et al., (2018) prepared and evaluated 5- Fluorouracil loaded gold nanoparticle for local application in the treatment of skin cancer. 5- Fluorouracil was loaded onto gold nanoparticles capped with cetyltrimethylammonium bromide using ionic interactions. The molar ratios of 5-Fluorouracil/cetyltrimethylammonium bromide and pH have affected the entrapment efficiency of 5- Fluorouracil and drug release from the gold nanoparticle. 5- Fluorouracil loaded gold nanoparticle gel and cream prepared from the nanoparticle dispersion was evaluated for their viscosity, skin permeability and *in vivo* anticancer study. *In vivo* anticancer study in C57BL/6 mice were performed by implanting subcutaneous A431 skin cancer cells (4×10^5) and started

topical application of gel and cream on 24th day of visualization of tumor in mice. The results obtained demonstrated that 5- Fluorouracil loaded gold nanoparticle gel and cream has significantly reduced the tumor volume and increased the body weight of mice (36).

1.3 JUSTIFICATION

The incidence of melanoma has increased in the last decade which accounts 75% of all skin cancer death every year, and is expected to continue to rise for the next 20 years. If melanoma is found and treated in its early stages, the chances of recovery are very good. If melanoma detection is not done early, then it can grow deeper into the skin and metastasize to other parts of the body. Once it has evolved to malignant melanoma, it is difficult to cure and results in a high death rate. The current clinical approach and therapy for melanoma includes surgery, chemotherapy or immunotherapy, and/or the combination of the two. Surgery remains the best intervention for patients with early stage melanoma. The combination of chemotherapy or immunotherapy is associated with higher response rates than single-agent therapy but this has not translated into improved survival. Major obstacles in the successful treatment of melanoma are development of multi-drug resistance and severe adverse effects. Therefore, interest has been grown for phytoconstituents having high anti-cancer potential mostly to be used for the treatment of melanoma.

The phytoconstituents such as resveratrol and piperine have exciting pharmacological potential against melanoma and have recently attracted a lot of research attention. Both the phytoconstituents exerts the different therapeutic activity viz. antioxidant, anti-cancer, anti-inflammatory, anti-diabetic, anti-microbial, cardioprotective, and neuroprotective. However, poor pharmacokinetic properties like low aqueous solubility, extensive first pass metabolism and low photostability problems results in poor bioavailability by parenteral or oral route which hinders an immense potential of resveratrol. To overcome these problems, resveratrol and piperine in combination can be delivered transdermally. However, stratum corneum is the main

barrier in transdermal delivery which decreases the permeability of these phytoconstituents through the skin and their high lipophilicity which resulted into poor local bioavailability.

To improve the stability, safety and efficacy of resveratrol and piperine for melanoma therapy, an emerging approach have been employed by a novel potential nanocarrier i.e. cubosome. The cubosomes have bioadhesion, thermodynamic stability, high loading capacity, penetration enhancement property and ability to encapsulate hydrophilic, lipophilic and amphiphilic drugs by which their potential utility in melanoma can be enhanced over other nanocarriers.

Many researchers have demonstrated resveratrol and piperine as potential phytoconstituents that can be used for the treatment of melanoma. However, the applicability of resveratrol and piperine loaded cubosomal nanoformulation as novel drug delivery system for targeting melanoma has not been performed so far. Thus, in the present investigation, an attempt is being made to design resveratrol and piperine loaded cubosomal nanoformulation and evaluate its efficacy in the treatment of melanoma.

1.4 OBJECTIVES AND PLAN OF WORK

AIM

To investigate the effect of cubosomal nanoformulation of resveratrol and piperine against Melanoma.

OBJECTIVES

- To formulate, evaluate and optimize resveratrol and piperine loaded cubosomal nanoformulation.
- To study anticancer activity of optimized cubosomal nanoformulation against Melanoma.

STUDY PLAN

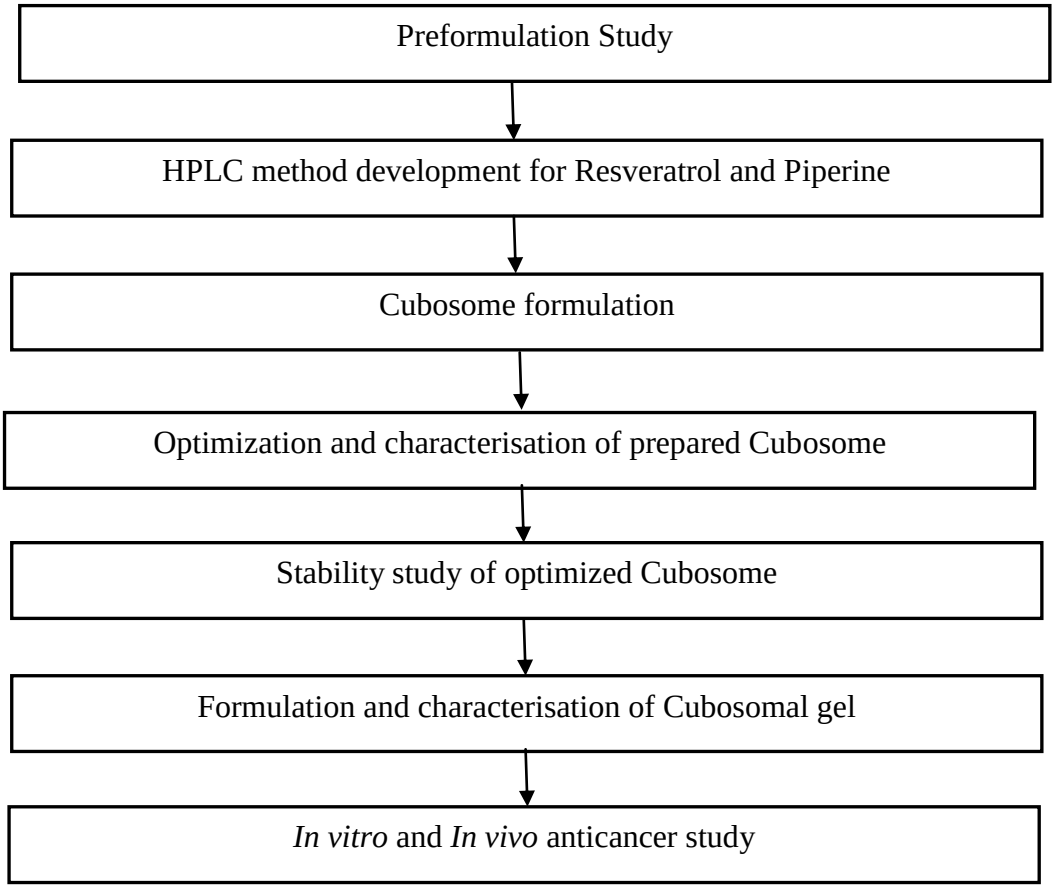

2. MATERIALS AND METHOD

Table 1: List of Instruments

S.No.	Instrument name	Model	Make
1	Electronic balance	AUW 220D	Shimadzu
2	Magnetic stirrer	RCT Basic	IKA
3	FTIR	IR Affinity-1S	Shimadzu
4	Differential scanning calorimetry	DSC-60	Shimadzu
5	High-performance liquid chromatography	LC-20AD Prominence	Shimadzu
6	pH meter	CyberScan pH 510	Eutech Instruments
7	Homogenizer	T25 digital Ultra Turax	IKA
8	Probe sonicator	Rivotek™ Ultrasonic sonicator	Riviera Glass Pvt Ltd
9	Bath sonicator	CPX 1800 H-E	Branson
10	Inverted microscope	TCM 400	Labomed
11	High resolution-transmission electron microscope	JEM, 2100	Jeol
12	Zetasizer	Nano ZS	Malvern instruments
13	High speed refrigerated Centrifuge	Floor model 7000	Kubota
14	Franz diffusion cell	V6B-02 and 31011	Perme Gear
15	Homogenizer	RQT-127A	Remi Laboratory Instruments
16	Fluorescence microscope	BX41	Olympus
17	Ultra-low temperature freezer	U410-86	New Brunswick
18	Freeze dryer	Alpha 1-2 LD plus	Christ
19	X-ray diffractometer	PW-3710	Philips
20	CO_2 incubator	Galaxy 170R	New Brunswick
21	Microtiter plate reader	Lisa Plus	Rapid Diagnostic Pvt. Ltd.
22	Viscometer	CAP 2000+	Brookfield
23	Micro centrifuge	Spinwin MC-02	Tarson

Table 2: List of chemicals

S.No.	Chemical	Supplier
1	Resveratrol	Sami Labs Ltd., Bangalore, India
2	Piperine	Sami Labs Ltd., Bangalore, India
3	Glyceryl monooleate	Mohini Organics Pvt. Ltd., Mumbai.
4	Pluronic F-127	Sigma Aldrich, USA
5	Potassium dihydrogen phosphate	Merck, India
6	Sodium hydroxide	Merck, India
7	Coumarin 6	Sigma Aldrich, USA
8	Mannitol	Himedia Laboratories, India
9	3-(4,5-dimethylthiazol-2-yl)- 2,5-diphenyltetrazolium bromide (MTT)	Sigma Aldrich, USA
10	Ethidium bromide	Sisco Research Laboratories Pvt. Ltd, India
11	Acridine orange	Himedia Laboratories, India
12	4',6-Diamidino-2-phenylindole (DAPI)	Sigma Aldrich, USA
13	Dimethyl sulfoxide	Qualigens, India
14	Carbopol 934	Lubrizol Advanced Materials India Private Limited, India
15	Acetonitrile	Fisher Scientific, India
16	Methanol	Fisher Scientific, India
17	Chloroform	Fisher Scientific, India
18	Ortho phosphoric acid	Fisher Scientific, India
19	Paraformaldehyde	Himedia Laboratories, India
20	Fetal bovine serum	Gibco, USA
21	Dulbecco's modified Eagle's medium (DMEM)	Gibco, USA

2.1 Analytical method for simultaneous estimation of RV and PI

HPLC (Shimadzu HPLC prominence system, LC-20AD, Japan) associated with prominence diode array (PDA) detector, pump (LC-20AD), autosampler, degasser and column oven was used to estimate the RV and PI concentration at common isosbestic point. Briefly, sample solutions were run on the chromatographic system using Luna C18 column (4.6 × 250 mm i.d.; particle size 5 µm, Phenomenex, USA) and eluted with a mobile phase comprising of acetonitrile : phosphate buffer (ACN:PB; pH 6, 55:45 % v/v). The pH of buffer was adjusted to 6 using sodium hydroxide. The flow rate of the mobile phase was kept at 1 mL/min with 35 °C column temperature. Samples and mobile phase were filtered through filter membranes (PVDF, 0.45 µm) prior to HPLC analysis. For simultaneous quantification of RV and PI, the common isosbestic point (330 nm) was selected for further analysis.

2.1.1 Preparation of stock and standard solutions:

Methanolic stock solutions (1 mg/mL) of RV and PI were prepared individually and used for calibration standard preparations of both the drugs in the series of concentrations of 0.25 to 8 µg/mL, by diluting stock with mobile phase. All solutions were kept in light resistant volumetric flasks to prevent possible photoisomerization.

2.1.2 Validation studies:

Validation of developed method was done by using system suitability, linearity, limit of detection (LOD), limit of quantification (LOQ), precision, accuracy and robustness as per ICH guidelines. The linearity was determined by evaluating a series of concentrations of RV and PI standards (0.25-8 µg/ml) in triplicates. Both inter-day (on three succeeding days) and intra-day (on the same day) precision analysis were performed at different concentrations (low, medium and high) under the same analytical conditions. In accuracy (recovery) study known

concentrations of RV and PI were spiked to their preanalyzed sample and its percentage recovery was evaluated by correlating the original and measured concentration. LOD (limit of detection) and LOQ (limit of quantification) are the analytes lowest detectable and quantifiable concentration which gives signal to noise ratio of 3:1 and 10:1 respectively. LOD and LOQ was calculated from slope and standard deviation (SD) of intercept, such as [LOD=3.3 (SD/slope)] and [LOQ=10 (SD/slope)].

2.2 Experimental design of the study

A 2-factor 3-level (3^2) factorial design was utilized to optimize the RPC, wherein concentrations of lipid - GMO (X1) and stabilizer - PF-127 (X2) were selected as independent variables and particle size (PS, Y1), and entrapment efficiency (EE, Y2) were selected as the response variables (Table 3). Optimization was done with the help of Design-Expert software (Version 7.0.0, Stat- Ease Inc., MN, USA).

Table 3: Variables utilized in 3^2 factorial design for the RPC nanoformulation

Coded level	**-1 (low)**	**0 (medium)**	**+1 (high)**
Independent variables			
X1- Lipid (%w/w)	3	5	7
X2- Stabilizer (%w/w)	0.5	1	1.5
Dependent variables			
Y1– Particle size	Minimize		
Y2- Entrapment efficiency	Maximize		

2.3 Preparation of RV and PI-loaded cubosome (RPC)

RPC was prepared by using top-down method. Fragmentation techniques were used to formulate cubosomes using high-speed homogenization method followed by probe sonication (37). Briefly,

PF-127 and GMO were liquefied in separate container on a magnetic stirrer at 65°C. RV and PI (each 0.1% w/v) was added in melted GMO and was mixed with liquefied PF-127 solution. This mixture was then added drop by drop to preheated water with constant stirring on a magnetic stirrer. Homogenization (IKA T25 digital Ultra Turax, Germany) was performed at 15,000 rpm for 15 min to form a fine dispersion and thereafter, probe sonicated (RivoTEK, Mumbai) for 5 min to form RPC nanoformulation. Coumarin–6-loaded cubosomes (C6-CUB, 0.05% w/v) was also formulated using the same procedure, except both drugs were replaced with Coumarin–6.

2.4 Freeze-drying

In order to perform the DSC, XRD and FTIR studies, it is important to convert the cubosome nanodispersion to a powder form. The powder of Blank cubosome (BC) and optimized RPC were obtained by lyophilization. In the lyophilization process mannitol (5% w/v) was added to cubosome dispersion as a cryoprotectant. The frozen (using ultra-low-temperature freezer at -20°C and -80 °C sequentially for 24 h) cubosome formulations were lyophilized by using Christ freeze dryer (Alpha 1-2 LD plus, Germany) in main drying and final drying stages. The dried powder was stored in air tight container for further analysis.

2.5 Characterization of prepared RPC

2.5.1 Physicochemical characterization of RPC

A) Particle size (PS), polydispersibility index (PDI), and zeta potential (ZP)

The physicochemical characterization of RPC was done for the average particle size, their distribution i.e. PDI, and ZP values as per the standard protocol using dynamic light scattering (DLS), and M3-phase analysis light scattering (PALS) techniques, respectively, using Zetasizer Nano ZS90 (Malvern Instruments, Malvern, United Kingdom).

B) Fourier-transform infra red (FTIR) spectroscopy

FTIR spectroscopy of pure RV, PI, GMO, PF-127 and RPC nanoformulation were performed by KBr pellet method and spectras were run (4000-400 cm^{-1}) using FTIR spectrophotometer (IR Affinity-1S, Shimadzu, Japan).

C) Differential scanning calorimetry (DSC)

DSC analysis of pure RV, PI, GMO, PF-127 and RPC nanoformulation were performed by heating (30-350 ^{o}C at 5 ^{o}C/min under constant Nitrogen supply) the aluminum pans containing the samples to determine the thermal behavior of drugs and their mixtures using DSC (DSC, DSC-60, Shimadzu, Kyoto, Japan).

D) X-ray diffraction (XRD)

XRD analysis (Xpert MPD, Philips Holland) of pure RV, PI, blank cubosome (BC) and RPC nanoformulation were performed using standard protocols to provide information about crystalline properties for the samples.

E) pH and viscosity

The pH value and rheological properties of RPCs were also determined as per the standard procedure using digital pH meter (CyberScan pH 510, Eutech instruments) and Brookfield viscometer (CAP 2000+, Brookfield Engineering Laboratories, MA, USA) respectively.

2.5.2 Entrapment efficiency (EE)

The RPC dispersion samples were centrifuged (High Speed Refrigerated Centrifuge, Floor Model, 7000, Kubota, Japan) at 15000 rpm for 30 min (37). The supernant liquid was collected, diluted appropriately and analyzed for the RV and PI content by using the developed HPLC method. The percent EE was determined as:

$$\% \text{ EE} = \frac{(A-B)}{A} X\ 100 \text{----(1)}$$

A- Total amount of RV and PI added in cubosome dispersion, and B - amount of RV and PI in supernant

2.5.3 Transmission electron microscopy (TEM)

The morphology of RPC was observed by high-resolution TEM (Jeol/JEM, 2100). A drop of diluted RPC was placed on a 200-mesh carbon-coated copper grid and stained with 2 % w/v phosphotungstic acid solution for 2 min. The grid was air-dried and observed under TEM (200kV and 40,000X) to get images along with a random selected area electron diffraction (SAED) .

2.5.4 *In vitro* RV and PI release from RPC

In vitro RV and PI release from optimized RPC was determined by using a dynamic dialysis method (USP II method) (38). The drug release study was done by using a tablet dissolution testing apparatus (Electrolab, EDT-08LX) equipped with low-volume conversion kit (EDT-08L/08L x 150 ml, Figure 7) which was specifically utilized for nanoformulation.

Figure 7: Dissolution testing apparatus (Electrolab, EDT-08LX) equipped with low volume conversion kit (EDT-08L/08L x 150 ml)

Briefly, RPC nanoformulation (5 mL) was transferred to a dialysis bag, which was immersed in 100 mL of PBS (pH 6.8) containing Tween 80 (1.5%). The temperature of the dissolution medium was kept at 37±0.5 ^{o}C with stirring speed of 50 rpm. The aliquots (1 mL) were withdrawn at specific time intervals. The withdrawn aliquots of the drug release medium were replaced with same volume of fresh buffer to maintain the sink condition. Concentrations of RV and PI released in the dissolution medium were determined by using HPLC method, as specified above. The drug release mechanism from cubosome formulation was determined by using different drug release kinetic models (39).

2.6 Stability study

In the short-term stability study, the cubosome nanoformulations were placed at room temperature away from light for 3 months and were then evaluated by estimating the mean PS, PDI, ZP, and % EE. Sample solutions were analyzed in triplicates (40).

2.7 Formulation and characterization of resveratrol and piperine loaded cubosomal gel (RPC-Gel)

For better skin applicability, the optimized RPC was formulated as RPC-Gel using Carbopol 934 (41). The RPC-Gel was prepared by directly incorporating carbopol 934 (1% w/v) into the optimized batch of RPC with constant stirring on a magnetic stirrer for 4 h. RV and PI gel (RP-Gel) was formulated to compare with RPC-Gel. The gel thus obtained was checked visually for its color, homogeneity, spreadability, and analyzed for its pH and viscosity. The drug content of the gel was determined by dissolving weighed, accurate quantity of RPC-Gel (0.1 g) in 10 mL of methanol. For complete solubilization of the drug, the solution was stirred at 500 rpm for 15 min and sonicated for 4 min. Finally, the solution was filtered using 0.45 μm syringe filter and

evaluated by HPLC after suitable dilution. The drug content was indicated in terms of percentage (42).

2.7.1 *Ex vivo* skin permeation and retention study

Ex vivo RV and PI permeation from RPC-Gel (equivalent of 0.5 mg of each RV and PI) through the skin of balb/c mice (25 ± 5 g) was carried out using PermeGear Franz diffusion cell with a diffusion surface area of 1.767 cm^2 and receptor chamber containing methanolic PBS (pH 6.4; 50:50, 12 ml, 37.0 ± 0.5 °C, and 100 rpm stirring). At specific time intervals, the aliquots (1 mL) were withdrawn and evaluated by HPLC. The withdrawn aliquots were replaced with the same volume of buffer to maintain sink conditions. The different parameters from the permeation study were estimated as follows.

$$\text{Flux(J)} = \text{quantity of RV and PI}\frac{\text{permeated}}{\text{time}}\text{X skin diffusion area} \text{----------(2)}$$

$$\text{Permeability coefficient (Kp)} = \frac{\text{J}}{\text{RV and PI concentration in donor compartment}} \text{--------(3)}$$

$$\text{Enhancement ratio (ER)} = \frac{\text{J of cubosomal gel}}{\text{J of the control (RP-gel)}} \quad \text{----------(4)}$$

At the end of study after 24h, the amount of RV and PI deposited within the skin was investigated. Briefly, the cut section of skin was homogenized (RQT-127A, Remi, India) with methanol and extracted for RV and PI. The final aliquot obtained was filtered (0.45 μm) and evaluated for RV and PI content using HPLC (35).

2.8 *In vitro* assays of RPC for targeting melanoma

Human melanoma (A375), mice melanoma (B16F10) and normal mouse fibroblast (L929) cell lines were procured from the National Centre of Cell Sciences, Pune, India.

Cells were grown in a mixture of Dulbecco's Modified Eagle Medium (DMEM), Fetal Bovine serum (FBS,10 %) and Pen step antibiotics (1 %) in CO2 incubator (Eppendorf, New Brunswick, Galaxy 170R, Germany) at 37 °C with 95% humidity.

2.8.1 *In vitro* cytotoxicity study

MTT (3-[4, 5-dimethylthiazol-2-yl]-2, 5-diphenyltetrazolium bromide) assay was used to measure the cytotoxic effects of resveratrol and piperine (RP), blank cubosome (BC), and optimized RPC on A375 and L-929 cell lines (43). Briefly, both cell lines were cultured in 96-well plates (6 x 10^3cells/well) and incubated for 24 h with DMEM media at 37°C with 95% humidity in CO_2 (5%) incubator. After 24 h, the media was discarded and replaced with fresh media with different concentrations of RP solution and optimized RPC (2.5 - 80.0 µg/mL) and the control were treated with equal volumes of media and BC without any test compound followed by incubation for 48 h. After the incubation period, the media from each well was discarded and the wells were gently washed with PBS. Subsequently, cells were treated with 20 µL of MTT solution (5mg/mL in PBS) and the plate was re-incubated at 37 °C for 4 h. After 4 h, the supernatant was discarded and dimethyl sufoxide (DMSO) (100 µL) was added to each well to dissolve the formazan crystals and analyzed by plate reader (Lisa Plus, India) to calculate the % cell viability.

2.8.2 Cell uptake studies by fluorescence microscopy

For qualitative cell uptake study, A375 cells were cultured in 6-well plates (5 x 10^4 cells/well) and incubated overnight. The cells were treated with coumarin–6 (C6) solution and coumarin–6-loaded cubosomes (C6-CUB) (equivalent to 1µg/mL of C6) for 3 h and 5 h of incubation. Cells were fixed with 4% paraformaldehyde (PFA) (Merck, India) and observed under a fluorescence microscope (44).

For quantitative cellular uptake analysis, A375 cells were incubated with equivalent concentrations of RP, and optimized RPC (equivalent to 10 µg/mL) at 37 °C and 5 % CO_2 for 5 h. After incubation, the media was discarded and the cells were washed four times with PBS and

lysed with 0.1% Triton X-100 followed by extraction with methanol for complete dissolution of RV and PI. Subsequently, centrifugation (10 min with 10,000 rpm) was performed, the cell lysate and supernatant obtained were used to analyze by HPLC (45).

2.8.3 Live and dead cell study and DAPI staining

A375 cells were seeded in 6-well plates (5 x 10^4 cells/well) in DMEM medium for 24h. The cells were treated with RP and optimized RPC (IC_{50}value) for 48 h, washed with PBS, and fixed with 4% PFA. Cells were then treated with ethidium bromide (EB) and acridine orange (AO) (each 5 µg/mL) for half an hour, and DAPI (0.1 mg/mL in PBS) for 10 min at 37^{o}C with 5% CO_2. Following incubation, the cells were washed with PBS for removing extra dye and the images of the cells were captured by fluorescence microscope (46).

2.9 *In vivo* evaluation of RPC-Gel

The animal experimental protocol was confirmed by the Committee for the Purpose of Control and Supervision of Experiments on Animals (CPCSEA) and the Institutional Animal Ethics Committee (IAEC), KLE College of Pharmacy, Belagavi, India (Ethical approval Letter No.: KLECOP/CPCSEA-Reg. No. 221/Po/Re/S/2000/CPCSEA/Res.26-13/10/2018). BALB/c male mice (25–30 g) were used for skin penetration, skin irritation and toxicity, and anticancer studies. The animals were housed in cages at room temperature (25 ± 3°C) and relative humidity of 30–70%, under 12 h-12 h light-dark cycle.

2.9.1 Skin irritancy and toxicity study

A skin irritancy test was performed to assess cubosomal gel compatibility with BALB/c mice skin. Two groups were made with three mice each. The first and second groups received applications of the RPC-Gel and marketed gel (Flonida 5%), respectively. This test was performed to confirm the cubosomal gel compatibility with the skin. Topical dose (equivalent to

20 µg of each of RV and PI) was applied to the left ear of the mouse using medical spatula with right ear as control. Observation was done every 7 days to check for erythema occurrence, which indicates cutaneous vascular dilatation. The average score obtained from the scoring scale of each day and finally the data interpretation was done as per Uttley and Van Abbe (1973) scoring method (47). Acute or sub-acute toxicity of the above gels were evaluated as per the procedure reported by Draize et al. (1944) (48). The first group was kept as sham control (no treatment) whereas the second group served as positive control (20% sodium lauryl sulfate [SLS] solution). The third and fourth groups had been applied with RPC-Gel and marketed gel locally, respectively. Daily application was done on the same area of mice. Grading of erythema and edema was done based on the scale of 0–4 at 1, 24, 48, and 72 h for the toxicity assessment (49). The application of gel was continued for 28 days after which the mice were sacrificed, and the treated skin part was collected and was processed for histopathological examination to check the toxicity of the developed RPC-Gel formulation (50,51).

2.9.2 *In vivo* anticancer study

Before injection of cells, the skin on the dorsal surface of the BALB/c male mice (25-30g) was shaved. Melanoma was induced in BALB/c male mice by injecting B16F10 cells (5×10^5) subcutaneously on the dorsal part (right side) of the mice (34,52). The experimental mice were divided into six groups, each group with six mice (Table 4). The application of formulation was continued up to the 6^{th} week. The tumor volume and body weight was measured on each week using a Vernier caliper and digital weighing balance respectively (53). Tumor volume was used as a parameter for tumor inhibition in anti-tumor activity (54) and it is calculated by following equation.

$$\text{Tumor volume} = \frac{[\text{length} \times (\text{width})^2]}{2} \quad \text{----------(5)}$$

Table 4: The experimental design for *in vivo* anticancer study

Group	Treatment	Animals required
I **Normal control**	Normal control- mice fed with standard diet	6
II **Carcinogen control**	Carcinogen control - subcutaneous (s.c.) injection of B16F10 cells (5×10^5)	6
Prophylactic treatment [From 1st day of s.c. injection of B16F10 cells (5×10^5)]		
III **Marketed Gel**	Carcinogen control + simultaneous application of Marketed Gel (Flonida 5%; equivalent to 50 mg/kg of 5-Flurouracil) – Daily	6
IV **RPC-Gel**	Carcinogen control + simultaneous application of RPC Gel (equivalent to 50 mg/kg of RV and PI) – Daily	6
Therapeutic treatment [Starting from 14th day of s.c. injection of B16F10 cells (5×10^5)]		
V **Marketed Gel**	Carcinogen + Marketed Gel (Flonida 5%; equivalent to 50 mg/kg of 5-Flurouracil) – Daily	6
VI **RPC-Gel**	Carcinogen + RPC gel (equivalent to 50 mg/kg of RV and PI) – Daily	6

2.9.3 Histopathological analysis

At 7th week, mice from each groups were sacrificed, the tumor tissues were removed and fixed with 10% formalin. Sections of the tumor tissues were stained with hematoxylin –eosin (H & E stain) dye and the images were observed under the light microscope (Olympus, Delhi).

3. Statistical analysis

The optimization of the RPC nanoformulations was accomplished using Design-Expert® software (Stat-Ease Inc., MN, USA). The Analysis of variance (ANOVA) was used to confirm the significance of the model and model terms. The statistical analysis of *in vitro* and *in vivo* studies was performed using GraphPad Prism software (GraphPad Software Inc., CA, USA).

4. RESULTS

4.1 HPLC method development of RV andPI

The UV spectra of methanolic solutions of drugs (10 µg/ml) were obtained in the range of 200–400 nm, in which RV exhibited maximum absorption at 306 nm while PI at 341 nm. Based on the UV spectra, detection wavelength 330 nm was selected as an isosbestic point, where both the drugs show maximum absorption (Figure 8).

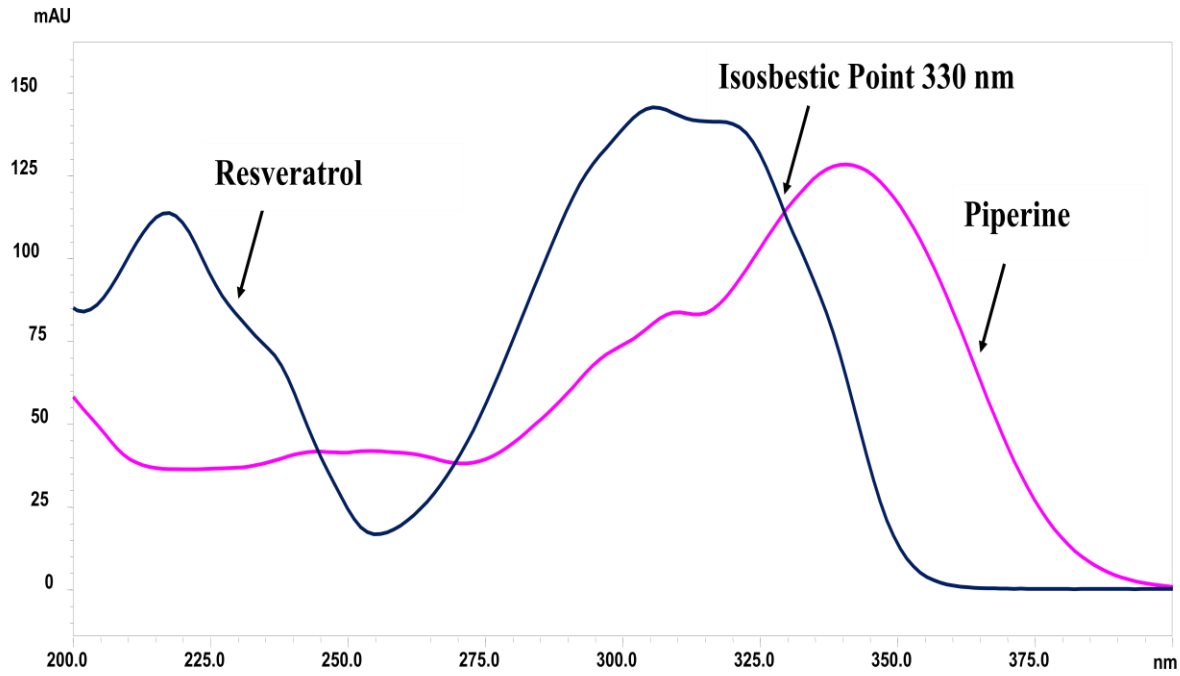

Figure 8:UV spectra of resveratrol (RV) and piperine (PI) showing an isosbestic point

HPLC analysis was performed in simultaneous for RV and PI and the retention time was found to be 3.3 and 9.19 min at 330 nm respectively. The HPLC chromatogram for methanolic solution of RV and PI and both the drugs loaded in the cubosome (RPC) were shown in Figure 9.The system suitability parameters were found to be within the acceptance limits; relative standard deviation of the peak area (% RSD<2.0%), tailing factor (T<2.0) and number of theoretical

plates (N>2000). The regression analysis data for the calibration curve shows linear relation over the concentration range of 0.25–8 µg/mL for RV and PI. The correlation coefficient (R^2) value was found to be > 0.999. The regression equation for RV and PI calibration curve was y = 77001x + 2858 and y =63831x – 4212 respectively (Figure 10). The % RSD values for intraday precision was ranged between 0.14-0.49% (for RV) and 0.24-0.77% (for PI) and for interday precision were ranged from 0.49-1.96% (for RV) and 0.63-1.96% (for PI). The mean percentage recovery of RV and PI were ranged between 98.06-101.47% and 98.51-101.74% respectively. The LOD and LOQ values were 0.02 and 0.08 µg/ml for RV and 0.04 and 0.11µg/ml for PI respectively. The slight variation in the flow rate, and mobile phase composition has insignificant effect on the chromatographic parameter such as % RSD of the retention time (<2.0%).

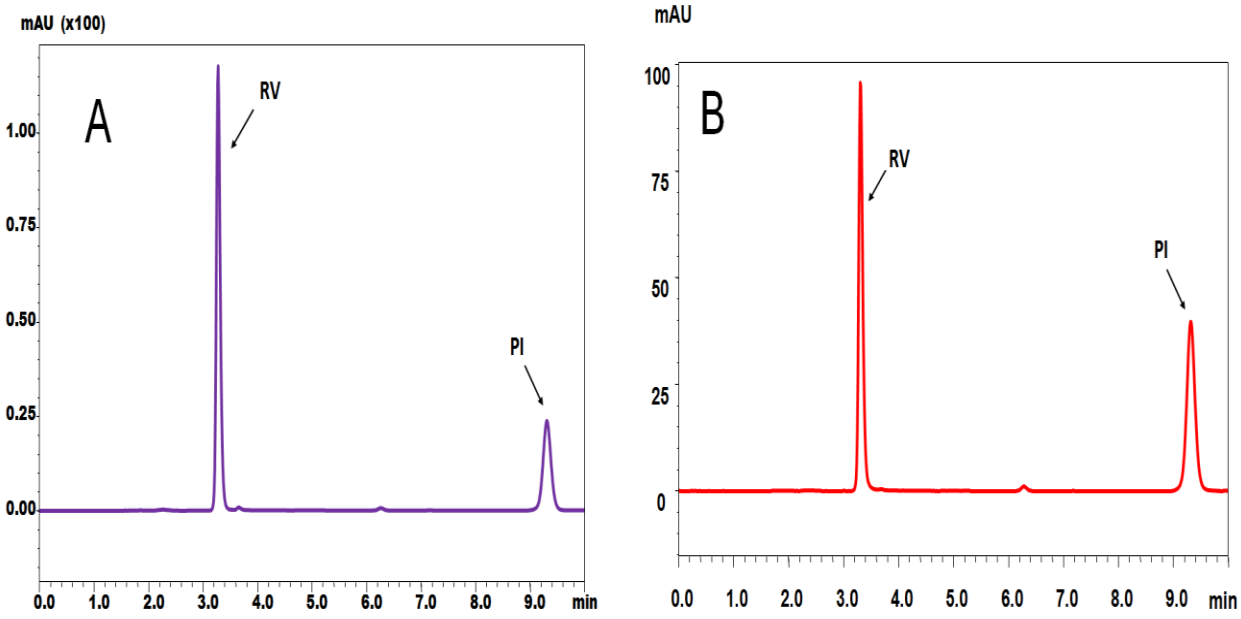

Figure 9: HPLC Chromatogram of methanolic solution of Resveratrol (RV) and Piperine (PI) (A) and both drugs loaded in the cubosome (B)

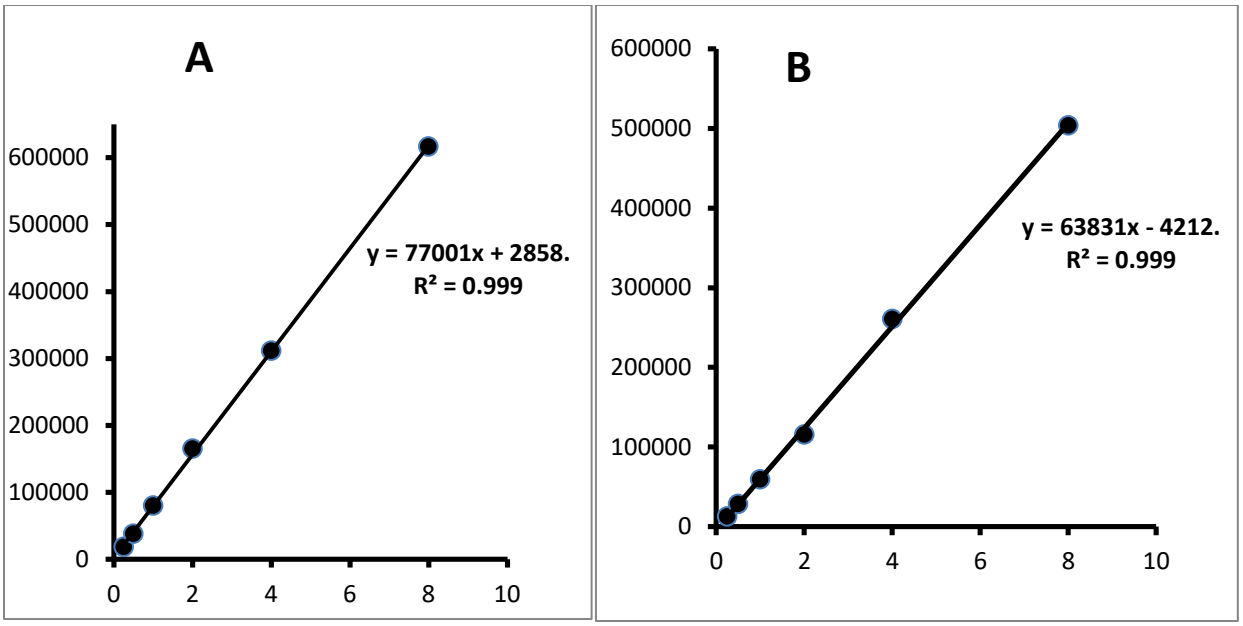

Figure 10: Linearity of chromatograms (A) Resveratrol (RV) and (B) Piperine (PI)

4.2 Preparation, optimization and characterization of RPC

RPC was prepared using high speed homogenization followed by probe sonication method. Since it is observed that lipid and stabilizer concentration are two most important factors governing performance properties of cubosome namely PS, and % EE. A 3^2 full factorial design was employed to yield an optimized formulation. The factor combination and performance properties of cubosome formulation batches are listed in Table 5.

Table 5: Observed responses from 3^2 factorial design of RPC formulation batches

Batch	Independent variables				Dependent variables			PDI	ZP (mV)
	X1	X2	X1 (% w/w)	X2 (% w/w)	Y1 (nm)	Y2 (%) RV	Y2 (%) PI		
RPC1	-1	-1	3	0.5	144 ± 6.25	60.07 ± 1.21	58.98 ± 0.85	0.13 ± 0.04	-31.1 ± 0.17
RPC2	-1	0	3	1	113 ± 4.19	65.19 ± 1.14	65.03 ± 0.15	0.17 ± 0.07	-26.5 ± 0.53
RPC3	-1	+1	3	1.5	99 ± 2.16	67.0 ± 0.85	69.10 ± 0.85	0.24 ± 0.14	-28.1 ± 0.55
RPC4	0	-1	5	0.5	143 ± 4.09	72.83 ± 0.75	72.22 ± 0.98	0.28 ± 0.15	-31.6 ± 0.29
RPC5	**0**	**0**	**5**	**1**	**110 ± 3.30**	**88.12 ± 1.54**	**85.17 ± 0.25**	**0.16 ± 0.07**	**-34.3 ± 1.04**
RPC6	0	+1	5	1.5	102 ± 1.25	82.30 ± 1.35	80.37 ± 0.75	0.32 ± 0.11	-24.9 ± 1.67
RPC7	+1	-1	7	0.5	160 ± 3.74	49.87 ± 0.25	48.13 ± 0.32	0.28 ± 0.13	-49.7 ± 0.96
RPC8	+1	0	7	1	149 ±2.49	59.03 ± 0.95	56.27 ± 0.55	0.21 ± 0.09	-32.2 ± 0.26
RPC9	+1	+1	7	1.5	134 ± 2.16	63.90 ± 0.79	58.30 ± 0.36	0.29 ± 0.11	-40.1 ± 1.10

mean ± SD, (n=3), X1 - GMO (% w/w), X2 – Pluronic F127 (%w/w), Y1 - Particle size (nm), Y2 - Entrapment efficiency (%), PDI – Polydispersibility index, ZP- Zeta potential (mV)

4.2.1 Particle size analysis

Mean PS of formulated RPC ranged between 99-160 nm (Table 5). The polynomial equation 6 generated from the Design-Expert® Software shows the effect of independent variables on the particle size of RPC.

$$PS = +113.89 + 14.33\,X_1 - 18.67X_2 + 4.75\,X_1X_2 + 14.67{X_1}^2 + 6.67{X_2}^2 \text{------- (6)}$$

Where PS is particle size, X_1 and X_2 is GMO and PF-127 concentration (%w/w), respectively.

The effect of GMO (X_1) and PF-127 (X_2) on the particle size is illustrated in Figure 11A and 11D. The equation and graph shows that the GMO concentration was directly proportional with particle size whereas PF-127 concentration was inversely correlated to it.

4.2.2 Analysis of entrapment efficiency (EE)

EE is an important parameter used to determine drug delivery capability of cubosome nanoformulation. The EE was found to be in the range of 49.87 - 88.12 % and 48.13 - 85.17 % for RV and PI respectively as shown in Table 5. The polynomial equation 7 and 8 shows the effect of independent variables on the EE of RV and PI respectively.

$$EE = +84.22 - 3.33\,X_1 + 4.83\,X_2 - 1.50X_1X_2 - 20.33{X_1}^2 - 4.83{X_2}^2 \ldots\ldots\ldots\ldots (7)$$

$$EE = +81.89 - 5.17\,X_1 + 4.67\,X_2 - 0.000X_1X_2 - 19.83{X_1}^2 - 4.33{X_2}^2 \ldots\ldots\ldots\ldots (8)$$

The effect of GMO (X_1) and PF-127 (X_2) on the EE is illustrated in Figure 11B, C, E and F. The equation and graph shows that the PF-127 concentration was directly proportional with % EE whereas GMO concentration was inversely proportional to it.

The results obtained for all cubosome formulation batches were simultaneously fitted to the different polynomial models using theDesign Expert® Software to obtain the best suitable model. Based on the results, the quadratic model was observed as best-fit model (Table6). The quadratic model has given the high values of multiple correlation coefficients (R^2).The PRESS values for quadratic model were small compared to the other polynomial models. For both response variables, the predicted R^2 is in reasonable agreement with the adjusted R^2 that means the difference is less than 0.2 (Table 6).

Table 6: Summary of results of regression analysis for dependent variables

Models	SD	R^2	Adjusted R^2	Predicted R^2	PRESS	Remark
Response 1: Particle size						
Linear	10.67	0.8294	0.7725	0.6423	1433.28	
2FI	10.89	0.8519	0.7631	0.4093	2367.06	
Quadratic	4.97	0.9815	0.9506	0.8146	742.81	**Suggested**
Response 2 (a): Entrapment efficiency of RV						
Linear	0.74	0.2043	-0.0609	-0.5752	6.43	
2FI	0.80	0.2155	-0.2552	-2.0268	12.35	
Quadratic	0.18	0.9763	0.9369	0.8137	0.76	**Suggested**
Response 2 (b): Entrapment efficiency of PI						
Linear	11.89	0.2552	0.0070	-0.4636	1667.84	
2FI	13.03	0.2552	-0.1917	-1.8584	3257.26	
Quadratic	2.85	0.9785	0.9428	0.8293	194.51	**Suggested**

SD-Standard deviation, PRESS-Predicted residual error sum of square, 2FI-Two-factor interaction, R^2: multiple correlation coefficients

The ANOVA results for the suggested quadriatic model mentioning an adequate precision, which measures the signal to noise ratio, was found to be 16.254 for PS and 12.907 and 14.731 for % EEof RV and PI respectively, which is >4 considered as desirable.

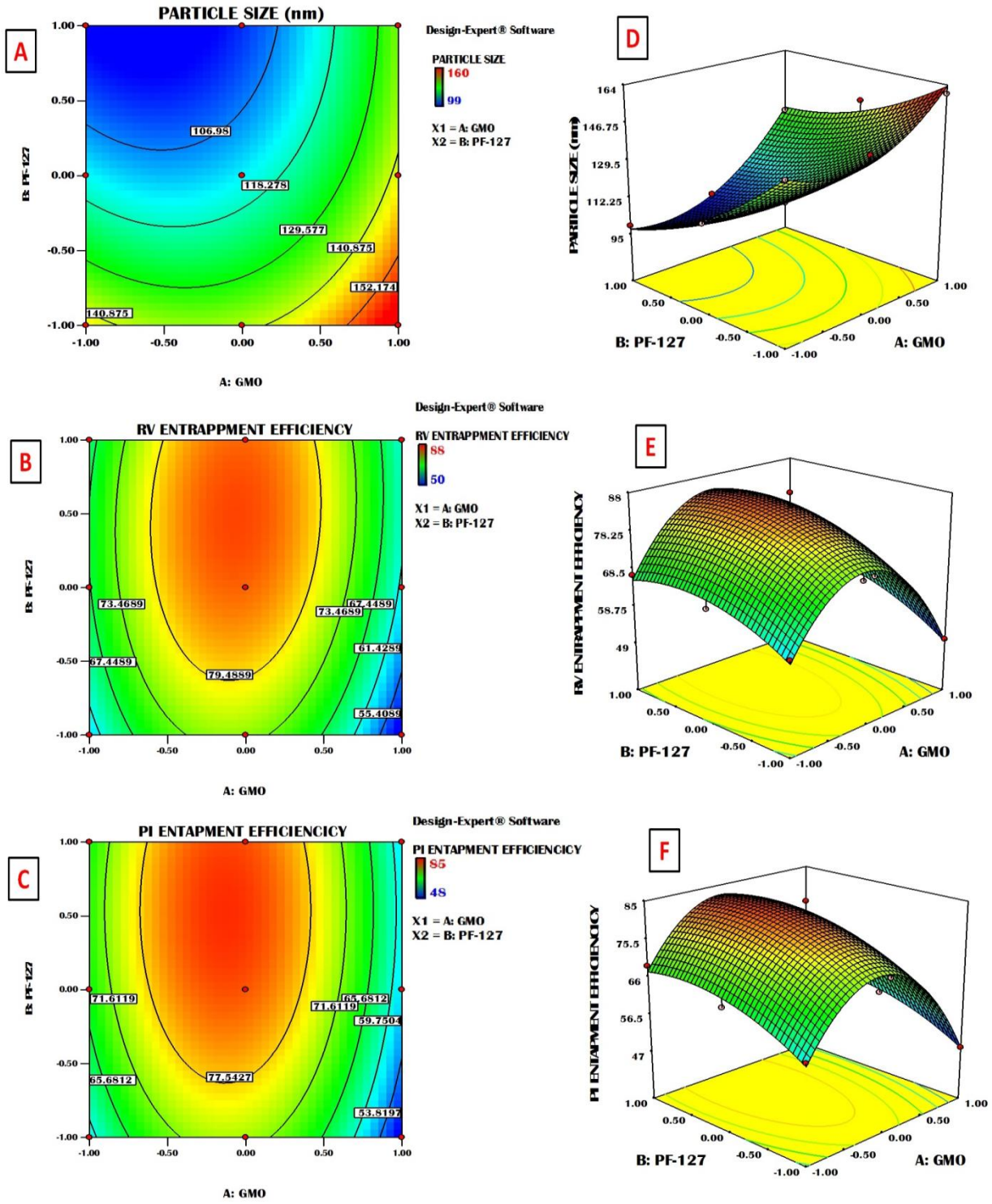

Figure 11:2D-contour (A, B, C), 3D-response surface (D, E, F) displaying the effect of GMO and PF-127 on particle size, and EE of RPC formulations.

4.2.3 Selection of optimized cubosomal dispersion

The optimized cubosome batch was selected from the nine cubosome formulations based on the requirement of maximum entrapment efficiency and lowest particle size. Based upon the results obtained for dependent variables, RPC5 batch having the concentrations of GMO (5 % w/w) and PF-127 (1% w/w) was selected for further evaluation studies, as it is having maximum EE (88.12% and 85.17% for RV and PI respectively) with less particle size (110 nm). The optimized cubosome batch (RPC5) was used for further evaluation studies.

4.3 Characterization of cubosomes

4.3.1. ZP and PDI

The ZP and PDI values ofall RPC batches are shown in Table 5. The ZP and particle size distribution of optimized cubosome batch (RPC5) were shown in Figure 12. The PDI of all prepared RPC nanoparticles ranged between 0.13-0.32, indicating the narrow homogeneous particle size distribution. The ZP was found to be in the range of -24.9 to -49.7mV (Table 5).

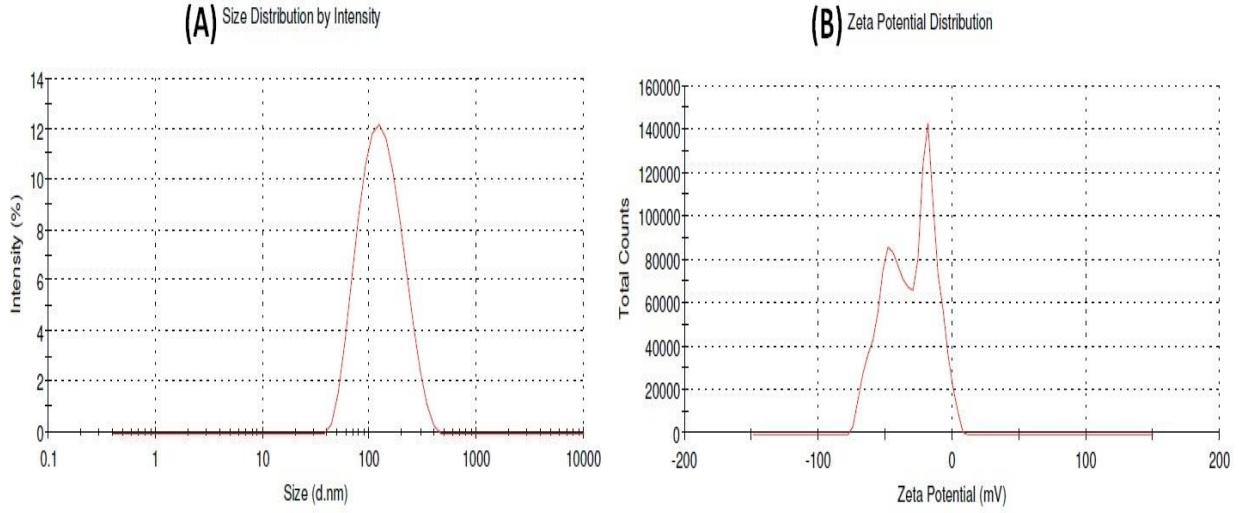

Figure 12:Particle sizedistribution (A), and ZP (B) of optimized cubosome formulation (RPC5)

4.3.2. FTIR spectrum analysis

The infrared spectra of RV, PI, GMO, PF-127, and RPC5 are shown in Figure 13.

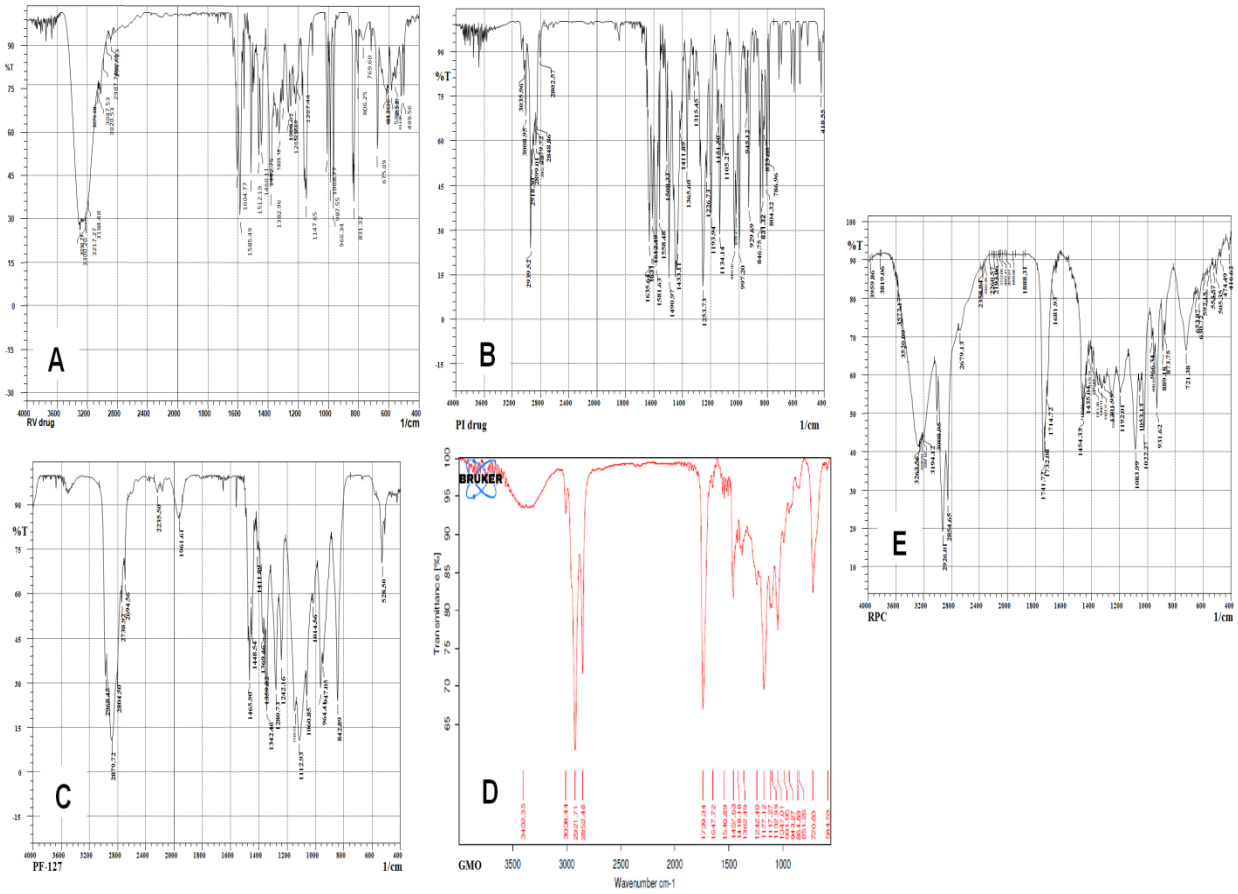

Figure 13: FTIR spectra of RV(A), PI (B), PF-127 (C), GMO (D), and RPC5 (E)

The FTIR peak values of RV displayed at the wave numbers of 3300 and 1512 cm^{-1}, for –OH and C=C functional group respectively, whereas, PI displayed at the wave numbers of 1635 and 1508 cm^{-1}, for C=O and C=C functional group respectively.

FTIR spectra of GMO represents the peak at the wave numbers of 1739 and 3402 cm^{-1} for C=O and –OH functional group respectively, while PF-127 at 1465, 1342, 2968, and 342cm^{-1} for C=O, C=C, –OH , -CH_3 functional group respectively.

The FTIR spectra of the RPC5 exhibited all the major characteristic peaks with slight shifting for GMO and PF-127, representing the absence of any interaction between the RV and PI with these excipients. Similarly, RPC5 spectra showed slightly shifted but reduced characteristics peaks of RV and PI which indicates the entrapment of RV and PI in the cubosomes nanoparticles.

4.3.3. TEM analysis

The surface morphology and structure of optimized RPC nanoformulation (RPC5) was evaluated and confirmed by high resolution transmission electron microscopy (HR-TEM) imaging. These cubosome particles appeared to be cubic, uniform, smooth surface with less curvature (Figure 14A and B). The scattered particles are in the nano range. A random selected area electron diffraction (SAED) pattern of RPC nanoparticles indicated the brightness nature surrounding to centrally placed lid, which exhibits crystalline nature for the cubosome nanoparticles (Figure 14C).

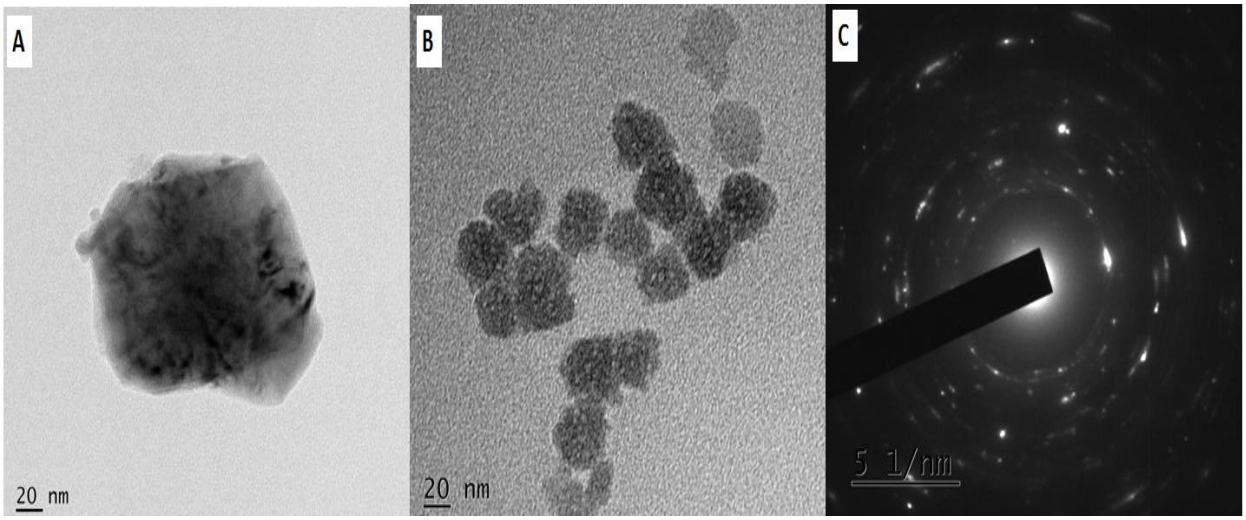

Figure 14:HR-TEM (A and B) and SAED (C) images of optimized cubosome nanoparticles (RPC5)

4.3.4. DSC Analysis

The DSC curves of pure RV, PI, GMO, PF-127, mannitol and optimized-RPC (RPC5) are shown in Figure 15. The DSC thermogram of pure RV and PI (figure 15B and A), demonstrated a sharp endothermic peak at 269.39 °Cand 132.34 °C respectively corresponding to its melting temperature, such sharp peak indicates the crystalline state of the drug. The lipid GMO exhibit a common feature of temperature dependent phase transition which shows endothermic peak at 33.21 °C (figure 15C), whereas the stabilizer PF-127 (figure 15E) showed endothermic peak at 59.81 °C due to its melting. Mannitol which was used as cryoprotectant to obtain the freeze dried powder of RPC had shown a sharp endothermic peak at 176.70 °C (figure 15D).

In the DSC thermogram of RPC5 (figure 15F), the lower shift of mannitol endothermic peak was detected at 158.11 °C, due to the formation of bicontinuous structures in the cubosome nanoformulation. In the same DSC thermogram of RPC5, the RV and PI sharp peaks were completely disappeared, indicating its conversion to the non-crystalline state. These results suggest that the RV and PI were molecularly encapsulated in the bicontinuous structure of the cubosome.

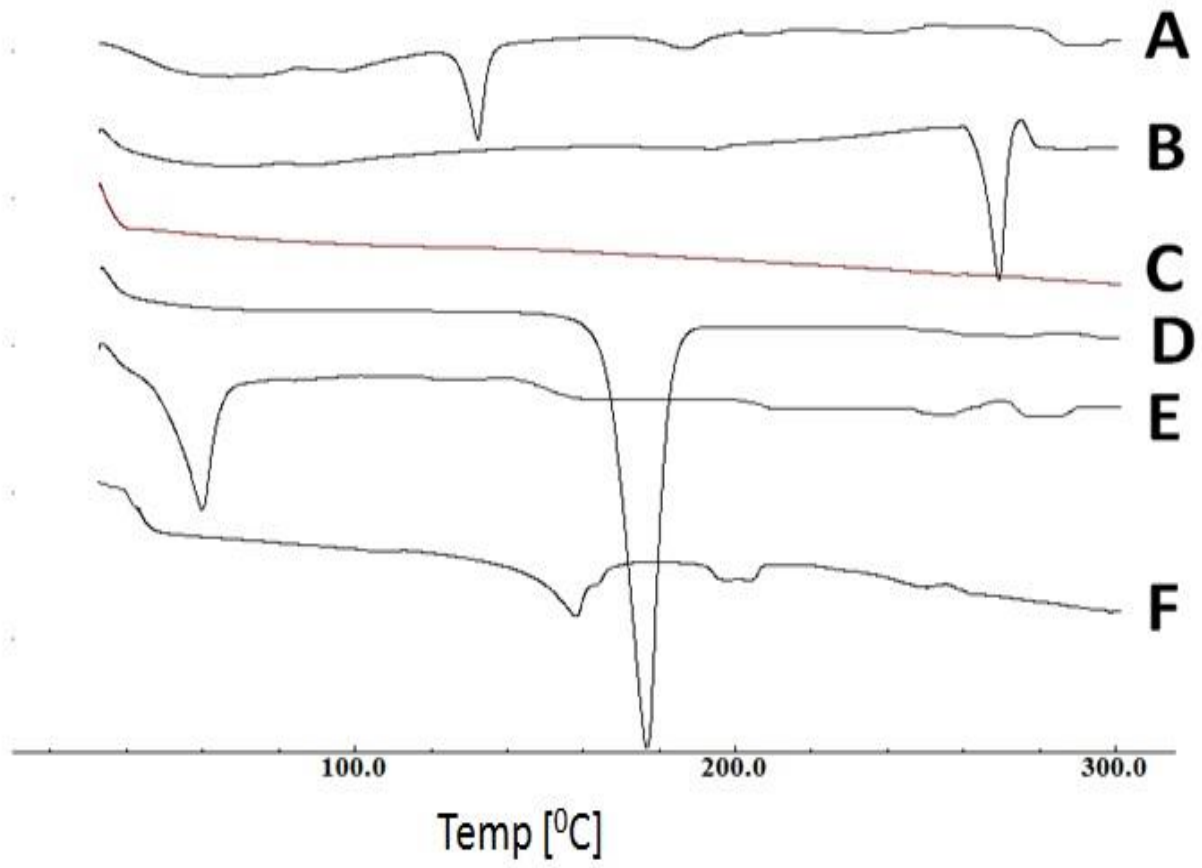

Figure 15:DSC thermogram of PI (A), RV (B), GMO (C), Mannitol (D), PF-127 (E), and RPC5 (F).

4.3.5. XRD study

XRD patterns of pure RV, PI, RPC5 and BC are shown in Figure 16. The diffractogram of the pure RV and PI exhibited characteristic specific sharp crystal peaks at diffraction angles (2θ) of 16.34, 19.14, 22.31, 28.24 and at 14.15, 22.52, and 25.80 respectively, indicating their crystalline nature. However, these high intensity peaks of RV and PI disappeared in the X-ray diffraction pattern of RPC5. Moreover, the powder X-ray diffraction pattern for the RPC5 was without any remarkable difference when compared to the powder X-ray pattern for BC. These results follow

the DSC findings which indicates that the RV and PI was molecularly dispersed or in non-crystalline state when incorporated into the bicontinuous structures of cubosome.

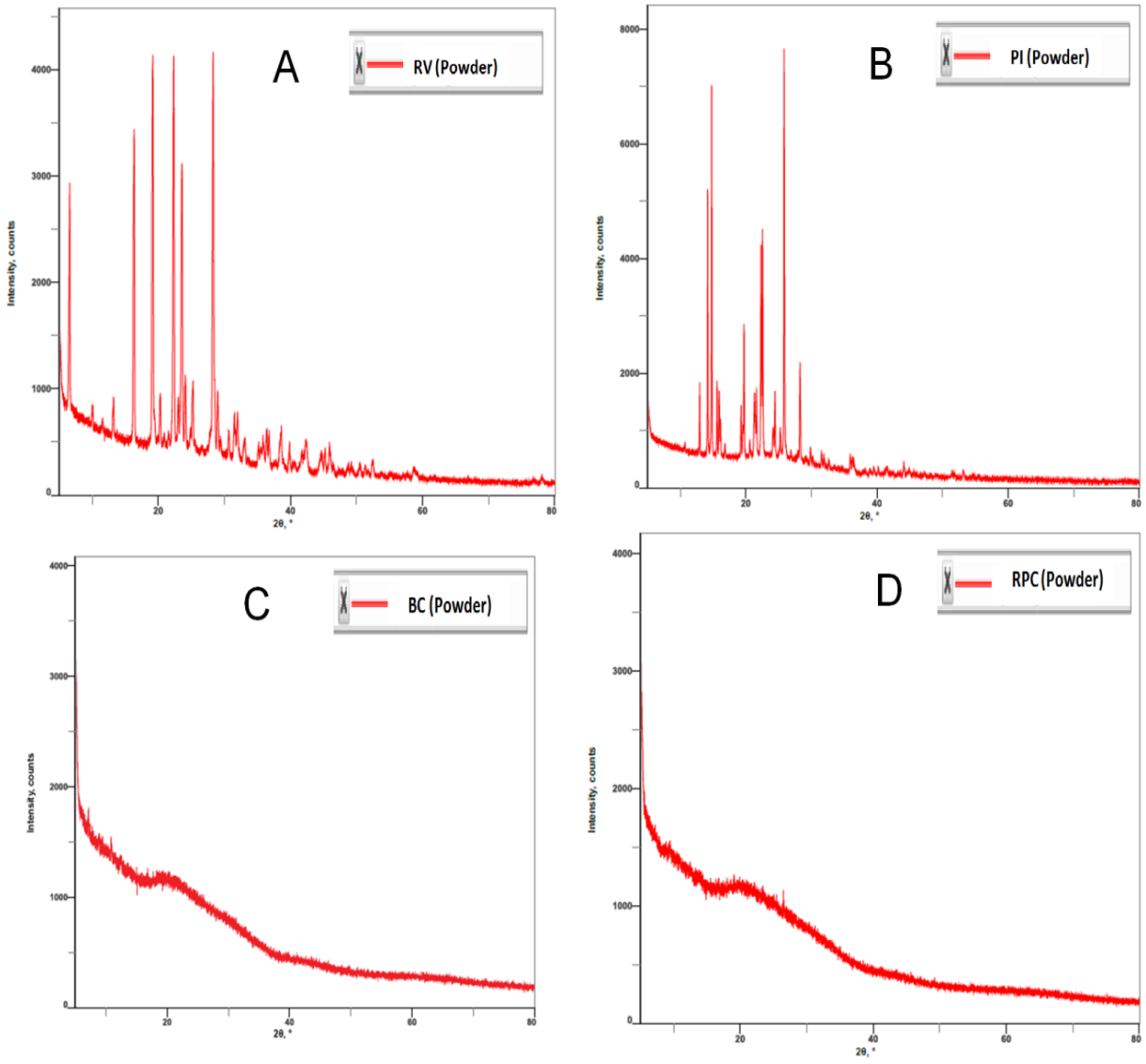

Figure 16:XRD patterns of RV (A), PI (B), BC (C), and RPC5 (D).

4.3.6. pH value measurement and rheological behavior for RPC

The pH values and viscosities of all cubosome batches are listed in table 7. The pH values for all RPC batches were found to be in the range of 5.64 to 6.78. The cubosome formulations showed viscosity values that ranged from 3.57 to 19.97cP. Increasing the amount of GMO and PF-127 in

the RPC nanoformulations led to the formation of more liquid crystal-like materials that increased the formulation viscosity.

Table 7: pH values and viscosities of RPC nanoformulations

Formulation Code	pH	Viscosity (cP)
RPC1	5.64 ±0.04	3.57 ±0.04
RPC2	6.12 ±0.04	3.85 ±0.04
RPC3	6.46 ±0.06	3.65 ±0.05
RPC4	6.96 ±0.05	7.82 ±0.07
RPC5	6.43 ±0.07	7.97 ±0.05
RPC6	6.69 ±0.04	8.09 ±0.06
RPC7	6.72 ±0.09	15.06 ±0.08
RPC8	6.80 ±0.08	17.79 ±0.09
RPC9	6.78 ±0.09	19.97 ±0.06

Values represent mean ± SD (n=3)

4.3.7. Drug release study

The *in vitro* drug release profile of RV and PI from cubosome and their solution are represented in Figure 17. The release study of RV and PI from the optimized batch of RPC nanoformulation (RPC5) and RV and PI (RP) solution in phosphate buffer pH 6.8 containing Tween 80 was evaluated by the tablet dissolution testing apparatus equipped with low volume conversion kit. A rapid and complete release of RV and PI from RP solution was obtained in 12 h. Generally, the bicontinuous cubosome nanoformulations shows a biphasic burst release with a release mechanism of diffusion from the cubic-phase matrix structure (1). The RV and PI drug release from the cubosome was biphasic, with an initial burst release of approximately 22.43% and

16.40% respectively in 1 h, followed by sustained prolonged drug release was observed up to 24 hr (Figure 17).

After fitting the results of dissolution study of RPC5 with the different release kinetic models, Higuchi model had shown the best fitting with the highest R^2 of 0.923 and 0.936 for RV and PI respectively.

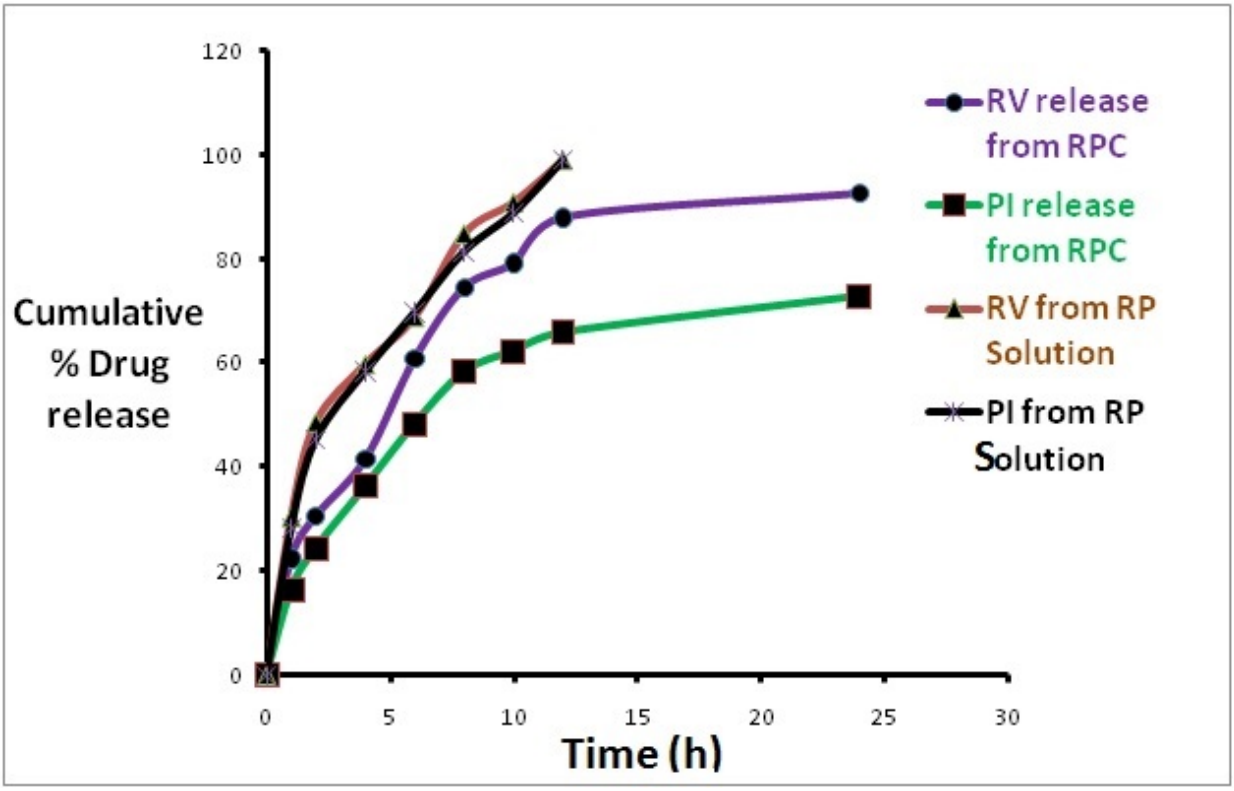

Figure 17: *In vitro* release profiles of RV and PI from aqueous solution (RP solution) and optimized batch of cubosomes (RPC5) (mean±SD, n=6).

4.4 Stability study

The optimized cubosome dispersion was studied for the stability study stored for 3 months at room temperature and were characterized for the PS, PDI, ZP, EE, and % drug release. The results are summarized in the table 8.

Table 8: Results showing characterization of optimized cubosomal dispersion at 0 month and after 3 months stored at Room Temperature

Optimized RPC batch (RPC5)	PS (nm)	%EE		PDI	ZP (mV)	%Drug release	
		RV	PI			RV	PI
0 month	110 ±3.3	88.12±1.54	85.17±0.25	0.16±0.07	-34.3±1.04	92.7±2.08	72.48±3.36
3 months	120 ±7.23	86.23±0.72	84.05±0.34	0.19±0.09	-34.55±1.51	95.49±1.40	75.08±3.54

mean ± SD (n=3).

PS- Particle size, EE- Entrapment efficiency, PDI- Polydispersibility index, ZP- Zeta potential, RV- Resveratrol, PI- Piperine

4.5 Formulation of RPC-Gel

The cubosomal gel was formulated from the optimized batch (RPC5) of cubosome dispersion (equivalent to 0.1% w/v of RV and PI) by directly dispersing Carbopol (1% w/v) as gel former. Methyl paraben (0.05 % w/v) was incorporated as preservative in RPC-Gel. Visual appearance, spreadability, and clarity of prepared cubosomal gel were observed for the presence of any particulate matter. SimpleRP-Gel was formulated by dispersing RV and PI (each 0.1% w/v)into Carbopol dispersion (1% w/v).

4.6 Characterization of cubosomal gel (RPC-Gel)

Various parameters of the RP-Gel and RPC-Gel were evaluated, and the results were mentioned in Table 9.

Table 9: Characterization of RPC- Gel and RP- Gel

Formulation	pH	Viscosity (cP)	Drug content (%)	
			RV	PI
RPC-Gel	6.79 ± 0.09	145.9 ± 0.9	97.53 ± 1.39	99.28 ± 1.43
RP- Gel	4.25 ± 0.08	110.2 ± 0.8	86.77 ± 1.68	90.72 ± 1.19

mean ± SD (n=3).

Both the prepared gels were found to be white, viscous creamy formulations with a smooth and homogenous appearance and pH value were found to be 6.79 and 4.25 for the RPC-Gel and RP-Gel, respectively. RP-Gel has slightly acidic pH compared to RPC-Gel, due to the Carbopol content which can decreases the pH of the RP-Gel, whereas, in addition to Carbopol, the GMO and PF-127 may stabilize the pH of RPC-Gel. The viscosity of the gel formulation was determined by using Brookfield viscometer, which was found to be 110 and 145 cP for RP- and RPC-Gel, respectively. The drug content of the RPC-Gel was found to be 97.53% and 99.28 % for RV and PI respectively, which showed that the RPC nanoparticles were uniformly and properly distributed in the gel formulation.

4.6.1. *Ex vivo* skin permeation and retention studies

The *ex vivo* skin permeation and retention of RV and PI across the hair removed mouse skin was carried out using a Franz diffusion cell apparatus. The RPC-Gel was compared with RP-Gel for cumulative amount of drug permeated for 24 h, transdermal flux, permeability coefficient, amount of drug deposited and enhancement ratio, and the results are depicted in Table 10.

The results indicate that the cumulative amount of RV and PI permeated from the RPC-Gel was 176.35 and 148.97 µg/cm^2 andthat of from RP-Gel was 34.12 and 28.54 µg/cm^{2}respectively. Permeation flux value for RPC-Gel was found to be 4.15 and 3.51 µg/cm^2/h whereas the RP-Gel

showed the value of 0.80 and 0.67 µg/cm^2/h for RV and PI respectively. Furthermore, the permeability coefficient and enhancement ratio for RPC-Gel was found to be higher than RP-Gel. The amount of RV and PI deposited in the skin were 10.36 and 11.47 µg/cm^2 respectivelyfor RPC-Gel which was considerably higher than RP-Gel.

Table 10: Result of *ex vivo* skin permeation and retention study of the RPC-Gel and RP-Gel

Formulation	Drug	Cumulative amount permeated (µg/cm^2)	Permeation flux (J,µg/cm^2/h)	Permeability coefficient (Kp, cm/h)	Enhance-ment ratio	Quantity of skin deposition (µg/cm^2)
RPC-Gel	RV	176.35±1.47	4.15 ± 0.03	11.19 ×10^{-3}	5.18	10.36 ± 0.77
	PI	148.97±1.16	3.51 ± 0.03	9.45 ×10^{-3}	5.23	11.47 ± 0.93
RP-Gel	RV	34.12 ± 1.93	0.80 ± 0.05	2.16 ×10^{-3}	1.0	9.15 ± 0.98
	PI	28.54 ± 1.41	0.67 ± 0.03	1.81 ×10^{-3}	1.0	8.69 ± 0.90

mean ± SD (n=3)

4.7 *In vitro* assays of RPC for targeting melanoma

4.7.1 *In vitro* cytotoxicity study

The *in vitro* cytotoxicity of pure RV and PI drugs (RP solution), BC, and optimized RPC were investigated against the L929 and the A375 cell lines over a period of 48h by MTT viability assay at different drug concentration (2.5 - 80.0 µg/ml). The viability of the L929 cells treated with different drug concentrations (Figure 18B) of different formulations remained in the range of 95-100% related to the untreated cells. The results obtained showed that BC does not have any cytotoxic effects to both L929 and A375 cells, which demonstrate their cytocompatibility and

significance as a bio-nanomaterial for targeting melanoma (Figure 18A and 18B). The RP solution and RPC have also does not shown cytotoxicity against normal L929 mouse fibroblast. Both RP solution and RPC showed no significant difference in cell viability which confirms its cytocompatibility (Figure 18B). But, in case of A375 human melanoma cells treated with RP solution and RPC, we found a significant reduction of cell viability in a concentration dependent manner (Figure 18A), where RPC demonstrated significantly higher cytotoxicity against A375 cells when compared to RP solution. The half maximal inhibitory concentration (IC_{50}) values of RP solution and RPC were found to be 51.75 and 17.04 µg/ml respectively. The enhanced cytotoxic activity of RPC in comparison to RV and PI solution could be because of enhanced uptake of cubosome nanoparticles by A375 cells.

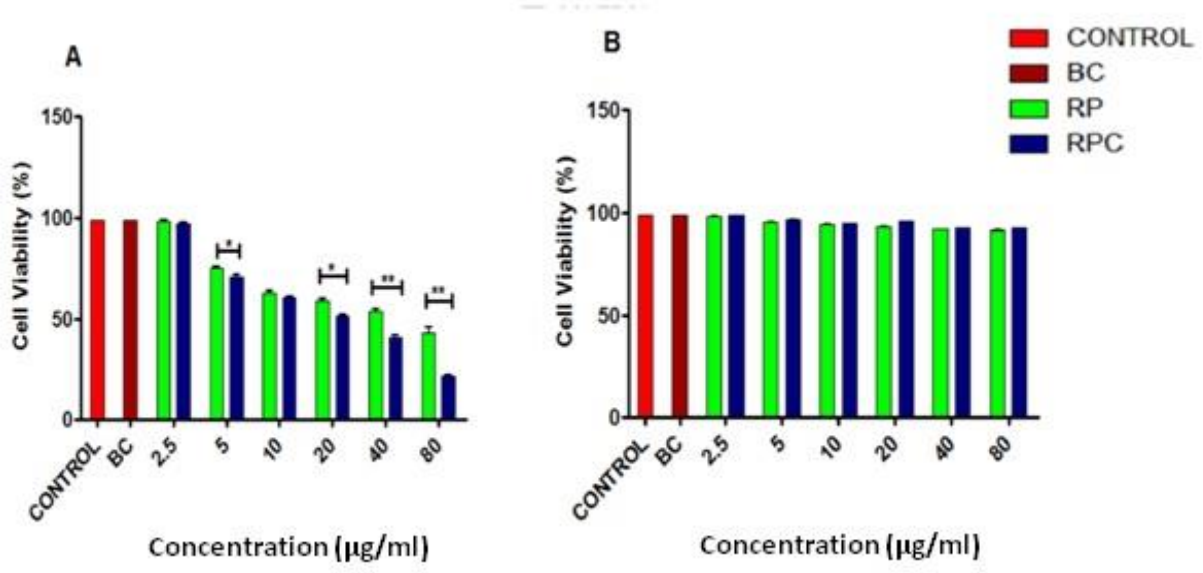

Figure 18: *In vitro* cytotoxicity of RP solution, Blank cubosome (BC), and Optimized RPC were investigated against the A375 human melanoma (A) and L929 mouse fibroblast (B) cell lines.

4.7.2 Cell uptake studies by fluorescence microscopy

Cellular uptake efficiency was evaluated by HPLC and fluorescence microscopy method for quantitative and qualitative methods, respectively (56). The cells treated with C6 solution showed no fluorescence up to 3 h (Figure 19A). Whereas, the cells under treatment with C6-CUB have shown maximum fluorescence intensity than that of C6 at the end 3 and 5h treatment period (Figure 19A-D), suggesting the enhanced cellular internalization of C6-CUB into the melanoma cells as compared to C6 solution. For the quantitative estimation of cell extract after 5 h treatment, the HPLC analysis showed 48.16 ± 8.30 % and 76.30 ± 7.42% for RV and 45.16 ± 8.30 and 79.30 ± 7.42% for PI, the cellular internalization of resveratrol and piperine (RP) drug solution and RPC, respectively.Bar graph representing (quantitative cell uptake) maximum cellular uptake of RPC in A375 cells compared to RV and PI solution at the end of 5 h of incubation evaluated by HPLC ($p<0.01$; Figure 19M).

4.7.3 DAPI staining and Live and Dead cell assay

The apoptotic profile of RP drug solution and RPC nanoformulation on A375 cells was evaluated qualitatively after 48 h of exposure using fluorescent microscope. The normal intact nuclei with blue DAPI staining have been reported by untreated cells and the cells on treatment with BC (Figure 19E-F). The cells treated with drug solution and RPC had shown nuclear blebbing, fragmentation and small apoptotic bodies which are the evidences of apoptotic induction. In comparison to non-treated and BC treated cells, it was found that drug solution and RPC nanoformulation induced apoptosis in human melanoma cells. (Figure 19G-H).

The AO/EB dye mixtures were used to stain live and dead A375 cells on treatment with BC, drug solution and RPC. Figure 19I-J reveals that untreated A375 cells and cells on treatment with BC showed green fluorescence due to penetration of AO into the live cells through intact cell

membranes.After the incubation (48 h) of cells with IC_{50} concentrations of drug solution and RPC, the cells exhibited orange-to-red nuclear staining, with EB entering through ruptured cell wall membranes of dead cells which causes nuclei condensation and apoptotic bodies, suggesting significant cell death (Figure 19K-L).

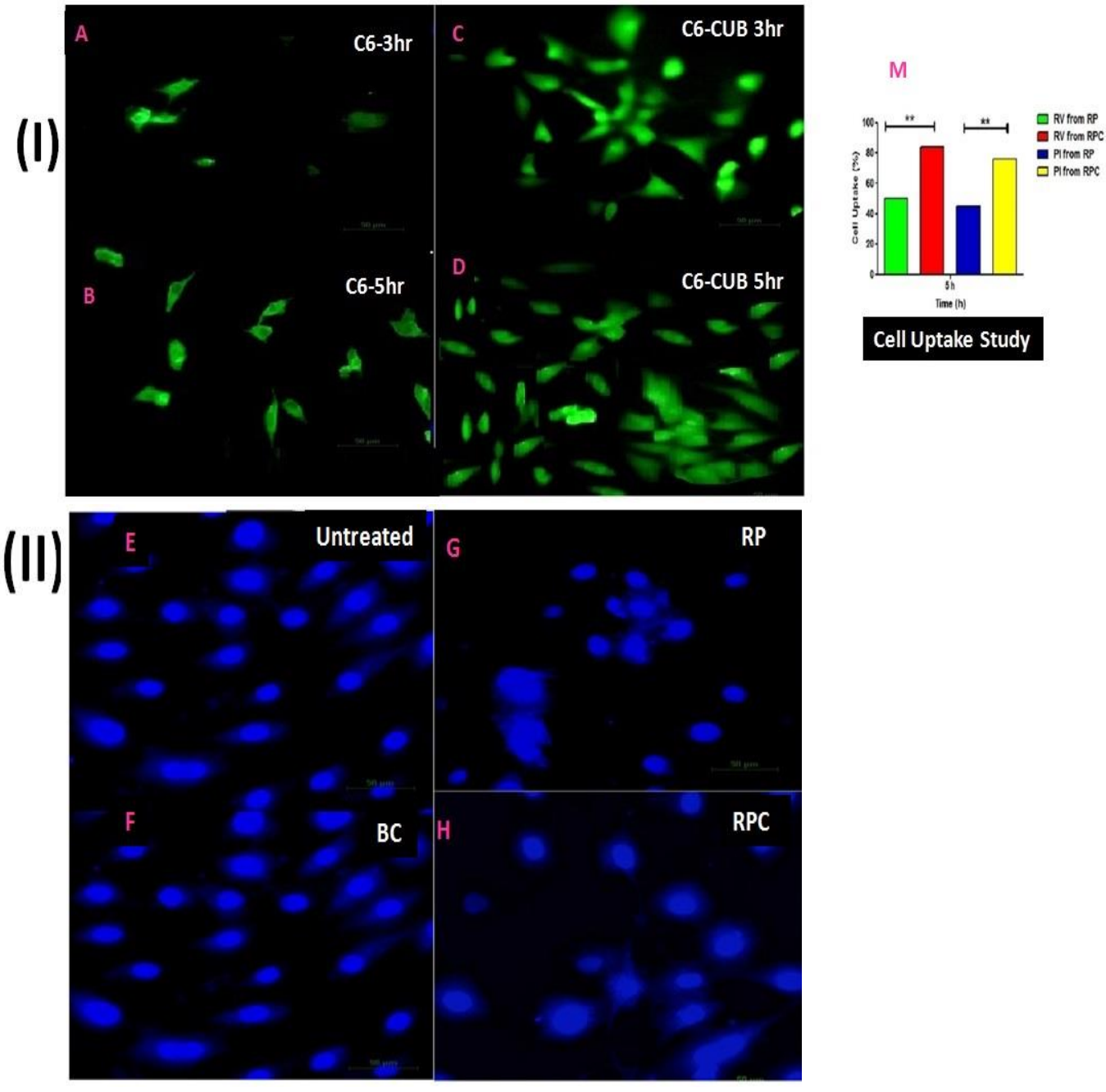

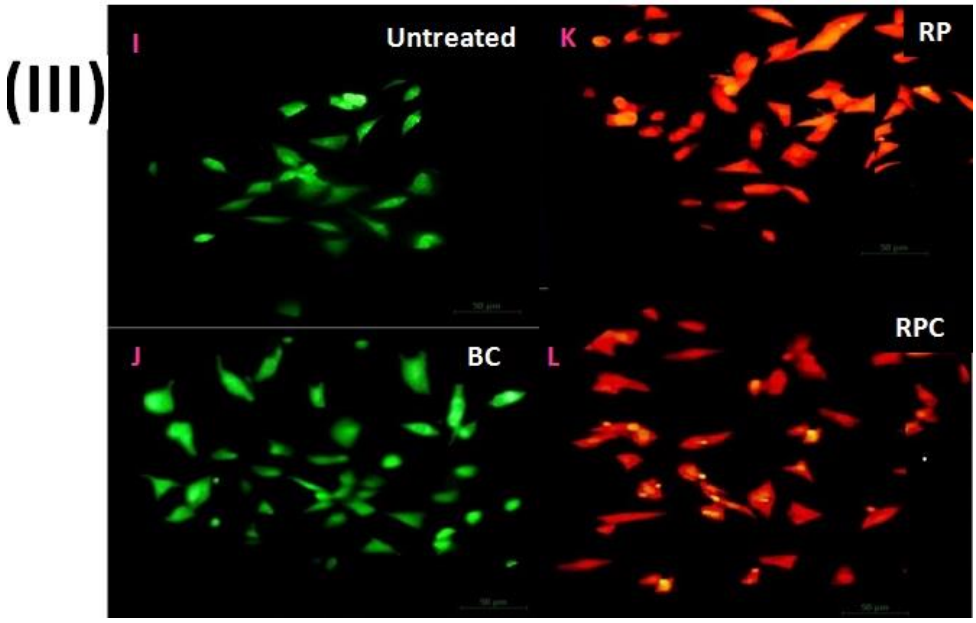

Figure 19. Fluorescence microscopic images showing qualitative cell uptake using (I) C-6 and C-CUB for 3h and 5h (A-D), (II) DAPI staining assay (E-H) and (III) live and dead cells assay using AO/EB staining (I-L) in A375 cells for RP solution, BC, and RPC. Bar graph is representing quantitative cell uptake for RP solution and RPC (M).

4.8 *In vivo*evaluation of RPC-Gel

4.8.1 Skin irritancy and toxicity study

The skin irritancy was performed for RPC-Gel and marketed gel as per by Uttley and Van Abbe (1973) test (3). It was found that the mean score of the skin irritancy for the RPC-Gel and marketed gel were 6.71 and 7.29, respectively (Table 11). The study demonstrated non-irritancy property of the developed cubosomal gel, as the values lie between 0-9.

Table 11: Scores of skin irritancy study for RPC-gel and Marketed gel as per Uttley and Van Abbe method

Formulation	Score after (day)							Mean score values
	1	2	3	4	5	6	7	
RPC-Gel	6	7	7	8	7	6	6	6.71
Marketed gel	6	6	7	8	8	8	8	7.29

(n=3)

The Draize test was used to perform acute and 28-days sub-acute skin toxicity study of RPC-gel and marketed gel (Table 12). The grading pattern 0-4 was used in this skin irritation test based on development of erythema and edema(4). The scoring was done for the data interpretation is as follows:

0–0.9: non-irritant and safe for human skin

1–1.9: mild irritant and need of preventive measures

2–3: irritant and not safe for topical use

Table 12: Score obtained after application of formulation for the skin irritation study (Draize method)

Formulation	Erythema				Edema			
	1h	24h	48h	72h	1h	24h	48h	72h
Normal control	0	0	0	0	0	0	0	0
RPC-GEL	0	0	0.67	0.67	0	0	0	0
Marketed gel	0	0	0.67	0.67	0	0	0	0
20% SLS	0	0.67	2.33	2.33	0	1.67	2.33	3

(n=3); Scores are defined as 0=no erythema, 1=very slight erythema (light pink), 2=well defined erythema (dark pink), 3=moderate to severe erythema (light red), 4=severe erythema (extreme redness). Similarly defined for edema.

There was no sign of erythema and edema after treatment of cubosomal gel in acute toxicity study. Marketed gel showed negligible erythema with absence of edema. SLS (20% w/v), a positive control in this study, caused reddening of skin which has shown high irritation with moderate to severe erythema and edema. In sub-acute toxicity study, after repeated application of above formulations up to 28 days have shown same results.

Also, the skin toxicity capability of formulated RPC-Gel and marketed gel were estimated by performing histopathology study of treated skin after 28 days of application (5). Figure 20 (A–D) shows the histopathological images of mice skins of normal control group, RPC- Gel, marketed gel, and SLS (20% w/v) as positive control, respectively. From the histopathological results, it reveals that SLS (20% w/v) caused complete damage of epidermal layer of the skin, and necrosis indicated the skin irritation potential of SLS (20% w/v). Whereas, RPC-Gel treated skin had shown continuous epidermal layer with negligible skin irritation potential, because of entrapment of both RV and PI in cubosome nanoparticles. Marketed gel has shown same results as that of cubosomal gel in comparison to normal skin. From the acute, sub-acute, and histopathology study, it can be concluded that the formulated RPC- Gel was safe for topical application.

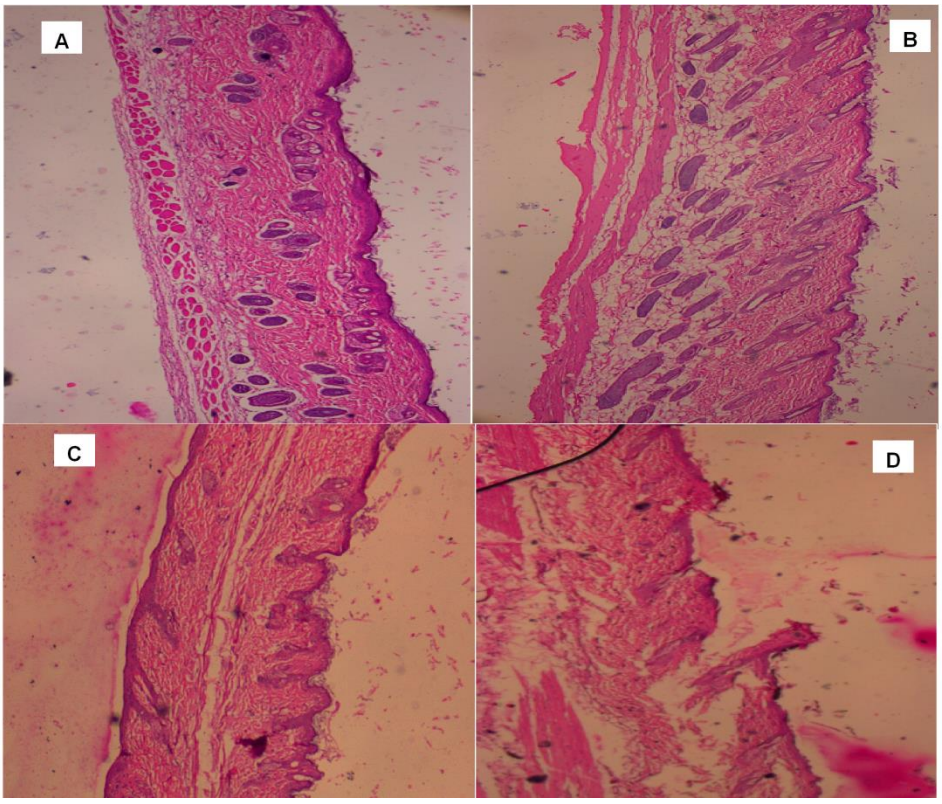

Figure 20 (A–D) shows the histopathological photos of hematoxylin and eosin stained cross sections of mice skin after 28 days of application of different formulations (A) Normal control group (B) RPC-Gel (C) Marketed gel (D) SLS (20%w/v) treated group(Magnification- 4X).

The histopathological photos of hematoxylin and eosin stained cross sections of Normal control group mice skin showing normal structure and epidermal layer of skin (Figure 20A). Mice skin treated with RPC- Gel (Figure 20B), and marketed gel (Figure 20C) demonstrated no structural differences in the mice skin as compared to normal mice skin. Mice skin on treatment with SLS (20% w/v) as positive control (Figure 20D) displayed structural damage and rupture of the epidermal layers of the skin. The results suggested that developed topical cubosomal gel was found to be non-irritant, non-toxic to mice skin.

4.8.2 *In vivo* anticancer study

Tumor volume and body weight were examined to investigate the efficacy of RPC-Gel on melanoma tumor bearing mice. The results of tumor volume and body weight measurements after 40 days of *in vivo* anticancer study are represented in Table 13. Observation of each mouse was done regularly for any physiological changes, signs of impairment, and illness. Body weight and tumor volume were recorded from the beginning on each week, until the end of the study (6). The mice belonging to normal control, carcinogen control, prophylactically and therapeutically treated with RPC-Gel and marketed gel are displayed in Figure 21 A-F respectively. In the carcinogen control (untreated) group (Figure B), there was considerable increase in the tumor volumewith damaged skin surface of tumor part and ulceration observed at the end of 6 weeks. The graphical results of tumor volume and body weight measurement of mice during and post treatment period was demonstrated in Figure 21 G-J. Prophylactically (280 mm^3) and therapeutically (412 mm^3) treated RPC-Gel has reduced the melanoma tumor volume in significant level compared to control (1080 mm^3) ($p<0.001$ and $p<0.01$ respectively). Marketed gel [prophylactically (293 mm^3) and therapeutically (428 mm^3)] also reduced the tumor volume ($p<0.01$) in the same manner as RPC-Gel. The results of body weight measurement demonstrated increase in the body weights of mice on prophylactic (36.47 gm) and therapeutic (36.67 gm) treatment with RPC-Gel ($p<0.05$) when compared with control mice (25.96 gm) The prophylactically treated mice with marketed gel showed significant increase in body weight (35.13 gm; $p<0.01$) however, there was no statistically significant difference was observed in the body weight of mice therapeutically treated with marketed gel (33.66 gm).

Finally, it was demonstrated from the anti-cancer study that RPC-Gel was nontoxic to BALB/c mice until the end of treatment and significantly reduced melanoma tumor growth, which indicated potential anti-melanoma activity.

Table 13: Tumor volume and body weight measurements after 40 days of *in vivo* anticancer study (n=6)

Group	Treatment	Tumor volume (mm^3)	Wt. of animal (gms)
I	Normal control	0.0	37 ± 2.26
II	Carcinogen control (s.c. injection of B16F10 cells)	1080 ±31.74	25.96 ±1.76
Prophylactic treatment			
III	Carcinogen + Marketed gel (Flonida 5%)	293±37.85	35.13±1.90
IV	Carcinogen + RPC gel	280±35.23	36.47±1.58
Therapeutic treatment			
V	Carcinogen + Marketed gel (Flonida 5%)	428±21.07	33.66± 1.52
VI	Carcinogen + RPC gel	412± 29.68	36.67±1.40

(n=6), Mean ± SD

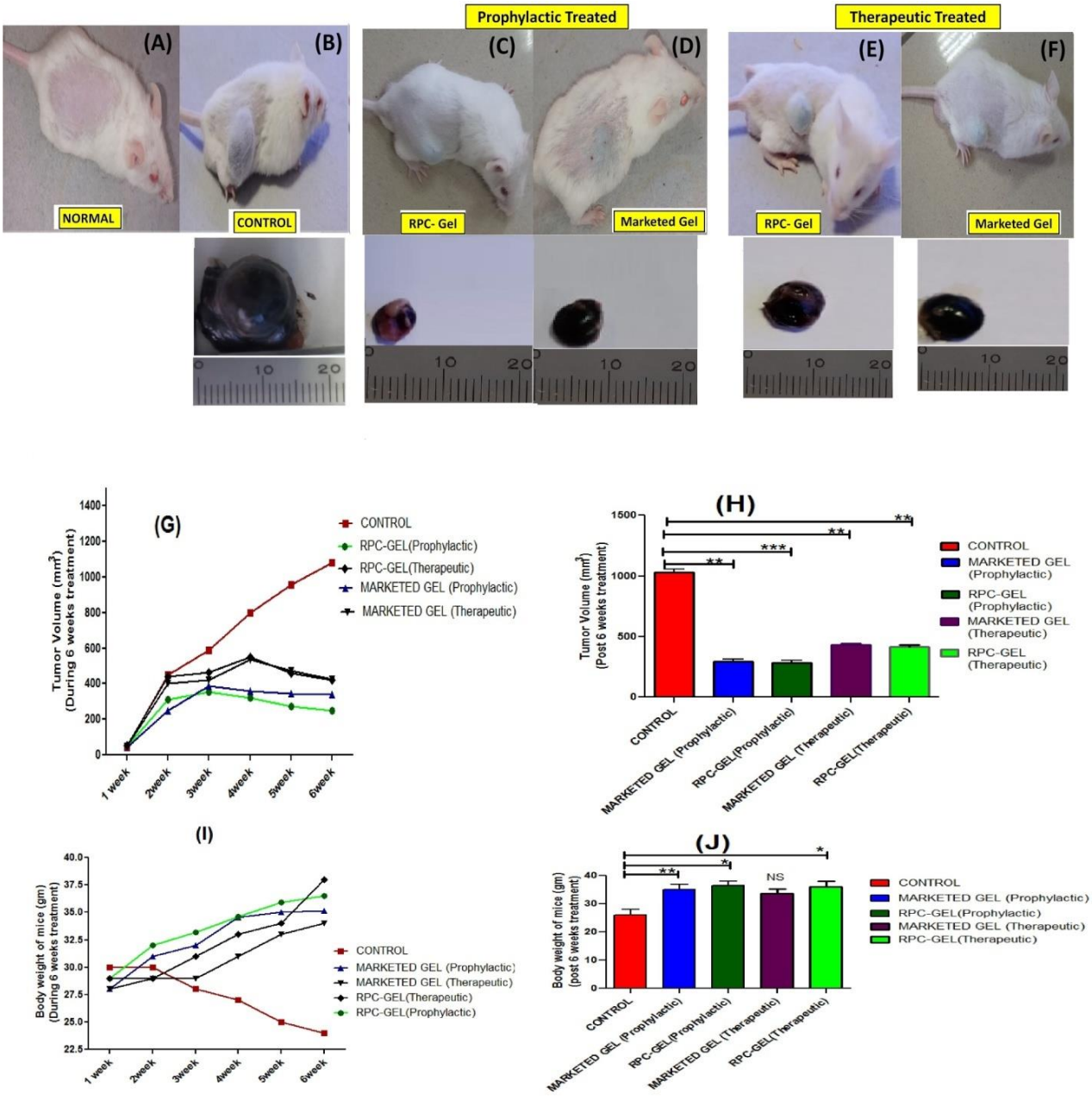

Figure 21:Melanoma growth regression and excised tumor images from different mice model groups: Normal (A), Disease control (B), Prophylactically and therapeutically treated with RPC-gel (C,E) and Marketed gel (D,F), Estimation of tumor volume and body weight (G and I) during 6 weeks treatment and post 6 weeks treatment (H and J) respectively. (n=6), (* P<0.001, ** P<0.01, * P<0.05, NS- not significant) vs control group.**

Figure 21 demonstrates assessment of *in vivo* prophylactic and therapeutic activity of RPC-Gel in B16F10 induced melanoma skin cancer BALB/c mice model. The tumor bearing mice without treatment (disease control) showing tumor nodule, structural damage of skin, ulcer formation at the end of 6 weeks after melanoma induction (Figure 21B). Tumor bearing mice prophylactically treated with RPC-Gel (equivalent to 50 mg/kg of RV and PI) andmarketed gel (Flonida 5%) applied topically (equivalent to 50 mg/kg of 5-fluorouracil) daily, showed reduction in tumor nodules and growth at the end of treatment period (Figure 21C & D). Similar results wereobtained for the mice therapeutically treated with RPC-Gel andmarketed gel, (Figure 21E&F). Estimation of tumor volume (mm^3) during 6 weeks treatment (Figure 21G) and post 6 weeks treatment (Figure 21H) with RPC-Gel and marketed gel demonstrated decrease the volume of tumor when compared with disease control group. Estimation of body weight (gm) during 6 weeks treatment (Figure 21I) and post 6 weeks treatment (Figure 21J) with RPC-Gel and marketed gel demonstrated increase in the body weights of mice when compared with disease control group.

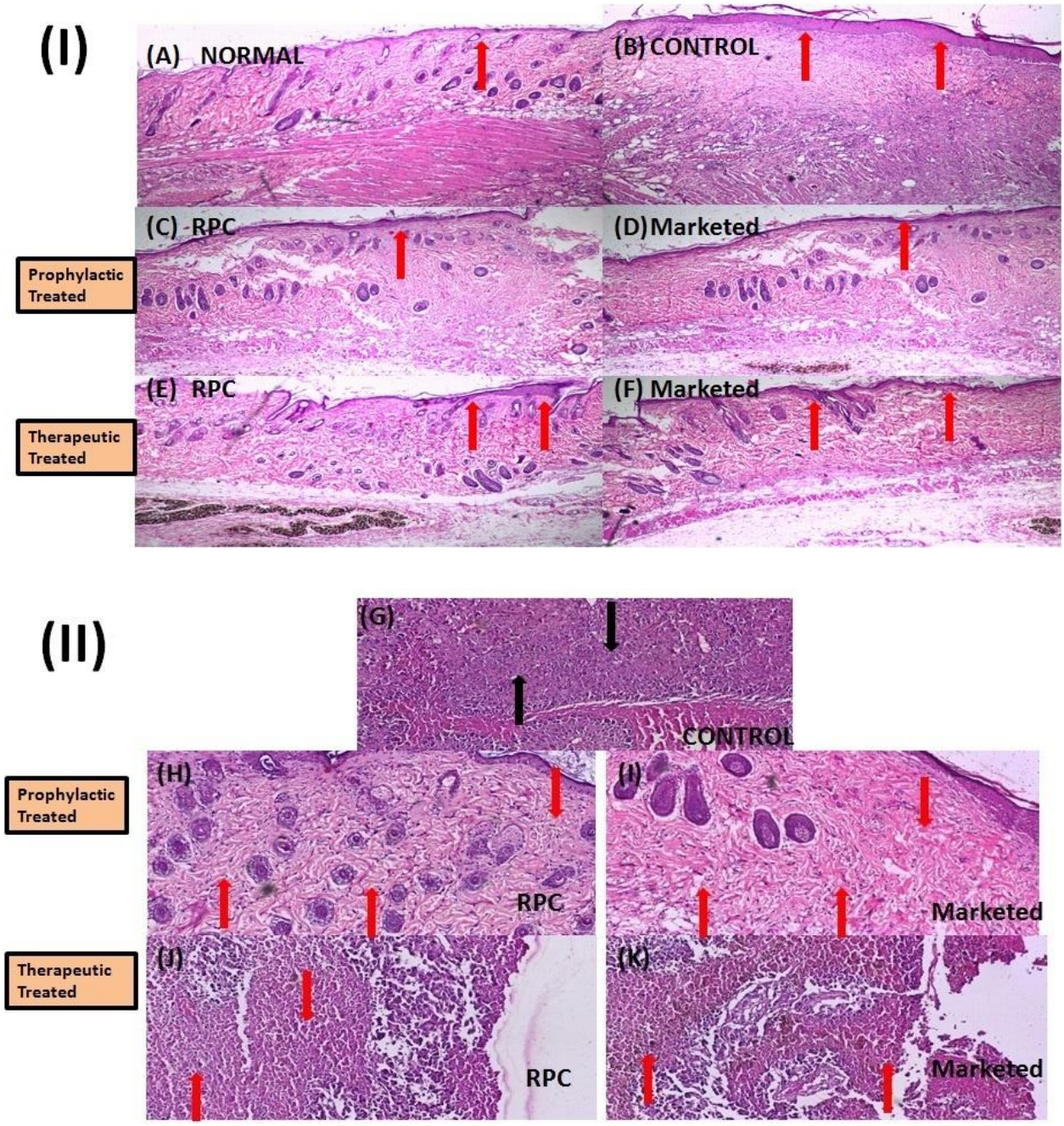

Figure 22: Representative Hematoxylin and Eosin stained images of tumor tissues obtained from BALB/c mice melanoma model in different groups demonstrating change in epidermis thickness (I) and tumor necrosis (II). Different groups represents as Normal skin (A), Untreated tumor (control) (B,G), Prophylactically and therapeutically treated with RPC-gel (C,H and E,J) and Marketed gel (D,I and F,K) respectively. (Magnification- 4X).

Histopathological examination of tumor tissues of different mice from each group is shown in Figure 22. In the Figure 22 the normal skin of mice (I-A) representing various normal layers of the skin and normal structure of epidermis. The red arrows indicate the change in the epidermis thickness due to the infiltrating tumor cells (Figure 22I B-F). There was an enlargement in the thickness of epidermis in untreated (control) mice (Figure 22I -B) and quite increased in mice therapeutically treated with RPC-Gel or marketed formulation (Figure 22I –E& F respectively). The RPC-Gel (Figure 22II-H, J) and marketed gel (Figure 22II-I, K) treated mice tumors shows more necrotic areas than untreated or control mice tumor (Figure 22II-G). The red arrows indicate presence of necrotic cells in excised tumor tissues of different groups.These results demonstrate that the extensive tumor necrosis may be due to movement of RPC nanoparticles within the melanoma tumor structure.

5. DISCUSSION

5.1 HPLC method development of RV andPI

Isosbestic point is the specific wavelength at which two compounds have the same molar absorptivities or the point which can correlate with a specific wavelength, where an absorption spectra of the two compounds can cross with each other. Although many compounds are simultaneously estimated based on the isosbestic point method, (59,60) none has been reported for estimation of piperine and resveratrol. Henceforth, with the help of an isosbestic point method, the simultaneous quantification of these phytoconstituents and finally, the data interpretation can be made simple.

An isosbestic point-based RP- HPLC method was developed and validated for simultaneous estimation of resveratrol and piperine in cubosome nanoformulation. All the validation parameter was observed to be within the acceptable range.

5.2 Characterization of RPC

5.2.1 Particle size

Nanoparticle size is one of the most important factor affecting not only transdermal drug delivery but also cellular uptake and biodistribution(61). The particles with < 300 nm can transfer entrapped drug into deep layer of the skin (62). In the present investigation, the particle size of RPC formulations were less than 300 nm, indicating that formulated cubosome nanoparticles are capable to enter into the skin.

The results indicate that increase in GMO (%w/w) led to increase in particle size and there was inverse relationship between PF-127 (%w/w) and particle size. As PF-127 concentration decreased in the formulations, the cubosomes with larger particle size were formed. This

happens because of the lesser amount of stabilizer causes reduced interfacial stability and leads to nanoparticles aggregation (63).

The results demonstrated that EE increases with increase in PF-127 concentrations. This might be due to the presence of PF-127 over the cubosome structures which can retain some amount of RV and PI by which EE can be increased. This enhancement in the EE is also due to availability of large surface area from the structure of the cubosome (64).

5.2.2 PDI and ZP

ZP was studied to determine the charge on the surface of cubosome nanoparticles which can affect the physical stability and skin permeation of cubosome formulation. The high ZP values provide long-term physical stability to cubosome nanoformulation, as it prevents aggregation between the particles of same charge due to the electric repulsion. (65).

The negative charge imparted might be due to the presence of the free fatty acid in the GMO (66). Generally, cubosome nanoparticles is formed with more negative charge values after adding PF-127 to the cubosome nanodispersion due to the interaction between hydroxyl ions of PF-127 with the aqueous medium i.e. water (67,68). It has been reported by Kohli and Alpar, that only negatively charged particles could permeate through the skin via channels produced by the repulsive forces exerted between the negatively charged particles and skin lipids (69). Hence, negatively-charged cubosome nanoparticles can easily permeate through the skin through transdermal application.

5.2.3 TEM Analysis

Morphological examination of cubosome was evaluated by HR-TEM after negative staining using phosphotungstic acid and images clearly showed cubic shaped nanoparticles with uniform size distribution. The reason for formation of cubic shape structural morphology could be due to

the hydrophobic nature of the lipids which when exposed to an aqueous environment led to spontaneous formation of closed bilayers exposing the polar hydrophilic layer to the outer surface of cubosome. The shape and surface morphology of the cubosome was found to be smooth cubic shaped nanoparticles.

5.2.4 DSC

DSC is a rapid and reliable method in evaluating the physicochemical drug-excipients interactions and detecting polymorphic modifications. The DSC thermogram of RPC (F) demonstrated the RV and PI were completely entrapped inside the cubosome nanoparticles, as the sharp endothermic peaks of PI and RV were disappeared which indicated non-crystalline state of cubosome (70).

5.2.5 XRD

XRD was carried out to confirm the physical state of RPC in comparison to pure RV, PI and BC. The crystallanity and physical state of the RPC was determined and confirmed by XRD spectras of RV (A), and PI (B), BC (C), and RPC (D). The diffractogram of the RPC suggested complete absence of sharp crystal peaks when compared with pure RV and PI which demonstrated that the physical state of RPC was same in comparison to BC.

5.2.6 pH and rheological behavior of RPC

The pH of the cubosomal dispersion was measured in order to examine any possible skin irritation that could happen due to change in the skin pH upon *in vivo* application. The pH values for all RPC batches were found to be in the range of 5.64 to 6.78 which are within the acceptable nonirritant pH range (71,72).

The flow properties of the cubosome formulations can affect the spreadability and the residence time of the formulation at the application site. Cubosome formulations with higher

concentrations of lipid showed maximum viscosities. This might be due to more viscous nature of GMO tends to form more liquid crystal-like materials that increased the viscosity of cubosome.

5.2.7 *In vitro* drug release study

In vitro drug release profile of RV and PI from the optimized cubosome nanoformulation was exerted biphasic release pattern. The results of drug release were in accordance with that obtained by Nasr *et al* (39) who stated that the release pattern of cubosome was also biphasic with initial burst release followed by sustained release. The initial burst release might be attributed to the weakly bound or inadequately adsorbed RV and PI on the large surface of cubosome nanoparticles. On the other hand, after 1h slow RV and PI release prolonged for 24 h may be due to the architecture of cubosome system that can assists as a rate controlling membrane matrix structure, with decreased RV and PI release (55). Also, the slow release may be because of limited diffusion of RV and PI from the aqueous channels, where diffusion is controlled by the relatively narrow pore size of the aqueous channels (73). Another reason for the slow drug release is GMO, which forms a bicontinuous structure in the cubosomes causes slow partitioning of drug from the lipid medium to aqueous medium (74). RV and PI both are hydrophobic drugs has a strong interaction with the lipophilic part of cubosome leading to the sustained release. Higuchi model was found to be the best fitting model with the highest regression value. Higuchi model could describe the biphasic release pattern with initial burst release followed by sustained release, with a release mechanism of diffusion controlled (55,75).

5.3 Stability study

The results of stability study suggest that there were insignificant changes in the obtained results of stored cubosome formulation as compared to freshly prepared formulation (0 month). The

GMO maintains the integrity of the cubosome and PF-127 stabilizes this nanoformulation by which cubosome can be considered as thermodynamically stable. The obtained results suggest that cubosome formulation were stable at the room temperature storage conditions.

5.4 Formulation of RPC-Gel

The developed RPC-Gel formulation was found to have same physical nature as that of colloidal dispersion. Low viscosity and dispersion like nature of cubosome in turn leads to poor patient compliance due to number of reasons, like short residence time of cubosome at the application site, difficult to apply an effective dose, loss during application, and thus leads to poor drug retention. Hence, to overcome these limitations, optimized-RPC nanoformulation was developed as bioadhesive gel by mixing with a gel former to form pharmaceutically elegant RPC-Gel formulation.

5.4.1 *Exvivo* skin permeation and retention studies

The results obtained from the e*x vivo* skin permeation and retention studies confirms the enhanced skin permeation of RV and PI from the cubosomal gel due to the physicochemical properties of the cubosomes (particle size, surface charge) (76) and synergistic effect of both GMO and PF-127. The nanosized and negatively-charged cubosome nanoparticles enhance the permeation of RV and PI through the skin. GMO can perturb the ordered structure of the skin by forming hydrophobic interaction with the skin lipid (77,78). The PF-127 a non-ionic surfactant, acts as penetration enhancer by emulsifying sebum of skin, thereby enhancing the thermodynamic coefficient of the drugs (79).

For effective treatment of melanoma, the drug delivery system should be able to deliver the drug into the deep layers of the epidermis where melanocytes are located. The sustained RV and PI diffusion pattern through the skin was achieved due to the formation of a depot by cubosome

nanoparticles in the lipid part of the stratum corneum. This may be due to the similarity between the structure of cubosome nanoparticles and the stratum corneum (80,81).

5.5 *In vitro* assays of RPC for targeting melanoma

5.5.1 *In vitro* cytotoxicity study

The viability of the L929 cells treated with different drug concentrations (Figure 18B) of different formulations remained in the range of 95-100% related to the untreated cells. The results obtained showed that BC does not have any cytotoxic effects to both L929 and A375 cells, which demonstrate their cytocompatibility and significance as a bio-nanomaterial for targeting melanoma (Figure 18A and 18B). The drug solution and RPC have also does not shown cytotoxicity against normal L929 mouse fibroblast. Both drug solution and RPC showed no significant difference in cell viability which confirms its cytocompatibility (Figure 18B)(56). But, in case of A375 human melanoma cells treated with drug solution and RPC, we found a significant reduction of cell viability in a concentration dependent manner (Figure 18A), where RPC demonstrated significantly higher cytotoxicity against A375 cells when compared to drug solution.

5.5.2 Cell uptake studies

The cells under treatment with C6-CUB have shown maximum fluorescence intensity than that of C6 at the end 3h and 5h treatment period (Figure 19A-D), suggesting the time dependent enhanced cellular internalization of C6-CUB into the melanoma cells as compared to C6 solution. The improved cellular uptake of the RPC nano formulation might be attributed to their particle size, shape, surface charge, and composition of cubosome containing GMO and PF-127.

5.5.3 DAPI and Live and Dead cells assays

DAPI staining assay reported that the RP drug solution and RPC nanoformulation induced apoptosis in human melanoma cells in comparison to non-treated and BC treated cells.

In live and dead cells assay, AO penetrates into the live A375 cells through intact cell membranes, showed green fluorescence. The A375 cells on treatment with BC showed green fluorescence, indicated biocompatible nature of cubosome formulation. The A375 cells on treatment with drug solution and RPC (IC_{50} value) displayed orange-red fluorescence, as EB entering through ruptured cell wall membranes of dead cells which stains damaged nuclei. The RPC treatment for 48 h demonstrated maximum staining to dead cells as compared to drug solution.

5.6 *In vivo* evaluation of RPC-Gel

5.6.1 Skin irritancy and toxicity study

Skin irritancy test using Uttley and Van Abbe (1973) method demonstrated non-irritancy property of the developed cubosomal gel, as the values lie between 0-9, probably due to RV and PI entrapped inside the cubosome nanoparticles. Upon its release from the nanoparticles, it will cause irritation to the skin and death to the melanoma cancer cells, but not to the normal cells. There was no sign of erythema and edema after treatment of cubosomal gel in acute toxicity study performed by using Draize method.

From the histopathological results, it was seen that SLS (20%w/v) caused complete damage of epidermal layer of the skin, and necrosis indicated the skin irritation potential of SLS (20%w/v). Whereas, RPC-Gel treated skin had shown continuous epidermal layer with negligible skin irritation potential, because of entrapment of both RV and PI in cubosome nanoparticles. Marketed gel has shown same results as that of cubosomal gel in comparison to normal skin.

From the acute, sub-acute, and histopathology study, it can be concluded that the formulated RPC- Gel was safe for topical application.

5.6.2 *In vivo* anticancer study

Prophylactic and therapeutic anti-cancer activity of RPC-Gel was evaluated in the B16F10 induced BALB/c mice animal model. In prophylactic treatment simultaneous gel application was done till the end of experiment. In therapeutic treatment gel application was started from 14th day of subcutaneous injection of B16F10 cells. Tumor volume and weight of mice were assessed in all groups during six weeks of treatment to compare the efficiency of RPC-Gel with marketed gel. Prophylactically and therapeutically, RPC-Gel and marketed gel was significantly reduced the tumor volume ($p<0.001$, $p<0.01$). Thus after 40 days of study the tumor volume was 3.8- and 2.6- fold lower in the mice treated with RPC-Gel, prophylactically and therapeutically respectively, compared with the carcinogen control mice. Furthermore, prophylactic and therapeutic treatment received from marketed gel (5% Flonida) achieved 3.6- and 2.5- fold lower tumor volume compared with carcinogen control mice, respectively. The better effect was observed for RPC-Gel might be related to the ability of cubosome nanoparticles to enhance drug penetration through mice skin.

RV and PI are known to prevent the progression of cancer by targeting multiple cellular targets affecting the cellular proliferation and growth: apoptosis, inflammation, invasion, angiogenesis, and metastasis. Gatouillat et al. revealed that RV stopped the growth of doxorubicin-resistant B16 melanoma cell subline (B16/DOX) by both *in vitro* and *in vivo* studies (10). Kutan et al. have found same results which demonstrated that PI has reduced the melanoma growth progression and lung metastasis in C57BL/6 mice in significant manner (17).

Hematoxylin and eosinstained tumor skin revealed increased thickness of the epidermis by the infiltration of tumor cells. Mice on treatment with RPC-gel and marketed formulation showed regression of epidermal infiltration by malignant cells. Also, RPC-gel and marketed formulation treated mice showed minimal hyperkeratosis in the epidermal layer as compared to untreated mice (Figure 22 IA-F). Tumor treated with RPC-Gel and marketed formulation showed more necrotic cells than the live tumor cells. (Figure 22 E –F). The untreated tumor (control) showed more live tumor cells than the necrotic cells (Figure 22 G).

These results demonstrate that the extensive tumor necrosis may be due to movement of RPC within the melanoma tumor structure.

SUMMARY

Resveratrol (RV) is a nutraceutical which have exciting pharmacological potential which demonstrates antioxidant, cardioprotective, neuroprotective, immunomodulatory, anti-inflammatory and anticancer properties. This exciting pharmacological potential and multi-targeting ability of resveratrol make it perfect drug candidate for targeting melanoma. However, its poor solubility, instability, and poor oral bioavailability were major barriers in the designing of formulation. Piperine (PI) is an alkaloid which exerts potential therapeutic activity against various diseases including obesity, inflammation, arthritis, and different types of cancers. In addition to these activities piperine enhances the bioavailability of other drugs. The combinational nanoparticulate approach of resveratrol and piperine through transdermal application has taken into the consideration to increase their effectiveness for better targeting to melanoma. In the present investigation, resveratrol and piperine loaded cubosomal nanoformulation was developed and evaluated for its potential treatment of melanoma through transdermal application.

An isosbestic point based reversed phase-HPLC method was developed and validated as per ICH guidelines for the simultaneous estimation of resveratrol and piperine in cubosome nanoparticles. The resveratrol and piperine loaded cubosomes was successfully formulated using homogenization technique followed by probe sonication. A 2-factor 3-level (3^2) factorial design approach was used for the optimization of cubosome nanoformulations and evaluation was done for the possible 9 batches using the Design-Expert software.

The results obtained fitted to different polynomial models and the best-fit model was selected on the basis of different statistical parameters. The contour and response surface plots thus generated from the Design-Expert software were demonstrated the relationship between the

independent and dependant variables. The optimized batch of cubosome was chosen based on the maximum entrapment efficiency and smaller particle size. Zeta sizer were used to evaluate the particle size, PDI, and ZP of cubosome formulation. The surface morphology of the cubosome nanoparticles was confirmed by using the HR-TEM analysis. Entrapment efficiency of cubosome was determined by using high speed centrifugation technique.

The characterization and compatibility of the drug with other excipients were confirmed by using FTIR and DSC analysis. The crystalline properties and thermal behavior of the freeze-dried powders of optimized cubosome formulation were performed by XRD and DSC analysis.

The pH and viscosities of the RPC were determined using digital pH meter and Brookfield viscometer. *In vitro* RV and PI release from optimized RPC was determined by using a dynamic dialysis method employing the tablet dissolution testing apparatus equipped with low-volume conversion kit and the release mechanism was determined by fitting the results of drug release into different drug release kinetic models.

Optimized RPC was further formulated into cubosomal gel (RPC-Gel) by using carbopol (1% w/v) and for the comparison purpose simple resveratrol and piperine gel (RP-Gel) was prepared in the same manner. The formulated gel systems were evaluated for their pH, viscosity, and drug content. *Ex vivo* permeation and deposition of formulated gel systems were studied by using Franz diffusion cell apparatus. Stability study of the optimized cubosome formulation was studied for 3 months by storing the formulation at room temperature, and further evaluated for particle size, PDI, ZP and Drug release. The *in vitro* cytotoxicity of resveratrol and piperine (RP), Blank-cubosome (BC), and optimized RPC was evaluated against the mouse fibroblast (L-929) and human melanoma (A-375) cell lines by MTT assay. Biocompatibility of optimized RPC was observed towards L929, with enhanced anticancer activity against A375 cell lines, when

compared to pure RV and PI. The results of *in vitro* cytotoxicity were further confirmed by using qualitative and quantitative cell uptake studies. DAPI staining assay was utilized for visualizing the nuclear changes in the A375 cells.

Skin irritancy study performed by using Uttley and Van Abbe, and Draize tests demonstrated that the composition of RPC-Gel has been proved non-irritant to the mice skin. The histopathology study showed that the formulated RPC- Gel was safe for topical application with lack of skin irritation. It was demonstrated from the anti-cancer study that topical application of RPC-Gel into melanoma-bearing BALB/c mice up to six weeks resulted in tumor regression, and histopathological examination of tumor tissues of BALB/c mice demonstrated extensive tumor necrosis in the same mice on treatment with RPC-Gel. The results of *in vitro* and *in vivo* studies thereby proposing, RPC-Gel to be a promising drug delivery system through transdermal application for the melanoma treatment.

CONCLUSION

In the present research work, an attempt was done to improve the efficacy of melanoma treatment in combination with RV and PI by using a novel cubosome. RV and PI entrapped cubosome was successfully formulated and optimized by using 3^2 factorial design. The optimized cubosome nanoformulation (RPC5) with GMO: PF-127 ratio (5:1) shown desirable particle size and greater entrapment efficiency. The XRD and DSC studies demonstrated successful encapsulation of RV and PI in the cubosome nanoparticles. TEM study for cubosome revealed that cubosome nanoparticles have cubic shape. *In vitro* drug release for RPC has shown a biphasic burst release with a release mechanism of diffusion controlled over 24 h. The optimized RPC was transferred into cubosomal gel (RPC Gel) and characterized for pH, drug content, and viscosity. RPC gel has shown high amount of RV and PI permeation, and deposition capacity through mice skin when compared to traditional RV and PI gel (RP Gel). The *in vitro* biocompatible nature of RPC was confirmed by the absence of cytotoxicity against L929 cell line. MTT and cell uptake studies showed increased uptake of RPC in A375 cells, in comparison to free RV and PI. The qualitative and quantitative cell uptake studies revealed that RV and PI entrapped cubosome nanoparticulate system was an effective drug delivery system to induce cytotoxicity in A375 cells. From the skin irritancy and toxicity study RPC-Gel was proved to be nonirritant in nature by showing no sign of edema, and erythema in mice skin. The histopathological examination demonstrated the biocompatibility of the developed cubosomal gels. *In vivo* anticancer study has shown potential therapeutic effect of RPC-Gel on B16F10 induced BALB/c mice. Overall, developed RPC drug delivery system has promising potential in the prevention and treatment of melanoma by transdermal application. Further studies using

advanced preclinical models are required to prove the efficacy of this cubosome formulation for melanoma treatment.

8. Bibliography

1. Ward WH, Farma JM. Cutaneous melanoma Etiology and Therapy.Codon Publications, Australia, 2017.
2. Bray F, Ferlay J, Soerjomataram I, Siegel RL, Torre LA, Jemal A. Global cancer statistics 2018: GLOBOCAN estimates of incidence and mortality worldwide for 36 cancers in 185 countries. CA Cancer J Clin. 2018;68(6):394–424.
3. Domingues B, Lopes J, Soares P, Populo H. Melanoma treatment in review. ImmunoTargets Ther. 2018;7:35–49.
4. Summerlin N, Soo E, Thakur S, Qu Z, Jambhrunkar S, Popat A. Resveratrol nanoformulations: Challenges and opportunities. Int J Pharm [Internet]. 2015;479(2):282–90. Available from: http://dx.doi.org/10.1016/j.ijpharm.2015.01.003
5. Varoni EM, Lo Faro AF, Sharifi-Rad J, Iriti M. Anticancer Molecular Mechanisms of Resveratrol. Front Nutr. 2016;3:1-15.
6. Sanna V, Roggio AM, Siliani S, Piccinini M, Marceddu S, Mariani A, et al. Development of novel cationic chitosan- and anionic alginate – coated poly (d, l -lactide- co - glycolide) nanoparticles for controlled release and light protection of resveratrol. Int J nanomedicine. 2012;7:5501–5516.
7. Kurangi B, Jalalpure S. A Validated Stability-indicating RP-HPLC Method for Piperine Estimation in Black Pepper, Marketed Formulation and Nanoparticles. Indian J Pharm Educ Res. 2020;54(3):677–686.
8. Salehi B, Mishra AP, Nigam M, Sener B, Kilic M, Sharifi-Rad M, et al. Resveratrol: A double-edged sword in health benefits. Biomedicines. 2018;6(3):1–20.
9. Berman AY, Motechin RA, Wiesenfeld MY, Holz MK. The therapeutic potential of

resveratrol: a review of clinical trials. npj Precis Oncol [Internet]. 2017;1(35). Available from: http://dx.doi.org/10.1038/s41698-017-0038-6

10. Gatouillat G, Balasse E, Joseph-Pietras D, Morjani H, Madoulet C. Resveratrol induces cell-cycle disruption and apoptosis in chemoresistant B16 melanoma. J Cell Biochem. 2010;110(4):893–902.

11. Osmond GW, Augustine CK, Zipfel PA, Padussis J, Tyler DS. Enhancing melanoma treatment with resveratrol. J Surg Res [Internet]. 2012;172(1):109–115. Available from: http://dx.doi.org/10.1016/j.jss.2010.07.033

12. Fang Y, Bradley MJ, Cook KM, Herrick EJ, Nicholl MB. A potential role for resveratrol as a radiation sensitizer for melanoma treatment. J Surg Res [Internet]. 2013;183(2):645–653. Available from: http://dx.doi.org/10.1016/j.jss.2013.02.037

13. Niles RM, McFarland M, Weimer MB, Redkar A, Fu YM, Meadows GG. Resveratrol is a potent inducer of apoptosis in human melanoma cells. Cancer Lett. 2003;190(2):157–163.

14. Asensi M, Medina I, Ortega A, Carretero J, Bano MC, Obrador E, et al. Inhibition of Cancer Growth by Resveratrol is related to its low Bioavailability. Free Radic Biol Med. 2002;33(3):387–398.

15. Sunila ES, Kuttan G. Immunomodulatory and antitumor activity of Piper longum Linn. and piperine. J Ethnopharmacol. 2004;90(2–3):339–346.

16. Bhardwaj RK, Glaeser H, Becquemont L, Klotz U, Gupta SK, Fromm MF. Piperine, a major constituent of black pepper, inhibits human P-glycoprotein and CYP3A4. J Pharmacol Exp Ther. 2002;302(2):645–650.

17. Pradeep CR, Kuttan G. Effect of piperine on the inhibition of lung metastasis induced B16F-10 melanoma cells in mice. Clin Exp Metastasis. 2002;19(8):703–708.

18. Fofaria NM, Kim S-H, Srivastava SK. Piperine causes G1 phase cell cycle arrest and apoptosis in melanoma cells through checkpoint kinase-1 activation. PLoS One. 2014;9(5).

19. Hashimoto K, Yaoi T, Koshiba H, Yoshida T, Maoka T, Fujiwara Y, et al. Photochemical isomerization of piperine, a pungent constituent in pepper. Food Sci Technol Int Tokyo. 1996;2(1):24–29.

20. Ganesh Bhat B, Chandrasekhara N. Studies on the metabolism of piperine: Absorption, tissue distribution and excretion of urinary conjugates in rats. Toxicology. 1986;40(1):83–92.

21. Wightman EL, Reay JL, Haskell CF, Williamson G, Dew TP, Kennedy DO. Effects of resveratrol alone or in combination with piperine on cerebral blood flow parameters and cognitive performance in human subjects: A randomised, double-blind, placebo-controlled, cross-over investigation. Br J Nutr. 2014;112(2):203–213.

22. Huang W, Chen Z, Wang Q, Lin M, Wu S, Yan Q, et al. Piperine potentiates the antidepressant-like effect of trans-resveratrol: Involvement of monoaminergic system. Metab Brain Dis. 2013;28(4):585–595.

23. Tak JK, Lee JH, Park JW. Resveratrol and piperine enhance radiosensitivity of tumor cells. BMB Rep. 2012;45(4):242–246.

24. Johnson JJ, Nihal M, Siddiqui IA, Scarlett CO, Bailey HH, Mukhtar H, et al. Enhancing the bioavailability of resveratrol by combining it with piperine. Mol Nutr Food Res. 2011;55(8):1169–1176.

25. Jiang T, Xu G, Chen G, Zheng Y, He B, Gu Z. Progress in transdermal drug delivery systems for cancer therapy. Nano Res. 2020;13(7):1810–1824.

26. Karami Z, Hamidi M. Cubosomes: Remarkable drug delivery potential. Drug Discov Today [Internet]. 2016;21(5):789–801. Available from: http://dx.doi.org/10.1016/j.drudis.2016.01.004

27. Lakshmi N, Yalavarthi P, Vadlamudi H, Thanniru J, Yaga G, K H. Cubosomes as Targeted Drug Delivery Systems - A Biopharmaceutical Approach. Curr Drug Discov Technol. 2014;11(3):181–188.

28. Duttagupta AS, Chaudhary HM, Jadhav KR, Kadam VJ. Cubosomes: Innovative Nanostructures for Drug Delivery. Curr Drug Deliv. 2016;13(4):482–493.

29. Naves LB, Dhand C, Venugopal JR, Rajamani L, Ramakrishna S, Almeida L. Nanotechnology for the treatment of melanoma skin cancer. Prog Biomater. 2017;6(1–2):13–26.

30. Kurangi BK, Jalalpure SS. Review of selected herbal phytoconstituents for potential melanoma treatment. Indian J Heal Sci Biomed Res. 2018;11(1):3.

31. Carletto B, Berton J, Ferreira TN, Dalmolin LF, Paludo KS, Mainardes RM, et al. Resveratrol-loaded nanocapsules inhibit murine melanoma tumor growth. Colloids Surfaces B Biointerfaces [Internet]. 2016;144:65–72. Available from: http://dx.doi.org/10.1016/j.colsurfb.2016.04.001

32. Morsi NM, Abdelbary GA, Ahmed MA. Silver sulfadiazine based cubosome hydrogels for topical treatment of burns: Development and in vitro/in vivo characterization. Eur J Pharm Biopharm [Internet]. 2014;86(2):178–189. Available from: http://dx.doi.org/10.1016/j.ejpb.2013.04.018

33. Sharma R, Kaur G, Kapoor DN. Fluconazole Loaded Cubosomal Vesicles for Topical Delivery. Int J Drug Dev Res. 2015;7(3):32–41.

34. Tupal A, Sabzichi M, Ramezani F, Kouhsoltani M, Hamishehkar H. Dermal delivery of doxorubicin-loaded solid lipid nanoparticles for the treatment of skin cancer. J Microencapsul. 2016;33(4):372–380.

35. Khan MA, Pandit J, Sultana Y, Sultana S, Ali A, Aqil M, et al. Novel carbopol-based transfersomal gel of 5-fluorouracil for skin cancer treatment: In vitro characterization and in vivo study. Drug Deliv. 2015;22(6):795–802.

36. Safwat MA, Soliman GM, Sayed D, Attia MA. Fluorouracil-Loaded Gold Nanoparticles for the Treatment of Skin Cancer: Development, in Vitro Characterization, and in Vivo Evaluation in a Mouse Skin Cancer Xenograft Model. Mol Pharm. 2018;15(6):2194–2205.

37. Ahirrao M, Shrotriya S. In vitro and in vivo evaluation of cubosomal in situ nasal gel containing resveratrol for brain targeting. Drug Dev Ind Pharm [Internet]. 2017;43(10):1686–93. Available from: http://dx.doi.org/10.1080/03639045.2017.1338721

38. Luo Q, Lin T, Zhang CY, Zhu T, Wang L, Ji Z, et al. A novel glyceryl monoolein-bearing cubosomes for gambogenic acid: preparation, cytotoxicity and intracellular uptake. Int J Pharm. 2015;493(1–2):30–39.

39. Nasr M, Ghorab MK, Abdelazem A. In vitro and in vivo evaluation of cubosomes containing 5-fluorouracil for liver targeting. Acta Pharm Sin B [Internet]. 2015;5(1):79–88. Available from: http://dx.doi.org/10.1016/j.apsb.2014.12.001

40. Elnaggar YSR, Etman SM, Abdelmonsif DA, Abdallah OY. Novel piperine-loaded Tween-integrated monoolein cubosomes as brain-targeted oral nanomedicine in Alzheimer's disease: Pharmaceutical, biological, and toxicological studies. Int J Nanomedicine. 2015;10:5459–5473.

41. Mitkari BV, Korde SA, Mahadik KR, Kokare CR. Formulation and evaluation of topical liposomal gel for fluconazole. Indian J Pharm Educ Res. 2010;44(4):324–333.

42. Esposito E, Ravani L, Mariani P, Contado C, Drechsler M, Puglia C, et al. Curcumin containing monoolein aqueous dispersions: A preformulative study. Mater Sci Eng C [Internet].2013;33(8):4923–4934. Available from: http://dx.doi.org/10.1016/j.msec.2013.08.017

43. Ding Y, Ding Y, Wang Y, Wang C, Gao M, Xu Y, et al. Soluplus®/TPGS Mixed Micelles for Codelivery of Docetaxel and Piperine for Combination Cancer Therapy. Pharm Dev Technol [Internet]. 2019;0(0):1–18. Available from: http://dx.doi.org/10.1080/10837450.2019.1679834

44. Garg NK, Singh B, Kushwah V, Tyagi RK, Sharma R, Jain S, et al. The ligand (s) anchored lipobrid nanoconstruct mediated delivery of methotrexate: An effective approach in breast cancer therapeutics. Nanomedicine Nanotechnology, Biol Med [Internet].2016;12(7):2043–2060. Available from: http://dx.doi.org/10.1016/j.nano.2016.05.008

45. Peram MR, Jalalpure S, Kumbar V, Patil S, Joshi S, Bhat K, et al. Factorial design based curcumin ethosomal nanocarriers for the skin cancer delivery: in vitro evaluation. J Liposome Res [Internet]. 2019;29(3):291–311. Available from: https://doi.org/10.1080/08982104.2018.1556292

46. Yin Win K, Feng SS. Effects of particle size and surface coating on cellular uptake of polymeric nanoparticles for oral delivery of anticancer drugs. Biomaterials. 2005;26(15):2713–2722.

47. Uttley M, Van Abbe N. Primary irritation of the skin : mouse ear test and human patch test procedures. J Soc Cosmet Chem. 1973;227:217–227.

48. Draize JH, Woodard G, Calvery HO. Methods for the Study of Irritation and Toxicity of Substances Applied Topically To the Skin and Mucous Membranes. J Pharmacol Exp Ther. 1944;82(3):377–390.

49. Han S, Shen JQ, Gan Y, Geng HM, Zhang XX, Zhu CL, et al. Novel vehicle based on cubosomes for ophthalmic delivery of flurbiprofen with low irritancy and high bioavailability. Acta Pharmacol Sin [Internet]. 2010;31(8):990–998. Available from: http://dx.doi.org/10.1038/aps.2010.98

50. OECD. Test No. 410: Repeated Dose Dermal Toxicity: 21/28-day Study. OECD Guidelines for Testing of Chemicals [Internet]. 1981; 1–8. Available from: https://www.oecd-ilibrary.org/environment/test-no-410-repeated-dose-dermal-toxicity-21-28-day-study_9789264070745-en

51. Sahu P, Kashaw SK, Sau S, Kushwah V, Jain S, Agrawal RK, et al. pH Responsive 5-Fluorouracil Loaded Biocompatible Nanogels For Topical Chemotherapy of Aggressive Melanoma. Colloids Surfaces B Biointerfaces [Internet]. 2019;174:232–245. Available from: https://doi.org/10.1016/j.colsurfb.2018.11.018

52. Overwijk WW, Restifo NP. B16 as a Mouse Model for Human Melanoma. Curr Protoc Immunol. 2000;39(1):1–29.

53. Yang H, Liu C, Zhang YQ, Ge LT, Chen J, Jia XQ, et al. Ilexgenin A induces B16-F10 melanoma cell G1/S arrest in vitro and reduces tumor growth in vivo. Int Immunopharmacol [Internet]. 2015;24(2):423–431. Available from: http://dx.doi.org/10.1016/j.intimp.2014.12.040

54. Zhai J, Tan FH, Luwor RB, Srinivasa RT, Ahmed N, Drummond CJ, et al. In Vitro and in Vivo Toxicity and Biodistribution of Paclitaxel-Loaded Cubosomes as a Drug Delivery Nanocarrier: A Case Study Using an A431 Skin Cancer Xenograft Model. ACS Appl Bio Mater. 2020;3(7):4198–4207.

55. Freag MS, Elnaggar YSR, Abdelmonsif DA, Abdallah OY. Stealth, biocompatible monoolein-based lyotropic liquid crystalline nanoparticles for enhanced aloe-emodin delivery to breast cancer cells: in vitro and in vivo studies. Int J Nanomedicine. 2016;11:4799-4818.

56. Jadhav K, Deore SL, Dhamecha D, Rajeshwari HR, Jagwani S, Jalalpure SS, et al. Phytosynthesis of silver nanoparticles : characterization , biocompatibility studies and anticancer activity. ACS Biomater Sci Eng. 2018; 4(3):892-899.

57. Kaur L, Jain SK, Manhas RK, Sharma D. Nanoethosomal formulation for skin targeting of amphotericin B: An in vitro and in vivo assessment. J Liposome Res [Internet]. 2015;25(4):294–307. Available from: http://dx.doi.org/10.3109/08982104.2014.995670

58. Bhowmick D, Bhar K, Mallick SK, Das S, Chatterjee N, Sarkar TS, et al. Para-Phenylenediamine Induces Apoptotic Death of Melanoma Cells and Reduces Melanoma Tumour Growth in Mice. Biochem Res Int. 2016.

59. Kumar S, Lather V, Pandita D. Stability indicating simplified HPLC method for simultaneous analysis of resveratrol and quercetin in nanoparticles and human plasma. Food Chem [Internet]. 2016;197:959–964. Available from: http://dx.doi.org/10.1016/j.foodchem.2015.11.078

60. Kurangi B, Jalalpure S, Jagwani S. A validated stability-indicating HPLC method for simultaneous estimation of resveratrol and piperine in cubosome and human plasma. J

Chromatogr B Anal Technol Biomed Life Sci [Internet]. 2019;1122–1123(May):39–48. Available from: https://doi.org/10.1016/j.jchromb.2019.05.017

61. Jagwani S, Jalalpure S, Dhamecha D, Jadhav K, Bohara R. Pharmacokinetic and Pharmacodynamic Evaluation of Resveratrol Loaded Cationic Liposomes for Targeting Hepatocellular Carcinoma. ACS Biomater Sci Eng. 2020;6(9):4969–4984.
62. Zhai Y, Xu R, Wang Y, Liu J, Wang Z, Zhai G. Ethosomes for skin delivery of ropivacaine: preparation, characterization and ex vivo penetration properties. J Liposome Res. 2015;25(4):316–324.
63. Mainardes RM, Evangelista RC. PLGA Nanoparticles Containing Praziquantel: Effect of Formulation Variables on Size Distribution. Int J Pharm. 2005; 290(1): 137–144.
64. Rizwan SB, McBurney WT, Young K, Hanley T, Boyd BJ, Rades T, et al. Cubosomes containing the adjuvants imiquimod and monophosphoryl lipid A stimulate robust cellular and humoral immune responses. J Control Release [Internet]. 2013;165(1):16–21. Available from: http://dx.doi.org/10.1016/j.jconrel.2012.10.020
65. Pal SL, Jana U, Manna PK, Mohanta GP, Manavalan R. Nanoparticle: An overview of preparation and characterization. J Appl Pharm Sci. 2011;1(6):228–234.
66. Hundekar YR, Saboji JK, Patil SM, Nanjwade BK. Preparation and evaluation of diclofenac sodium cubosomes for percutaneous administration. World J Pharm Pharm Sci. 2014;3(1):523–539.
67. Rizwan SB, Hanley T, Boyd BJ, Rades T, Hook S. Liquid crystalline systems of phytantriol and glyceryl monooleate containing a hydrophilic protein: characterisation, swelling and release kinetics. J Pharm Sci. 2009;98(11):4191–4204.

68. Rattanapak T, Young K, Rades T, Hook S. Comparative study of liposomes, transfersomes, ethosomes and cubosomes for transcutaneous immunisation: Characterisation and in vitro skin penetration. J Pharm Pharmacol. 2012;64(11):1560–1569.

69. Kohli AK, Alpar HO. Potential use of nanoparticles for transcutaneous vaccine delivery: effect of particle size and charge. Int J Pharm. 2004;275(1–2):13–17.

70. Zhang L, Li J, Tian D, Sun L, Wang X, Tian M. Theranostic combinatorial drug-loaded coated cubosomes for enhanced targeting and efficacy against cancer cells. Cell Death Dis [Internet]. 2020;11(1):1–12. Available from: http://dx.doi.org/10.1038/s41419-019-2182-0

71. Barry BW, BW B. Dermatological formulations: percutaneous absorption. J Pharm Sci. 1983;73(4):573.

72. Hadgraft J. Skin, the final frontier. Int J Pharm. 2001;224(1–2):1–18.

73. Clogston J, Craciun G, Hart DJ, Caffrey M. Controlling release from the lipidic cubic phase by selective alkylation. J Control release. 2005;102(2):441–461.

74. Abdelrahman FE, Elsayed I, Gad MK, Badr A, Mohamed MI. Investigating the cubosomal ability for transnasal brain targeting: In vitro optimization, ex vivo permeation and in vivo biodistribution. Int J Pharm. 2015;490(1–2):281–291.

75. Kurangi B, Jalalpure S, Jagwani S. Formulation and evaluation of resveratrol loaded cubosomal nanoformulation for topical delivery. Curr Drug Deliv. 2020;17:1–12.

76. Gour V, Agrawal P, Pandey V, Kanwar IL, Haider T, Tiwari R, et al. Nanoparticles and skin cancer [Internet]. Nano Drug Delivery Strategies for the Treatment of Cancers. INC; 2021; 245–273. Available from: http://dx.doi.org/10.1016/B978-0-12-819793-6.00011-4

77. Kwon TK, Kim J-C. Preparation and in vitro skin permeation of cubosomes containing hinokitiol. J Dispers Sci Technol. 2010;31(7):1004–1009.

78. Peng X, Zhou Y, Han K, Qin L, Dian L, Li G, et al. Characterization of cubosomes as a targeted and sustained transdermal delivery system for capsaicin. Drug Des Devel Ther. 2015;9:4209–4218.

79. Smith EW, Maibach HI. Percutaneous penetration enhancers. CRC Press; 1995; 393-405.

80. Norlén L, Al-Amoudi A. Stratum corneum keratin structure, function, and formation: the cubic rod-packing and membrane templating model. J Invest Dermatol. 2004;123(4):715–732.

81. Nasr M, Younes H, Abdel-Rashid RS. Formulation and evaluation of cubosomes containing colchicine for transdermal delivery. Drug Deliv Transl Res. 2020;10(5):1302–1313.

Animal Ethical Committee Approval letter

KLE College of Pharmacy
A Constituent Unit of
KLE Academy of Higher Education and Research
(Deemed to be University)
JNMC Campus, Nehru Nagar, Belagavi – 590 010, Karnataka, India
Phone: 0831-2471399 Fax: 0831-2472387 Web: http://www.klepharm.edu E-mail:principal@klepharm.edu

13-10-2018

CERTIFICATE

This is to certify that the research project,"**Cubosome based nano formulation of resveratrol and piperine for targeting Melanoma,**submitted by **Mr. Bhaskar K. Kurangi** under the guidance of Prof (Dr.) Sunil Jalalpure, has been approved in the Institutional Animal Ethics Committee meeting held on 13th October 2018, resolution No. KLECOP/CPCSEA-Reg.No.221/Po/Re/S/2000/CPCSEA, Res.26-13/10/2018 and was permitted to use -96-, sex Either Rats/ Mice/ Rabbits/Guinea pig.

You are hereby informed to strictly adhere to the protocol submitted for approval. Further you are required to keep the account of animals used for the project in specified Performa, Form D.

SECRETARY
Institutional Animal Ethical Committee,
KLES's College of Pharmacy,
BELGAUM - 590010

CPCSEA Nominee 13/10/18
Institutional Animal Ethics Committee
KLES's College of Pharmacy,
BELGAUM.

Journal of Chromatography B 1122–1123 (2019) 39–48

Contents lists available at ScienceDirect

Journal of Chromatography B

journal homepage: www.elsevier.com/locate/jchromb

A validated stability-indicating HPLC method for simultaneous estimation of resveratrol and piperine in cubosome and human plasma

Bhaskar Kurangi, Sunil Jalalpure*, Satveer Jagwani

Dr. Prabhakar Kore Basic Science Research Center, KLE Academy of Higher Education and Research, Nehru Nagar, Belagavi 590010, Karnataka, India
KLE College of Pharmacy, Belagavi, KLE Academy of Higher Education and Research, Nehru Nagar, Belagavi 590010, Karnataka, India

ARTICLE INFO

Keywords:
RP-HPLC
Resveratrol
Piperine
Stress degradation
Isosbestic point

ABSTRACT

Resveratrol and piperine are proven for their therapeutic benefits to treat various diseases. Due to their synergistic actions and combined drug delivery application, a rapid and specific RP-HPLC method was developed and validated as per ICH guidelines, by using an isosbestic point. The chromatographic separation was performed with Luna 5 µ 100 Å C-18(2) HPLC column by using acetonitrile (ACN): phosphate buffer (0.01% orthophosphoric acid) (55:45) as mobile phase, at 1 mL/min of flow rate and 330 nm. The developed method was found to be linear over the concentration range of 0.25–8 µg/mL with correlation coefficient value > 0.999. The developed method was accurate (percent recovery 98.06–101.74%), precise (percent relative standard deviation < 2.0%), and robust. The limit of detection and limit of quantification for resveratrol were found to be 0.02 and 0.08 µg/mL, respectively and 0.04 and 0.11 µg/mL, for piperine, respectively. The developed method was also validated in human plasma as per ICH guidelines. Moreover, stress degradation studies of both phytoconstituents were studied and the relevancy of the developed method was analyzed on cubosome nanoformulation. A good separation of drug peaks was observed in the presence of the degradation products. This method could thus be used for regular *in vitro* and *in vivo* estimation of piperine and resveratrol.

1. Introduction

The functional food phytoconstituents, especially alkaloids and polyphenols have attracted many researchers, as they have gained importance in the treatment of several diseases, including cancer. Resveratrol (3,4′,5-Trihydroxy-*trans*-stilbene; Fig. 1a) is a natural polyphenol phytoconstituent belonging to a stilbenoid family and present in grapes, wines, different berries, pistachios and peanuts. Even though resveratrol has a wide range of therapeutic applications, several studies have reported its bioavailability problem which has led to limitation of its therapeutic applicability [1]. Piperine [5-(3,4-methylenedioxyphenyl)-2,4-pentadienoylpiperidine; Fig. 1b] is a bioactive alkaloid, belonging to Piperaceae family and present in dried fruits of the black pepper (*Piper nigrum* Linn.), long pepper (*Piper longum* Linn.), and the fruits of other Piper species. It is commonly used for daily consumption and has application in diverse traditional systems.

Many studies have been carried out by combination-based techniques, which have led to improved resveratrol bioavailability, and its chemo-preventive and therapeutic responses [2,3]. Pre-clinical and clinical studies have shown that the co-supplementation of piperine with various other drugs significantly enhances their bioavailability [4–6]. These two phytoconstituents offer a promising therapeutic approach for cancer treatment by inducing apoptosis and have shown synergistic antidepressant effect [7,8]. Nowadays, to overcome the bioavailability problem of resveratrol, various researchers focus on the combinational strategies of these phytoconstituents to explore their beneficial synergistic effect through different nanotechnology-based delivery systems. Hence, in the present study, we ideate to formulate resveratrol and piperine entrapped cubosome nanoformulation. The required therapeutic activity of any drug can be correlated from the accurate estimation of drugs entrapped within the nanoformulation.

There are different types of analytical methods available for the estimation of resveratrol and piperine individually, but none are reported for a simple RP-HPLC method for simultaneous estimation of piperine and resveratrol in plasma and nanoformulation. In a study, Jasoliya and Jani developed RP-HPLC method for capsule dosage form containing resveratrol and piperine by simultaneous estimation method. The method seemed to be less realistic because of the absence of stability indicated by stress degradation study, and validation assay in plasma. Moreover, two different wavelengths - 305 and 336 nm were

* Corresponding author at: Dr. Prabhakar Kore Basic Science Research Center, KLE College of Pharmacy, Belagavi, KLE Academy of Higher Education and Research, Nehru Nagar, Belagavi 590010, Karnataka, India.
E-mail address: jalalpuresunil@rediffmail.com (S. Jalalpure).

https://doi.org/10.1016/j.jchromb.2019.05.017
Received 1 February 2019; Received in revised form 26 April 2019; Accepted 14 May 2019
Available online 16 May 2019

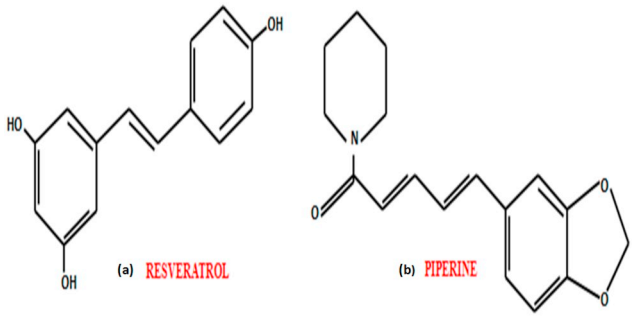

Fig. 1. Chemical structures of (a) resveratrol and (b) piperine.

used for the detection of resveratrol and piperine, demonstrating large differences which complicated the analysis [9]. In another study, by Qu et al., an ultra high-performance liquid chromatography (UPLC) method for simultaneous estimation of twelve components in Zuozhu Daxi (a Tibetan medicine) was developed. In this method, the maximum wavelength of detection (λ_{max}) was fixed at 306 nm for protopine, resveratrol and piperine [10]. In the present study, we aimed to develop and validate an isosbestic point-based HPLC method for simultaneous estimation of resveratrol and piperine.

Isosbestic point is the specific wavelength at which two compounds have the same molar absorptivities or the point which can correlate with a specific wavelength, where an absorption spectra of the two compounds can cross with each other (Fig. 2). Although many compounds are simultaneously estimated based on the isosbestic point method [11,12] none has been reported for estimation of piperine and resveratrol. Henceforth, with the help of an isosbestic point method, the simultaneous quantification of these phytoconstituents and finally, the data interpretation can be made simple.

The aim of the proposed research study was to develop and validate stability showing isosbestic point based RP-HPLC method for simultaneous analysis of resveratrol and piperine in accordance with ICH (International Conference on Harmonization) guidelines. This method was also applied in resveratrol and piperine entrapped cubosome nanoparticles and human plasma. Different stress or forced degradation study methods like acidic, alkaline, oxidative, thermal and sunlight were performed to confirm the suitability of the developed method.

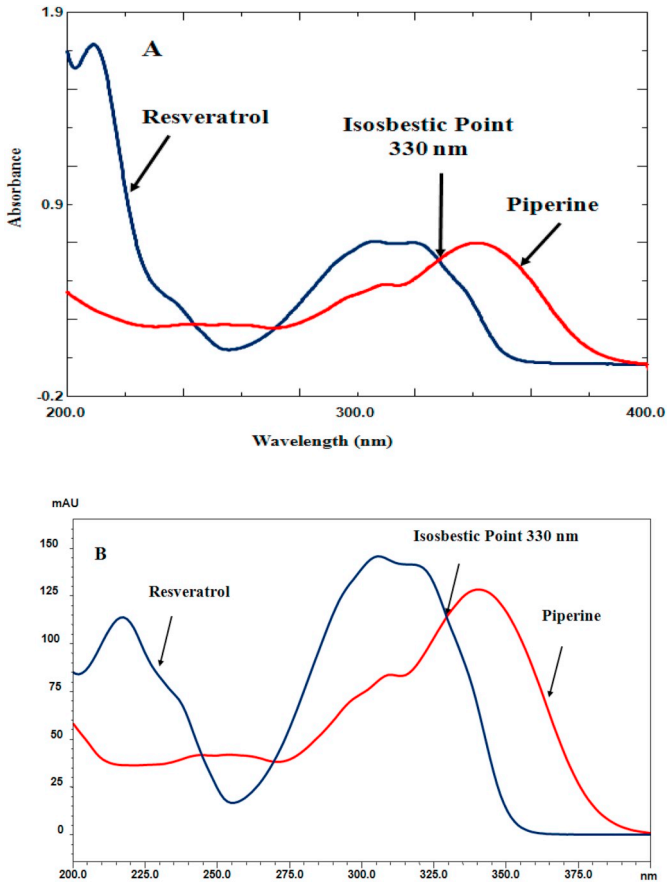

Fig. 2. UV–Vis absorption spectra displaying isosbestic λ max at 330 nm for resveratrol and piperine (A) and spectra obtained by PDA detector connected to HPLC (B).

2. Materials and methods

2.1. Reagents and solvents

Resveratrol (95%) and piperine (95%) were provided by Sami Labs Ltd. Bangalore, India. Glyceryl monooleate (GMO) and poloxamer 407 -P407(lutrol F127) were gifted by Mohini Organics Pvt. Ltd. Mumbai, India and BASF, Mumbai, India, respectively. HPLC-grade methanol, acetonitrile (ACN) and orthophosphoric acid (OPA) were purchased from Fisher Scientific Mumbai, India. The fresh blood sample was collected from KLE Hospital Blood Bank, Belagavi, India. Throughout the study, HPLC analytical-grade water (Merck, Mumbai, India) was used. All the other solvents or reagents used were of pharmaceutical or analytical grade.

2.2. Chromatography instrument and conditions

Shimadzu HPLC prominence instrument system (LC-20AD, Japan) equipped with SPD-M20A prominence diode array detector (PDA), LC-20AD pump, a SIL-20AC HT auto sampler, DGU-20A5 online degasser, rheodyne injection value with 20 µL loop and CTO-10AS VP column oven. The data interpretation and analysis were done using software Shimadzu LC solution (version 1.25).

Chromatographic separation and analysis were carried out using phenomenex Luna C18 analytical column C-18(2) 100 Å (250 × 4.60 mm internal diameter, 5 µm particle size, Phenomenex Inc., Canada, USA) at a column temperature of 35 °C. The optimized mobile phase ACN: Phosphate buffer [0.01% OPA; 55:45 v/v] was adjusted to pH 6 with sodium hydroxide and pumped through the column at a flow rate of 1 mL/min. Prior to use, the mobile phase was filtered through PVDF filter membrane (0.45 µm; Millex HV®, Millipore, USA) and ultrasonically degassed. The volume for injection was kept at 10 µL for the sample analysis. The isosbestic point of phytoconstituents i.e. 330 nm, was used for simultaneous estimation.

2.3. Primary stock and standard sample preparation

Primary stock solutions of resveratrol and piperine were individually prepared at a concentration of 1 mg/mL in methanol. The standard preparation of resveratrol, piperine and both the drugs were prepared in the concentration range of 0.25–8 µg/mL, by the dilution of stock solution using the mobile phase. All standard solution preparations were stored in light-resistant, amber-colored, tightly-stoppered volumetric flask and kept at 4 °C, prior to the HPLC analysis.

2.4. Method development

The development of method for simultaneous analysis of piperine and resveratrol was done by using different mobile phase ratios, concentration and pH values of OPA, flow rates, and column oven temperature.

2.5. Method validation

According to ICH guidelines the validation of the developed method was done for system suitability, linearity, limit of quantification (LOQ), limit of detection (LOD), accuracy, precision, ruggedness, and robustness.

2.6. Preparation of Cubosome nanoparticles

Top-down approach such as homogenization technique was used to prepare cubosome nanoparticles [13]. The cubosome formulation was optimized from the different concentrations of lipid (glycerol monooleate) and stabilizer (polymer i.e. lutrol F 127).

Briefly, the optimized batch containing glycerol monooleate (2100 mg) and lutrol F127 (150 mg) were melted in separate beaker in thermostatic water bath at 70 °C. Resveratrol (10 mg) and piperine (10 mg) were added in molten lipid and mixed into preheated, aqueous lutrol F127 solution. The mixture (7.5%) was subsequently added in drop-wise manner to the preheated water (92.5%) at the same temperature of mixture under constant stirring. Finally, the mixture was homogenized (IKA T25 digital Ultra Turax, Germany) at 15,000 rpm for 15 min, followed by probe sonication (RivoTEK, Mumbai) for 5 min. The cubosome formulation was allowed to equilibrate for 24 h and used for further investigation. The average particle size, distribution (polydispersity index - PDI), and zeta potential values of the prepared cubosome were analyzed by dynamic light scattering (Zetasizer, Malvern Instruments, Malvern, UK) [14]. The developed HPLC method was used for simultaneous estimation of resveratrol and piperine in optimized cubosome nanoformulation. Encapsulation efficiency of cubosome nanoformulation was evaluated by centrifugation (Kubota 6500, Japan) at 15,000 rpm for 30 min. The supernatant solution obtained after centrifuge was mixed with mobile phase and further analyzed by using HPLC [15,16]. For the recovery study in cubosomes the standard solutions of drugs were spiked to blank cubosome nanoparticles.

2.7. Extraction of drug from plasma and processing

The fresh human blood was obtained from the KLE Hospital blood bank, Belagavi. Plasma was collected by centrifugation of blood sample at 4000 rpm for 15 min and at 4 °C.

Stock solutions (1 mg/10 mL) of both resveratrol and piperine were prepared in methanol. Plasma standards for both the drugs were prepared by spiking plasma with the stock solution of drugs to obtain required concentrations. In each drug extraction process, 100 µL of plasma was added to 50 µL of stock solution of drugs and mixed for 1 min on the vortex mixer (Eppendorf, India). For getting high recovery, plasma protein was precipitated with the addition of 100 µL of ACN [17]; 50 µL of methanol was added to make up 300 µL volume, then vortexed for 1 min. Centrifugation was done at 15,000 rpm for 10 min, after which the supernatant solution was collected, filtered and injected (20 µL) for the analysis [18].

2.8. Validation of method in human plasma

The developed method was validated in human plasma for linearity, sensitivity, recovery, and stability according to ICH guidelines and US food drug administration bioanalytical method validation guidance [19,20].

2.8.1. Selectivity

The selectivity of the developed method was evaluated by analyzing six randomly selected human blank plasma extracted samples. The method selectivity was checked for endogenous interference or matrix effects of plasma components with the drugs.

2.8.2. Linearity

The linearity of the method in plasma was evaluated by injecting different concentrations of the standard solution of resveratrol and piperine. Stock solutions (1 mg/10 mL) of both were prepared in methanol. Plasma was spiked with appropriate amounts of respective standard stock solution to yield the concentrations in the ranges from 0.25 to 8 µg/mL.

2.8.3. Recovery

Plasma standards for both the drugs were prepared by spiking plasma with the respective stock solution to obtain the required concentrations such as 0.84, 1.66, and 2.5 µg/mL. The extraction recovery of resveratrol and piperine from the biological plasma matrix was estimated by comparing the concentrations measured in the plasma, with the concentrations added.

2.8.4. Sensitivity

The lower limit of detection (LLOD) and LOQ were calculated from a calibration curve.

2.8.5. Stability [21]

The stability study was conducted to determine the concentration of the studied drugs, after each storage period, and it was correlated with the initial concentration as zero cycle (samples that were freshly prepared and processed immediately).

2.8.5.1. Freeze–thaw stability. The freeze–thaw stability of the studied drugs was determined at low, medium, and high concentration samples (0.5, 2 and 8 µg/mL respectively), over 3 cycles within three days. In each cycle, the frozen plasma samples were thawed at room temperature for 2 h and refrozen for 24 h. After completion of each cycle the samples were analyzed and the results were compared with that of the zero cycle.

2.8.5.2. Short-term stability (bench-top stability). Aliquots each of the low, medium, and high concentration (0.5, 2, 8 µg/mL respectively) unprocessed samples were kept at room temperature for 24 h, following which the samples were analyzed and the results were compared with that of the zero cycle.

2.9. Forced or stress degradation studies

ICH recommended stress conditions like acidic, alkaline, thermal, oxidative, and photolytic conditions were employed for the controlled forced or stress degradation studies, for individual and mixed analytes matrix solutions of piperine and resveratrol [22]. Preparation of samples were done in each stress degradation conditions as, drug solutions stored under normal conditions at zero time and the drug solution supposed for the degradation for 1 h. In the study of acid-base degradation, 1 mL of stock solution of drug mixture containing resveratrol and piperine were treated with 1 mL of 1 N hydrochloric acid (HCl) and 1 mL of 1 N sodium hydroxide (NaOH) solutions, separately. After sealing, the amber-colored volumetric flasks containing the above-mentioned solutions, they were heated for 1 h at 80 °C. Before analysis, both the samples were neutralized. In a study of oxidative degradation, 1 mL of stock solution of the drug mixture was treated with 1 mL of 30% hydrogen peroxide (H_2O_2) solution. Thermal degradation study was performed by the treatment of 1 mL of stock solutions of drug mixture with 2 mL of methanol in an amber-colored volumetric flask. After sealing the volumetric flasks containing above-mentioned solutions, they were heated for 1 h at 80 °C. For studying the photochemical degradation, 1 mL of stock solution of drug mixture was taken in a transparent volumetric flask (10 mL) and diluted up to 10 mL with mobile phase. After sealing, volumetric flask was exposed to direct sunlight for 30 min to study their photochemical stability. For all the above-mentioned studies, the final volume was adjusted by mobile

phase up to 10 mL. After filtration through syringe filters (0.2 µm), further analysis was done by injecting sample solution into HPLC-chromatographic system [23,24].

3. Results and discussion

3.1. Development and optimization of the method

A new, robust and isosbestic point-based RP-HPLC method was established for the simultaneous determination of resveratrol and piperine. For getting an isosbestic point, the UV spectra for methanolic solution of both the drugs (10 µg/mL) was run at 200–400 nm range. The maximum UV absorption of resveratrol and piperine was observed at 306 and 341 nm, respectively. The selection of an isosbestic point for piperine and resveratrol was done on the basis of UV–absorption spectra and the spectra obtained from the HPLC system connected to DAD detector, where the spectra crossed with each other on a common point – 330 nm, which shows maximum absorbance (Fig. 2).

The different parameters such as mobile phase composition, their pH and flow rate, wavelength detection, and column oven temperature was optimized for the development of effective chromatographic method. In order to get sharp and well separated peaks, many trials were done with different mobile phase compositions which include ACN, methanol, diluted OPA, and water. Analysis of both the drugs was done at their respective λ_{max} and at the isosbestic point observed (Fig. 2). Initially, the composition of ACN: methanol: diluted OPA provided the acceptable results with good resolution but having less peak separation. In contrast, ACN: diluted OPA composition demonstrated the results as sharp well-defined peaks, with poor resolution and less separation. Hence, methanol and water were replaced, while ACN and diluted OPA were retained as components of the mobile phase. The 0.1% OPA produced broad peaks with less resolution, which occurs because of less efficient elution from the column. Improvement in the sharpness of the peak was observed by decreasing the concentration of OPA. Hence, the different compositions of ACN: 0.01% OPA was studied which yielded high resolution and good separation of peaks, without any tailing.

The pH effect was also studied by adding NaOH solution to OPA of the mobile phase. Phosphate buffer system consisting 0.01% concentration of OPA was selected for getting sharp peaks with greater resolution since both the drugs in acidic condition of 0.1% OPA yielded less intense peaks with poor resolution. Phosphate buffer (0.01% OPA v/v) with pH 6 gave sharper peak for piperine without affecting the peak characteristics of resveratrol. The column temperature has a considerable effect on retention time and peak shape of both drugs, which was tested by varying the temperature in between 20 °C to 40 °C. Optimized temperature was set as 35 °C based on the sharpness of peak and shortest retention time. The mobile phase composition containing ACN: phosphate buffer (0.01% OPA v/v) at ratio of 55:45 with 1 mL/min of flow rate was found to be most acceptable. The retention time was found to be 3.31 and 9.19 min for resveratrol and piperine, respectively. From Fig. 3, it was evident that both the drugs displayed excellent peak characteristics with less tailing.

3.2. Method validation

Validation of analytical method deals with the aim to ensure that the developed method is acceptable and reliable for its deliberate purpose. As per ICH guidelines (Q2R1), the developed HPLC method was validated for different validation characteristics such as system suitability, linearity, accuracy, precision, LOD, LOQ, robustness, and ruggedness.

3.2.1. System suitability

The system suitability ensures the validity and specificity of the developed method. This test represents an essential component of the method development and is utilized to confirm the resolution and reproducibility of the developed technique, for performing chromatographic analysis. The percent RSD of different parameters such as peak area, retention time (tR), theoretical plates, and tailing factor were determined (Table 1). The percent RSD of peak area (< 2), tailing factor (< 2), and theoretical plates ($N > 2000$) were within the acceptable limits. An isosbestic point based method thus assures and satisfies the system suitability parameters and ensures the suitability of the developed HPLC method. The peaks obtained for resveratrol and piperine were found to be sharp, well separated and with high resolution as shown in Fig. 3. The results obtained for the above parameters reveal the suitability of the selected chromatographic system for further validation and analysis of resveratrol and piperine.

3.2.2. Linearity

Linearity is the ability of the analytically-developed procedure to

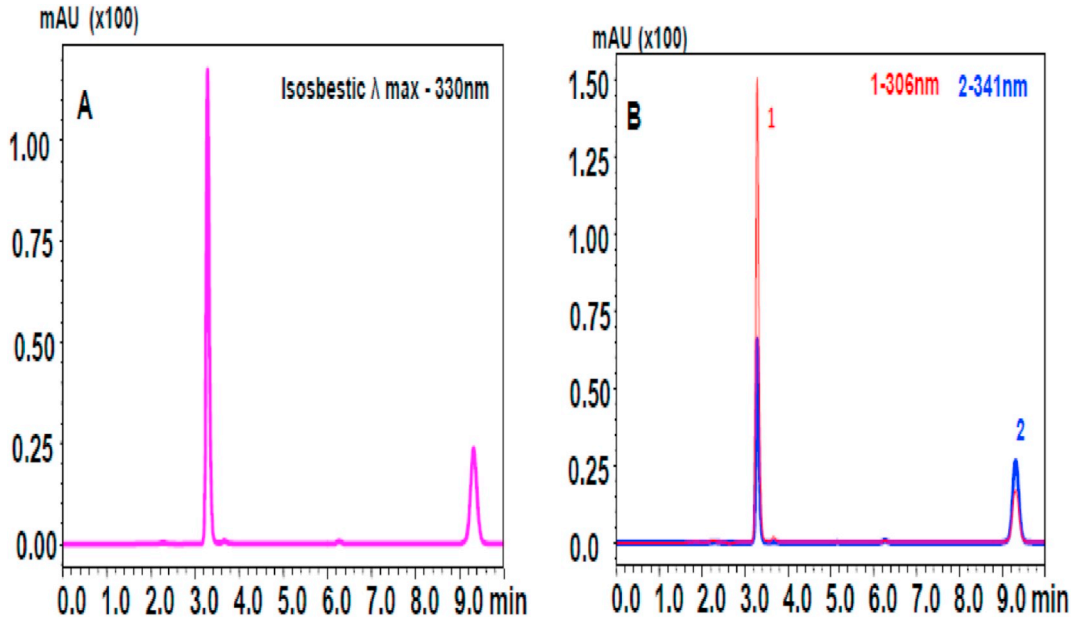

Fig. 3. HPLC chromatograms at A) isosbestic λ max - 330 nm, B) individual λ max - 306 (1) and 341 (2) nm with respective for resveratrol and piperine.

Table 1
System suitability study parameters for the developed method of resveratrol and piperine (N = 6).

Parameter	Resveratrol		Piperine	
	Mean ± SD	%R.S.D.	Mean ± SD	%R.S.D.
tR (min)	3.30 ± 0.00	0.09	9.28 ± 0.03	0.28
Peak area	384,300 ± 4784	1.24	225,540 ± 3786	1.68
Plate count	6916 ± 104	1.51	16,023 ± 145	0.91
Tailing factor	1.37 ± 0.02	1.22	1.07 ± 0.01	0.51

SD – Standard deviation; tR - retention time; RSD - relative standard deviation.

Table 2
Linear regression data and sensitivity parameters of the developed method.

Analyte	Concentration range (μg/mL)	Slope	Intercept	R^2	LOD (μg/mL)	LOQ (μg/mL)
At 306 and 341 nm (resveratrol and piperine respectively) - individual λ max						
Resveratrol	0.25–8	77,001	2858	0.999	0.03	0.10
Piperine	0.25–8	63,831	4212	0.999	0.04	0.12
At 330 nm - an isosbestic point						
Resveratrol	0.25–8	59,731	2155	0.999	0.02	0.08
Piperine	0.25–8	57,646	4107	0.999	0.04	0.11

R^2 - Regression coefficient; LOD - limit of detection; LOQ - limit of quantification.

check the result of the sample analytes whether it is linear to its concentration. Linearity of the method was tested by analyzing different concentration range (0.25–8 μg/mL) of piperine and resveratrol, individually, at their maximum wavelength of 341 and 306 nm, respectively, and simultaneously at 330 nm (isosbestic point). The regression analysis data for the calibration curve shows linear relation over this concentration range for resveratrol and piperine. The correlation coefficient values for both drugs were found to be $R^2 > 0.999$ which suggested excellent correlation and good linearity for the optimized method (Table 2).

3.2.3. Limit of quantification (LOQ) and limit of detection (LOD)

LOD and LOQ were calculated as:

$$LOD = 3.3 \times \delta/s \quad LOQ = 10 \times \delta/s$$

where

δ Standard deviation of y-intercept
s Mean slope of calibration curves

LOD is the lowest, detectable concentration of the analyte and provides a signal-to-noise ratio of 3, whereas LOQ is the analytes lowest, quantifiable concentration and gives the signal-to-noise ratio of 10. At the isosbestic point of the present study, LOD and LOQ were found to be 0.02 and 0.08 μg/mL for resveratrol and 0.04 and 0.11 μg/mL for piperine respectively. From the LOD and LOQ values, it was inferred that the optimized method was sensitive to determine the entrapment efficiency of resveratrol and piperine in cubosomal nanoparticles. Similarly, LOD and LOQ were also determined at their separate λ max where insignificant differences were observed as shown in Table 2.

3.2.4. Precision

Precision is a measure of degree of scattered readings of the developed method between the numbers of reading resulted from various samplings of a similar sample under the specified analytical procedures. In the present study, intra-day and inter-day assays were used to test the precision. Analysis of precision was done on the same day at different time intervals by determining repeatability (intra-day precision), and on three consecutive days, by determining intermediate precision (inter-day precision) for different concentrations of analytes such as low, intermediate and high (0.5, 2 and 4 μg/mL) concentrations. For intra-day precision, the percent RSD values ranged from 0.14 to 0.49% for resveratrol, 0.24–0.77% for piperine, respectively. In inter-day precision, the percent RSD values were ranged between 0.49–1.96% and 0.63–1.96% for resveratrol and piperine, respectively. As a result, the percent RSD values were lower than 2% in both the precision studies, which satisfied the acceptance criteria (Table 3) and indicated high precision of the developed method.

3.2.5. Accuracy

The closeness of experimental and true value or an accepted reference value signifies the accuracy of analytical procedure. Both the accuracy and precision are related to the method's repeatability and were determined by recovery experiments.

Known quantity of combined samples of resveratrol and piperine were spiked in triplicate injections at low, medium and high concentrations (50, 100, and 150% respectively) of a specified concentration to a previously analyzed sample solutions of resveratrol and piperine (5 μg/mL) and further analyzed by using developed method. The mean percentage recovery of resveratrol and piperine were found to be in the range of 98.06 to 101.47% and 98.51 to 101.74% respectively (Table 4), resulting in low percent RSD and high recovery values, which indicates an excellent accuracy for the developed method.

3.2.6. Ruggedness and robustness

Ruggedness and robustness of the developed method were measured by intentional changes in method conditions, which provide a reliable and authentic estimation of drug compounds.

Slight changes were made in the HPLC chromatography parameters

Table 3
Intraday and interday precision of resveratrol and piperine.

Compound	Active content (μg/mL)	Intraday (n = 3)		Interday (n = 3)					
				1st day		2nd day		3rd day	
		Found ± SD	RSD	Found ± SD	RSD	Found ± SD	RSD	Found ± SD	RSD
		(μg/mL)	(%)	(μg/mL)	(%)	(μg/mL)	(%)	(μg/mL)	(%)
Resveratrol	0.5	0.5 ± 0.002	0.31	0.49 ± 0.006	1.12	0.51 ± 0.010	1.96	0.49 ± 0.006	1.12
	2	2.04 ± 0.010	0.49	1.97 ± 0.020	1.02	2.04 ± 0.010	0.49	2.05 ± 0.015	0.74
	4	4.02 ± 0.016	0.14	3.92 ± 0.025	0.64	4.09 ± 0.045	1.10	3.97 ± 0.066	1.65
Piperine	0.5	0.49 ± 0.001	0.24	0.49 ± 0.006	1.17	0.51 ± 0.006	1.12	0.51 ± 0.010	1.96
	2	2.03 ± 0.015	0.75	2.04 ± 0.026	1.30	2.01 ± 0.036	1.79	1.97 ± 0.035	1.79
	4	3.97 ± 0.031	0.77	4.05 ± 0.035	0.87	3.99 ± 0.025	0.63	3.93 ± 0.046	1.18

RSD - relative standard deviation.

Table 4
Recovery studies of the developed method (n = 3).

Compound	Active Content (μg/mL)	Level (%)	Spiked quantity (μg/mL)	Recovered quantity (μg/mL)	Recovery (%)	RSD (%)
Resveratrol	5	50	2.41 ± 0.01	2.40 ± 0.02	99.63	0.87
	5	100	5.01 ± 0.09	4.91 ± 0.03	98.06	0.62
	5	150	7.45 ± 0.09	7.56 ± 0.07	101.47	0.97
Piperine	5	50	2.40 ± 0.02	2.41 ± 0.02	100.36	0.98
	5	100	4.93 ± 0.07	4.86 ± 0.05	98.51	0.93
	5	150	7.57 ± 0.09	7.70 ± 0.06	101.74	0.78

RSD - relative standard deviation.

Table 5
Robustness and ruggedness evaluation of developed method for piperine and resveratrol.

Parameters	Changes made	Resveratrol		Piperine	
		Retention time ± S.D.	RSD (%)	Retention time ± S.D.	RSD (%)
Composition of mobile phase [ACN: phosphate buffer (0.01% OPA)]	55:45	3.30 ± 0.006	0.17	9.30 ± 0.006	0.06
	53:47	3.29 ± 0.006	0.18	9.89 ± 0.025	0.25
	57:43	3.42 ± 0.010	0.29	8.93 ± 0.015	0.17
Concentration of OPA	0.01%	3.30 ± 0.006	0.17	9.30 ± 0.006	0.06
	0.10%	3.34 ± 0.010	0.30	9.32 ± 0.006	0.06
Flow rate	1 mL/min	3.30 ± 0.006	0.17	9.30 ± 0.006	0.06
	0.9 mL/min	3.56 ± 0.015	0.43	9.98 ± 0.006	0.06
	1.1 mL/min	3.01 ± 0.010	0.33	8.48 ± 0.015	0.18
Detection wavelength	330 nm	3.30 ± 0.006	0.17	9.30 ± 0.006	0.06
	332 nm	3.30 ± 0.010	0.30	9.30 ± 0.006	0.06
	328 nm	3.30 ± 0.006	0.17	9.30 ± 0.000	0.00
Column oven temperature	35 °C	3.30 ± 0.006	0.17	9.30 ± 0.006	0.06
	30 °C	3.36 ± 0.006	0.17	9.44 ± 0.017	0.18
pH of OPA	6	3.30 ± 0.006	0.17	9.30 ± 0.006	0.06
	3	2.41 ± 0.015	0.63	6.27 ± 0.049	0.80

RSD - relative standard deviation.

such as flow rate (± 0.1), concentration of OPA (± 0.09%), pH (± 3), mobile phase composition (± 2%), and λ_{max} (± 2). The instrument condition including column oven temperature (± 5 °C) was also changed. Analyte concentration for the present study was selected to be 10 μg/mL and the results showed that the percent RSD values (< 1) and retention time remained unaffected, which confirm the robustness of the developed HPLC method. However, the small changes in methodology did not influence the reliability of the method; hence it was more authentic one (Table 5).

3.3. Characterization of cubosome

The blank and drug-loaded cubosome nanoformulation prepared by using homogenization has shown the mean particle size to be 151 and 159 nm, respectively. The average PDI for blank and drug-loaded cubosome was 0.23 and 0.16, respectively, indicating that the PDI value is < 0.3 which showed narrow homogeneous particle size distribution. The zeta potential is the main parameter in determining the nanoparticulate system stability [25]. The average zeta potential for blank and drug-loaded cubosome was −21.1 and −17.60 mV, respectively. These zeta potential values suggest moderate degree of stability in cubosome nanoparticles. The negative charge was imparted due to the free fatty acids of glycerol monooleate lipid structure.

The developed RP-HPLC method was utilized to estimate the encapsulation efficiency (EE) of piperine and resveratrol in a cubosome nanoformulation. The HPLC chromatogram had shown intense characteristic peaks of resveratrol and piperine in cubosome nanoparticles [Fig. 4(c)]. The analysis of percent EE was done by estimating free and total drug in a cubosome nanoformulation and mean percent EE was obtained to be 90.18% for resveratrol whereas for piperine it was 94.66% (Table 6). The high percent EE of both drugs in cubosomes may be due to the surfactant concentration which is sufficient to solubilize high quantity of resveratrol and piperine in lipid vesicle, thereby significantly increasing their concentrations the cubosome formulation.

3.4. Recovery assay in cubosome

Recovery assay was utilized in the evaluation of accuracy of developed HPLC method for the quantification of resveratrol and piperine in cubosome nanoparticles. Triplicate injections containing both the drugs of known concentration at different levels such as 50%, 100% and 150% were spiked with known concentration of samples (pre-analyzed), and their percentage recovery was evaluated by comparing real and observed concentrations of the drugs. The mean percentage recoveries of resveratrol and piperine from cubosome were found to be between the 98–102% ranges, which were within the accepted limits (80–120%) as shown in Table 7. The high percent recovery values obtained thus proves the applicability of this developed method for wide range of sample analysis. The chromatogram of resveratrol and piperine containing cubosome nanoformulation sample was given in Fig. 4(c).

3.5. Method validation in plasma

As per ICH guidelines (M 10) and US food drug administration bioanalytical method validation guidance, the developed HPLC method

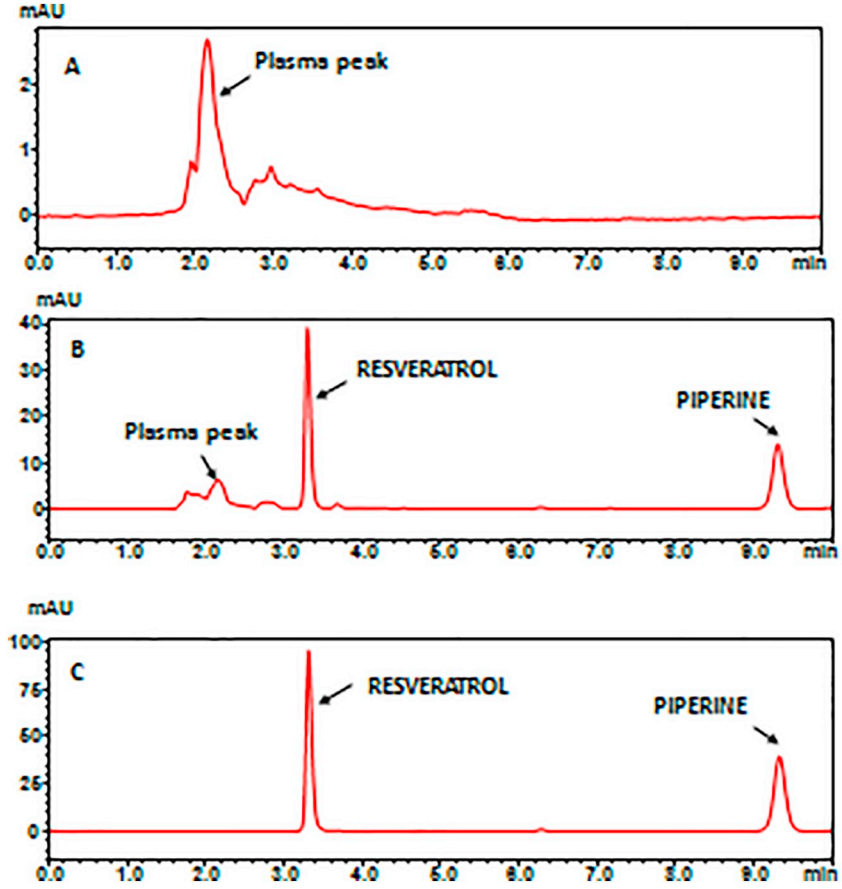

Fig. 4. HPLC chromatograms of blank human plasma (A), resveratrol and piperine in plasma sample (B) and in cubosome nanoparticles (C).

Table 6
Characterization of resveratrol and piperine entrapped cubosome.

Cubosome formulation	Particle size diameter (nm)	PDI	Zeta potential value (mV)	% EE	
				Piperine	Resveratrol
Blank cubosome	151 ± 9.07	0.23 ± 0.02	−21.1 ± 2.69	–	–
Resveratrol and piperine loaded cubosome	159 ± 11.02	0.16 ± 0.03	−17.60 ± 1.86	94.66 ± 3.7	90.18 ± 2.23

Mean ± SD, N = 6; EE - encapsulation efficiency; PDI - polydispersibility index.

was validated for different validation parameters like selectivity, linearity, sensitivity (LLOD and LOQ), recovery, and stability studies.

3.5.1. Selectivity

Absence of an interfering peak of plasma at the retention times of resveratrol and piperine is an evidence for method selectivity. This was clearly indicated from the chromatogram obtained from the blank plasma, and the drug samples in plasma preparations. Chromatograms of both blank human plasma and the samples of resveratrol and piperine in plasma are given in Fig. 4(a) and (b).

Table 7
Recovery studies of the spiked resveratrol and piperine from cubosome nanoformulation (n = 3).

Drug	Spiked (μg)	Found (μg)	% recovery
Resveratrol	5.12 ± 0.08	5.18 ± 0.06	101.24
	10.49 ± 0.09	10.28 ± 0.09	98.03
	15.30 ± 0.11	15.72 ± 0.09	102.77
Piperine	5.01 ± 0.10	5.08 ± 0.08	101.46
	10.23 ± 0.09	10.04 ± 0.10	98.17
	15.69 ± 0.09	15.58 ± 0.09	99.29

n - replicate number.

Table 8
Linear regression data and sensitivity parameters of the developed method in human plasma.

Analyte	Concentration range (μg/mL)	Slope	Intercept	R^2	LLOD (μg/mL)	LOQ (μg/mL)
At 306 and 341 nm (resveratrol and piperine respectively) - individual λ max						
Resveratrol	0.25–8	13,070	3281	0.999	0.06	0.20
Piperine	0.25–8	3699	2340	0.999	0.07	0.21
At 330 nm - an isosbestic point						
Resveratrol	0.25–8	10,203	2083	0.999	0.06	0.20
Piperine	0.25–8	3381	1889	0.999	0.07	0.22

R^2 - Regression coefficient; LLOD - lower limit of detection; LOQ - limit of quantification.

Table 9
Recovery studies of the spiked resveratrol and piperine from human plasma (n = 3).

Drug	Spiked (μg)	Found (μg)	% recovery
Resveratrol	0.84 ± 0.01	0.83 ± 0.08	98.33
	1.66 ± 0.01	1.68 ± 0.03	101.33
	2.5 ± 0.02	2.55 ± 0.06	102.16
Piperine	0.8 ± 0.03	0.79 ± 0.07	98.75
	1.62 ± 0.04	1.64 ± 0.02	101.23
	2.53 ± 0.06	2.53 ± 0.06	100.16

n - replicate number.

3.5.2. Linearity

Linearity of the assay method was tested by analyzing different concentration range (0.25–8 μg/mL) of piperine and resveratrol individually at their maximum wavelength 341 and 306 nm respectively and simultaneously at 330 nm (isosbestic point). The regression analysis data for the calibration curve shows linear relation over this concentration range. The correlation coefficient values for both drugs were found to be $R^2 > 0.999$ which suggest excellent correlation and good linearity for the optimized method as per ICH guidelines (Table 8).

3.5.3. Sensitivity

The LLOD and LOQ were found to be 0.06 and 0.20 μg/mL for resveratrol, and 0.07 and 0.21 μg/mL for piperine, respectively at their individual λ_{max}. Similarly, LLOD and LOQ were also determined at the isosbestic point where insignificant differences were observed as shown in Table 8. From the LLOD and LOQ values it was indicated that the optimized method was found to be a sensitive one.

3.5.4. Recovery

The measure of accuracy i.e. percentage recovery, was determined by observing the proximity of the observed drug concentration values with the actual concentration values. The recovery assay was performed by spiking a known concentration of standard (pre-analyzed) in triplicate at different levels such as 50%, 100% and 150%. The mean percentage recoveries of resveratrol and piperine from the plasma were found to be between 98 and 102%, as shown in (Table 9). The high percentage recovery values obtained thus proves the applicability of this developed method for wide range of sample analysis.

3.5.5. Stability

Freeze-thaw and bench-top (short-term) stability for resveratrol and piperine were evaluated at the low, medium and high concentration (0.5, 2, and 8 μg/mL, respectively) samples. The results revealed that both the drugs were stable in plasma for 24 h at room temperature. It was also observed that the plasma samples experiencing freezing and thawing (3 cycles) with resveratrol and piperine at all low, medium and high concentration levels did not influence their stability (Table 10).

3.6. Forced or stress degradation studies

The results of forced degradation studies for individual and mixed analytes matrix are presented in Table 11. From the results, it was clear that both the analytes such as resveratrol and piperine were less degraded in mixed matrix solution form as compared to the individual solutions under different forced degradation conditions. The applicability of the developed method can be proved from this study, as there was adequate separation observed between drug peaks and their degraded product peaks (Fig. 5).

For mixed analyte matrix solutions, in the acid degradation study, percent degradation of resveratrol and piperine was found to be 13.48% and 17.67%, respectively in 1 N HCl. Analysis of resveratrol showed one insignificant, small degraded peak whereas for piperine degrading peak was absent. The result for acid degradation study has demonstrated that both the drugs were stable and less prone to degradation in acidic condition. In alkaline degradation study, 19.82% resveratrol was degraded whereas piperine degradation was only 14.05%. Two degraded peaks of resveratrol were observed near the parent peak whereas piperine does not show any degrading peaks in alkaline condition. As resveratrol is weakly acidic in nature, it is more prone to degradation at alkaline condition. Hence, resveratrol was found to be more unstable in

Table 10
Stability of resveratrol and piperine in human plasma at different conditions (n = 3).

Drug	Spiked (μg)	Zero cycle 0 h (μg)	Found (μg) 24 h 1st cycle	Found (μg) 48 h 2nd cycle	Found (μg) 72 h 3rd cycle	Short term (bench top) stability found (μg) 24 h
Resveratrol	0.5	0.56 ± 0.02	0.56 ± 0.01	0.55 ± 0.01	0.55 ± 0.008	0.57 ± 0.01
	2	1.85 ± 0.01	1.85 ± 0.01	1.83 ± 0.005	1.81 ± 0.01	1.84 ± 0.04
	8	8.03 ± 0.07	8.04 ± 0.02	8.00 ± 0.01	7.81 ± 0.04	8.03 ± 0.14
Piperine	0.5	0.43 ± 0.01	0.43 ± 0.006	0.42 ± 0.007	0.41 ± 0.005	0.42 ± 0.01
	2	1.91 ± 0.02	1.90 ± 0.01	1.89 ± 0.005	1.86 ± 0.01	1.86 ± 0.02
	8	8.01 ± 0.09	7.93 ± 0.07	7.85 ± 0.07	7.76 ± 0.09	7.88 ± 0.10

n - replicate number.

Table 11
Results under the stress degradation studies for resveratrol and piperine (n = 3).

Exposed stress Degradation condition	% Degradation Individual analytes		% Degradation Mixed Analyte matrix	
	Resveratrol	Piperine	Resveratrol	Piperine
1 N HCl, 80° C, 1 h	17.88 ± 0.61	21.34 ± 0.60	13.48 ± 0.85	17.67 ± 0.79
1 N NaOH, 80° 1 h	25.72 ± 0.90	15.60 ± 0.34	19.82 ± 0.93	14.05 ± 0.60
Thermal, 80° C, 1 h	1.46 ± 0.24	1.72 ± 0.84	1.05 ± 0.06	1.95 ± 0.34
30% H_2O_2, 80° C, 1 h	11.53 ± 0.48	14.26 ± 0.76	7.69 ± 0.30	12.0 ± 0.51
Sunlight 30 minutes	42.81 ± 0.63	36.48 ± 0.94	40.96 ± 0.74	32.86 ± 0.61

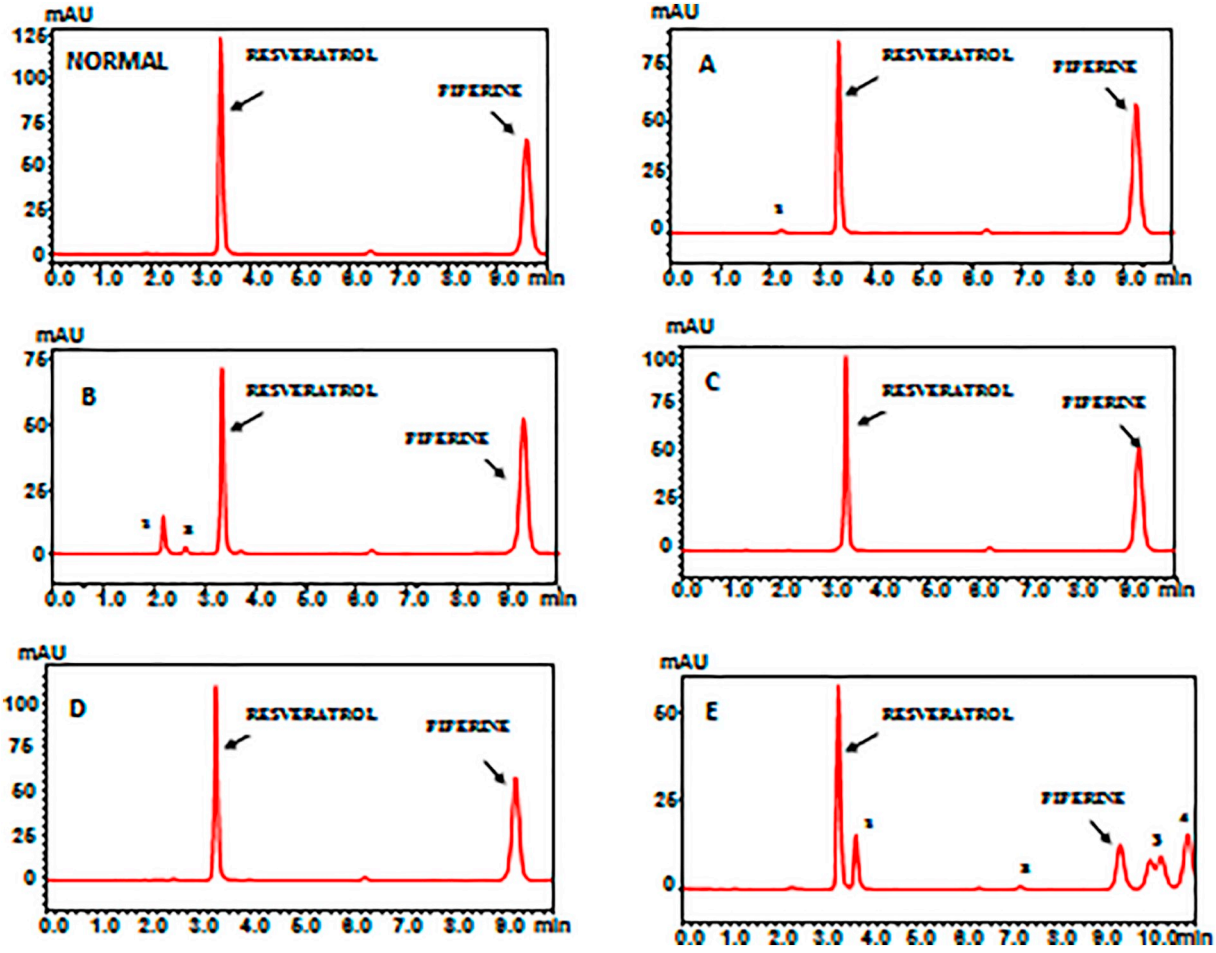

Fig. 5. HPLC chromatograms of resveratrol and piperine in forced degradation study under normal, acid (A), alkaline (B), thermal (C), oxidative (D) and photolytic (E) stress conditions.

alkaline environment than piperine. Thermal degradation for both resveratrol and piperine did not yield any peak indicating negligible % degradation. The results of thermal degradation suggest that, heating does not affect the stability behavior of both drugs as they have high melting points. Hence, both drugs were found to be stable in thermal degradation analysis. In 30% of H_2O_2 degradation study, small peroxide peak was observed at 2.3 min. In this condition, resveratrol slowly oxidizes with 7.69% degradation whereas piperine degradation was found to be 12.0%. In photolytic controlled stress condition, when both the drugs were exposed to direct sunlight for 30 min, resveratrol and piperine were degraded up to 40.96% and 32.86%, respectively. Under photolytic degradation condition resveratrol was found to be unstable in exposed sunlight where it converts into *cis*-resveratrol form which is isomer form of *trans*-resveratrol. As dilute solution of piperine is highly photosensitive, hence when piperine exposed to direct sunlight, it is prone to degradation for which two distinguishable degradation peaks were observed.

Under all circumstances, the integrity of peaks was maintained with no change in the retention time of the drugs (Fig. 5).

4. Conclusion

A novel RP-HPLC method was strategically developed for simultaneous quantification of piperine and resveratrol in newly-designed cubosome nanoformulation and spiked human plasma. The developed method, as per ICH guidelines was validated for different parameters which were within the acceptable limits and observed to be easy, fast, more sensitive, and efficient. The developed method has been improvised and economical with the use of an isosbestic point, for the analysis of resveratrol and piperine having different wavelengths. The developed method demonstrated excellent accuracy, precision, and linearity with low LOD and LOQ values. It also presents well resolved peaks and adequate quantification of both the encapsulated drugs without any interference of excipients in cubosome nanoparticles. The developed method was also validated in human plasma for different parameters, which were within the acceptable limits. It was concluded from forced degradation study that resveratrol and piperine were stable against acidic, alkaline, oxidative and at higher temperature conditions. But both were observed to be susceptible to degradation in photolytic conditions. Hence, this developed RP-HPLC method is useful for regular estimation of piperine and resveratrol in any type of formulation.

Declaration of Competing Interest

The authors declare no conflict of interests.

Acknowledgements

The authors acknowledge Dr. Prabhakar Kore Basic Science Research Center (BSRC), KLE Academy of Higher Education and Research and Regional Medical Research Centre – Indian Council of Medical Research (ICMR-NITM), Belagavi for providing the facility to

perform the research study. We would like to thank Sami Labs Ltd, Bangalore, Mohini Organics Pvt Ltd, Mumbai and BASF, Mumbai for providing the samples of the requisite materials as gifts.

This research did not receive any specific grant from funding agencies in the public, commercial, or not-for-profit sectors.

References

[1] C.A. Lastra, I. Villegas, Resveratrol as an antioxidant and pro-oxidant agent: mechanisms and clinical implications, Biochem. Soc. Trans. 35 (2007) 1156–1160, https://doi.org/10.1042/BST0351156.

[2] C.K. Singh, J. George, N. Ahmad, Resveratrol-based combinatorial strategies for cancer management, Ann. N. Y. Acad. Sci. 1290 (2013) 113–121, https://doi.org/10.1111/nyas.12160.

[3] B.K. Kurangi, S.S. Jalalpure, Review of selected herbal phytoconstituents for potential melanoma treatment, Indian J. Health Sci. Biomed. Res. 11 (2018) 3–11, https://doi.org/10.4103/kleuhsj.kleuhsj_319_17.

[4] E.S. Sunila, G. Kuttan, Immunomodulatory and antitumor activity of *Piper longum* Linn. and piperine, J. Ethnopharmacol. 90 (2004) 339–346, https://doi.org/10.1016/j.jep.2003.10.016.

[5] J.J. Johnson, M. Nihal, I.A. Siddiqui, C.O. Scarlett, H.H. Bailey, H. Mukhtar, N. Ahmad, Enhancing the bioavailability of resveratrol by combining it with piperine, Mol. Nutr. Food Res. 55 (2011) 1169–1176, https://doi.org/10.1002/mnfr.201100117.

[6] E.L. Wightman, J.L. Reay, C.F. Haskell, G. Williamson, T.P. Dew, D.O. Kennedy, Effects of resveratrol alone or in combination with piperine on cerebral blood flow parameters and cognitive performance in human subjects: a randomized, double-blind, placebo-controlled, cross-over investigation, Br. J. Nutr. 112 (2014) 203–213, https://doi.org/10.1017/S0007114514000737.

[7] J.K. Tak, J.H. Lee, J.W. Park, Resveratrol and piperine enhance radiosensitivity of tumor cells, BMB Rep. (2011) 242–246, https://doi.org/10.5483/BMBRep.2012.45.4.242.

[8] W. Huang, Z. Chen, Q. Wang, M. Lin, S. Wu, Q. Yan, F. Wu, X. Yu, X. Xie, G. Li, Y. Xu, J. Pan, Piperine potentiates the antidepressant-like effect of trans-resveratrol: involvement of monoaminergic system, Metab. Brain Dis. 28 (2013) 585–595, https://doi.org/10.1007/s11011-013-9426-y.

[9] J. Jasoliya, A. Jani, Method development and validation of RP-HPLC method for simultaneous estimation of resveratrol and piperine in combined capsule dosage form, World J. Pharm. Pharm. Sci. 3 (2014) 1096–1107.

[10] Y. Qu, J.H. Li, C. Zhang, C.X. Li, H.J. Dong, C.S. Wang, R. Zeng, X.H. Chen, Content determination of twelve major components in Tibetan medicine Zuozhu Daxi by UPLC, Zhongguo Zhongyao Zazhi 40 (2015) 1825–1830, https://doi.org/10.4268/cjcmm20150938.

[11] S. Kumar, V. Lather, D. Pandita, Stability indicating simplified HPLC method for simultaneous analysis of resveratrol and quercetin in nanoparticles and human plasma, Food Chem. 197 (2016) 959–964, https://doi.org/10.1016/j.foodchem.2015.11.078.

[12] H.M. Lotfy, S.S. Saleh, N.Y. Hassan, H.A. Salem, Comparative study of novel spectrophotometric methods based on isosbestic points; application on a pharmaceutical ternary mixture, Spectrochim. Acta A 126 (2014) 112–121, https://doi.org/10.1016/j.saa.2014.01.130.

[13] M. Ahirrao, S. Shrotriya, In vitro and in vivo evaluation of cubosomal in situ nasal gel containing resveratrol for brain targeting, Drug Dev. Ind. Pharm. 43 (2017) 1686–1693, https://doi.org/10.1080/03639045.2017.1338721.

[14] K. Jadhav, S. Deore, D. Dhamecha, S. Jagwani, S. Jalalpure, R. Bohara, Phytosynthesis of silver nanoparticles: characterization, biocompatibility studies, and anticancer activity, ACS Biomater. Sci. Eng. 4 (2018) 892–899, https://doi.org/10.1021/acsbiomaterials.7b00707.

[15] X. Jin, Z.H. Zhang, E. Sun, X.B. Tan, S.L. Li, X.D. Cheng, M. You, X.B. Jia, Enhanced oral absorption of 20(S)-protopanaxadiol by self-assembled liquid crystalline nanoparticles containing piperine: in vitro and in vivo studies, Int. J. Nanomedicine 8 (2013) 641–652, https://doi.org/10.2147/IJN.S38203.

[16] K. Jadhav, H.R. Rajeshwari, S. Deshpande, S. Jagwani, D. Dhamecha, S. Jalalpure, K. Subburayan, D. Baheti, Phytosynthesis of gold nanoparticles: characterization, biocompatibility, and evaluation of its osteoinductive potential for application in implant dentistry, Mater. Sci. Eng. C 93 (2018) 664–670, https://doi.org/10.1016/j.msec.2018.08.028.

[17] D. Pandita, S. Kumar, N. Poonia, V. Lather, Solid lipid nanoparticles enhance oral bioavailability of resveratrol, a natural polyphenol, Food Res. Int. 62 (2014) 1165–1174, https://doi.org/10.1016/j.foodres.2014.05.059.

[18] A. Katsagonis, J. Atta-Politou, M.A. Koupparis, HPLC method with UV detection for the determination of *trans*-resveratrol in plasma, J. Liq. Chromatogr. Relat. Technol. 28 (2005) 1393–1405, https://doi.org/10.1081/JLC-200054884.

[19] International Council for Harmonisation of Technical Requirements for Pharmaceuticals for Human Use, Bioanalytical Method Validation M10, (2019).

[20] Guidance for Industry, Bioanalytical Method Validation, 2013, http://www.fda.gov/Drugs/GuidanceComplianceRegulatoryInformation/Guidances/default.htm, and/or http://www.fda.gov/AnimalVeterinary/GuidanceComplianceEnforcement/GuidanceforIndustry/default.htm

[21] M.S. Elgawisha, S.M. Mostafa, A.A. Elshanawane, Simple and rapid HPLC method for simultaneous determination of atenolol and chlorthalidone in spiked human plasma, SPJ 19 (2011) 43–49, https://doi.org/10.1016/j.jsps.2010.10.003.

[22] Q1A(R2), ICH Stability Testing of New Drug Substances and Products, International Conference on Harmonization. Geneva, 2003.

[23] R. Pangeni, J. Ali, G. Mustafa, S. Sharma, S. Baboota, Design expert-supported development and validation of stability indicating high-performance liquid chromatography (hplc) method for determination of resveratrol in bulk drug and pharmaceutical formulation, Int. J. Pharm. Sci. Res. 6 (2015) 5115–5125 https://doi.org/10.13040/IJPSR.0975-8232.6(12).5115-25.

[24] M.R. Peram, S.S. Jalalpure, S.A. Joshi, M.B. Palkar, P.V. Diwan, Single robust RP-HPLC analytical method for quantification of curcuminoids in commercial turmeric products, Ayurvedic medicines, and nanovesicular systems, J. Liq. Chromatogr. Relat. Technol. 40 (2017) 487–498, https://doi.org/10.1080/10826076.2017.1329742.

[25] D. Dhamecha, S. Jalalpure, K. Jadhav, D. Sajjan, Green synthesis of gold nanoparticles using *Pterocarpus marsupium*: characterization and biocompatibility studies, Part. Sci. Technol. 34 (2015) 156–164, https://doi.org/10.1080/02726351.2015.1054972.

Send Orders for Reprints to reprints@benthamscience.net

Current Drug Delivery, 2021, *18*, 1-13

RESEARCH ARTICLE

Formulation and Evaluation of Resveratrol Loaded Cubosomal Nanoformulation for Topical Delivery

Bhaskar Kurangi[a,b], Sunil Jalalpure[*, a,b] and Satveer Jagwani[a,b]

[a]*Dr. Prabhakar Kore Basic Science Research Center, KLE Academy of Higher Education and Research, Nehru Nagar, Belagavi-590010, Karnataka, India;* [b]*KLE College of Pharmacy, Belagavi, KLE Academy of Higher Education and Research, Nehru Nagar, Belagavi-590010, Karnataka, India*

Abstract: ***Aim*:** The aim of the study was to formulate, characterize, and evaluate the resveratrol-loaded cubosomes (RC) for topical application.

***Background*:** Resveratrol (RV) is a nutraceutical compound with exciting pharmacological potential in different diseases, including cancers. Many studies on resveratrol have been reported for anti-melanoma activity. Due to its low bioavailability, the therapeutic activities of resveratrol are strongly limited. Hence, an approach with nanotechnology has been made to increase its activity through transdermal drug delivery.

***Objective*:** To formulate, characterize, and evaluate the resveratrol-loaded cubosomes (RC). To evaluate resveratrol-loaded cubosomal gel (RC-Gel) for its topical application.

***Methods*:** RC was formulated by homogenization technique and optimized using a 2-factor 3-level factorial design. Formulated RCs were characterized for particle size, zeta potential, and entrapment efficiency. Optimized RC was evaluated for *in vitro* release and stability study. Optimized RC was further formulated into cubosomal gel (RC-Gel) using carbopol and evaluated for drug permeation and deposition. Furthermore, developed RC-Gel was evaluated for its topical application using skin irritancy, toxicity, and *in vivo* local bioavailability studies.

***Results*:** The optimized RC indicated cubic-shaped structure with mean particle size, entrapment efficiency, and zeta potential were 113±2.36 nm, 85.07 ± 0.91%, and -27.40 ± 1.40 mV, respectively. *In vitro* drug release of optimized RC demonstrated biphasic drug release with the diffusion-controlled release of resveratrol (RV) (87.20 ± 3.91%). The RC-Gel demonstrated better drug permeation and deposition in mice skin layers. The composition of RC-Gel has been proved non-irritant to mice skin. *In vivo* local bioavailability study depicted the good potential of RC-Gel for skin localization.

***Conclusion*:** The RC nanoformulation proposes a promising drug delivery system for melanoma treatment simply through topical application.

ARTICLE HISTORY

Received: May 21, 2020
Revised: July 10, 2020
Accepted: July 20, 2020

DOI:
10.2174/1567201817666200902150646

Keywords: melanoma, cubosome, resveratrol, factorial design, cubosomal gel, local bioavailability.

1. INTRODUCTION

Melanoma is a malignant tumor originating from melanocytes (especially involving the skin) and is the most fatal kind of skin cancer. The death rate associated with melanoma is 90% which can also be related to cutaneous tumors. Globally, there is a 2-7% increase in the incidence rate annually [1, 2]. Nowadays, the treatments recommended for melanoma are surgery, chemotherapy, immunotherapy, or the combination of the two. Although the current chemotherapies have their advantages, they are either not effective enough or can cause severe adverse effects and assist in developing multi-drug resistance. The results of randomized clinical trials reported to date show that no single drug or combination of therapies is superior to the existing drugs [3]. Therefore, there is a need for herbal drugs which can offer better efficacy over existing chemotherapy for melanoma treatment.

Phytoconstituents such as carotenoids, flavonoids, and terpenoids have high anti-cancer potential and can be used for the treatment of melanoma [4-6]. Resveratrol (RV) is a

[*] Address correspondence to this author at the Dr. Prabhakar Kore Basic Science Research Center, and KLE College of Pharmacy, Belagavi, KLE Academy of Higher Education and Research, Nehru Nagar, Belagavi-590010 Karnataka, India; Tel: 0831-2470362; Fax: 0831-2470640; E-mail: jalalpuresunil@rediffmail.com

1567-2018/21 $65.00+.00

nutraceutical which has pharmacological potential and because of this recently attracted a lot of research attention. It is a phytoalexin compound found in many plants such as grapes, peanuts, berries, etc. RV has been found as an anti--cancer agent [7]. Many studies of RV have been reported for anti-melanoma activity like in doxorubicin resistant murine melanoma cells, the activity of resveratrol has been observed by inducing apoptosis and inhibiting the growth of melanoma tumors in mice [8]. In contrast, in another study, it was demonstrated that RV in combination with temozolomide has shown cytotoxicity against melanoma cells [9]. In addition to this, RV also performed a role as a radiation sensitizer in the treatment of melanoma [10] and apoptosis inducer and growth inhibitor for human melanoma cells [11]. Due to its poor bioavailability the *in vivo* anti-cancer activity of RV is strongly reduced [12]. Hence the approach is to be made to increase its bioavailability using either bioenhancer or nanotechnology. The effective management of melanoma using RV is obtained through maximizing its permeation and localization to form a depot at melanocytes. Such effective treatment can be achieved by the topical application RV formulation.

Nowadays, an increase in drugs delivery through transdermal route has been achieved with novel nanostructured liquid crystalline dispersion systems such as cubosomes. Cubosomes are colloidal dispersion of bicontinuous cubic liquid-crystalline structures in water developed using suitable surfactants in nanostructured systems. They provide a number of benefits over the traditional transdermal formulations owing to their unique properties like biocompatible nature, the capability to encapsulate all hydrophilic, lipophilic, and amphiphilic drugs, thermodynamic stability, simplicity, non-allergic, non-irritating, and non-toxic nature which has potential for controlled drug release. More importantly, these nano-cubic structures enhance the drug penetration in deep layers of the skin and increase their cell uptake capacity [13]. Cubosomes have a transdermal effect which might be due to their structural organization being similar to that of biomembranes [14-16].

Various innovative nano-drug delivery systems [lipid based nanoparticles like solid lipid nanoparticles, poly(lactic-co-glycolic acid) nanoparticles, niosomes, nanocapsules of RV] have been used in different treatment therapies [16-20]. Very few works of literature have reported where RV has been targeted to brain, liver, skin using cubosome as a nano-carrier system [21-24]. But, to date the application of RV loaded cubosomes (RC) as a novel nanostructured liquid crystalline dispersion system through transdermal application has not been reported.

Therefore, in the present study, we formulated and characterized RC nanoformulation for transdermal application in order to target melanoma. Furthermore, the optimized RC was used to formulate the cubosomal gel (RC-Gel) which was investigated for *in vivo* local bioavailability and skin toxicity in Swiss albino mice.

2. MATERIALS AND METHODS

2.1. Materials

RV (98%) was provided by Sami Labs Ltd., Bangalore, India. Glyceryl monooleate (GMO) was obtained as a gift sample from Mohini Organics Pvt. Ltd., Mumbai. Pluronic F-127 (PF-127) was purchased from Sigma Aldrich, USA. HPLC-grade Acetonitrile (ACN), methanol and ortho phosphoric acid (OPA) were procured from Merck and Fisher Scientific, Mumbai, India.

2.2. Preparation of RV-loaded Cubosome (RC)

RC was prepared by using the top-down method. The fragmentation techniques were used to formulate cubosomes using high speed homogenizer followed by probe sonicator [24, 25]. Briefly, PF-127 and GMO were liquefied in separate containers on a magnetic stirrer at 65°C. RV (0.1% w/v) was added in melted GMO and mixed with liquefied PF-127 solution. This mixture was then added in a drop--wise manner to preheated water with constant stirring on a magnetic stirrer [26]. Homogenization (IKA T25 digital Ultra Turax, Germany) was performed at 15,000 rpm for 15 min to form a fine dispersion and thereafter, probe sonicated (RivoTEK, Mumbai) for 5 min to form RC nanoformulation.

2.3. Experimental Design and Chromatographic Conditions of the Study

2.3.1. Experimental Design of the Study

A 2-factor 3-level (3^2) factorial design was utilized to optimize the RC wherein concentrations of GMO (X1) and PF-127 (X2) were selected as independent variables and particle size (PS, Y1), and entrapment efficiency (EE, Y2) were selected as the response variables. Optimization was done with the help of Design-Expert software (Version 7.0.0, Stat- Ease Inc., MN, USA). Table **1** illustrates the different variables and levels used in RC nanoformulation.

Table 1. Independent and dependent variables utilized in 3^2 factorial design for the RC nanoformulation.

Coded level	-1 (low)	0 (medium)	+1 (high)
Independent variables			
X1- Lipid (%w/w)	3	5	7
X2- Stabilizer (%w/w)	0.5	1	1.5
Dependent variables			
Y1– Particle size	Minimize		
Y2- Entrapment efficiency	Maximize		

2.3.2. Chromatographic conditions for RV

HPLC (Shimadzu HPLC prominence system, LC-20AD, Japan) was performed to estimate the RV concentration at 306 nm as previously reported by Kurangi, Jalalpure, Jag-

wani 2019 [27]. Briefly, samples analysis were performed by using Luna C18 column (4.6 × 250 mm, particle size 5 µm, Phenomenex, USA), eluted with a mobile phase consisting of acetonitrile: phosphate buffer (ACN:PBS; pH 6, 55:45 v/v) and keeping the flow rate at 1 ml/min with 35 °C column temperature. The HPLC method, thus developed was further used for the analysis of cubosomes and other samples.

2.4. Characterization of Prepared RC

2.4.1. Physicochemical Characterization of RC

The physicochemical characterization of RC was performed for the average particle size, their distribution (PDI), and zeta potential (ZP) values as per the standard protocol using dynamic light scattering (DLS), and M3-phase analysis light scattering (PALS) techniques, respectively, using Zetasizer Nano ZS90 (Malvern Instruments, Malvern, United Kingdom) [28, 29].

The fourier-transform infra red (FTIR) spectroscopy (IR Affinity-1S, Shimadzu, Japan), differential scanning calorimetry (DSC, DSC-60, Shimadzu, Kyoto, Japan), and X-ray diffraction (XRD, Xpert MPD, Philips Holland) of pure RV and RC nanoformulation were performed using standard protocols to provide information about drug-excipients compatibility, thermal behavior, and crystalline properties. Furthermore, the pH value and rheological properties of RC were also determined as per the standard procedure using digital pH meter (CyberScan pH 510, Eutech instruments) and Brookfield viscometer (CAP 2000+, Brookfield Engineering Laboratories, MA, USA) [30-32].

2.4.1.1. Entrapment Efficiency (EE)

The cubosome dispersion samples were centrifuged (Eppendorf laboratory centrifuge, 5424R, Germany) at 15000 rpm for 30 min [24, 30]. The supernatant liquid was collected, diluted appropriately and analyzed by using the developed HPLC method [27]. The percent EE was determined as:

$$\% \text{ EE} = \frac{(A-B)}{A} X\ 100 \quad \text{----(1)}$$

A- Total amount of RV added in cubosome dispersion, and B - amount of RV in supernatant

2.4.1.2. Transmission Electron Microscopy

The morphology of RC was observed by high resolution TEM (Jeol/JEM, 2100). A drop of diluted RC was placed on a 200-mesh carbon coated copper grid and stained with 2% w/v phosphotungstic acid solution for 2 min. The grid was air-dried and observed under TEM (200kV and 40,000X) to get images along with a randomly selected area electron diffraction (SAED) [33, 34].

2.4.2. In vitro RV Release from RC

In vitro RV release from optimized RC was determined by using a dynamic dialysis method (USP II method) [35, 36]. The drug release study was done by using a tablet dissolution testing apparatus (Electrolab, EDT-08LX) equipped with low volume conversion kit (EDT-08L/08L x 150 ml, Supplementary Fig. **1**) which was specifically utilized for nanoformulation. Briefly, RC nanoformulation (5 ml) was transferred to a dialysis bag, which was immersed into a 100 ml of PBS (pH 6.8) containing tween 80 (1.5%). The temperature of dissolution medium was kept at 37±0.5 °C with a stirring speed of 50 rpm. The aliquots (1 ml) were withdrawn at specific time intervals. The withdrawn aliquots of the drug release medium were replaced with same volume of fresh buffer to maintain the sink condition. Concentrations of RV released in the dissolution medium were determined by using HPLC method, as specified above. The drug release mechanism from cubosome formulation was determined by using different drug release kinetic models [24, 37, 38].

2.5. Formulation and Characterization of Cubosomal Gel (RC-Gel)

For better skin applicability, the optimized RC was formulated as RC-Gel using Carbopol [39]. The RC-Gel was prepared by directly incorporating carbopol (1% w/v) into the optimized batch of RC with constant stirring on a magnetic stirrer for 4 h. Resveratrol gel (RV-Gel) was formulated to compare with RC-Gel. The gel thus obtained was checked visually for its color, homogeneity, spreadability, and analyzed for its pH and viscosity [40]. The drug content of the gel was determined by dissolving weighed an accurate quantity of RC-Gel (0.1 g) in 10 ml of methanol. For complete solubilization of the drug, the solution was stirred at 500 rpm for 15 min and sonicated for 4 min. Finally, the solution was filtered using 0.45 µm syringe filters and evaluated by HPLC after suitable dilution. The drug content was indicated in terms of percentage [41, 42].

2.5.1. Ex vivo Skin Permeation and Retention Study

Ex vivo RV permeation from RC-Gel (equivalent of 0.5 mg RV) through the skin of Swiss albino mice (25 ± 5 g) was performed using PermeGear Franz diffusion cell with the diffusion surface area of 1.767 cm^2 and receptor chamber containing methanolic PBS (pH 6.4; 50:50, 12 ml, 37.0 ± 0.5 °C, and 100 rpm stirring). At specific time intervals, the aliquots (1 ml) were withdrawn and evaluated by HPLC. The withdrawn aliquots were replaced with the same volume of buffer to maintain sink conditions. The different parameters from the permeation study were estimated as follows.

$$Flux(J) = quantity\ of\ RV \frac{permeated}{time} X\ skin\ diffusion\ area \quad \text{--(2)}$$

$$Permeability\ coefficient\ (Kp) = \frac{J}{RV\ concentration\ in\ donor\ compartment} \quad (3)$$

$$Enhancement\ ratio\ (ER) = \frac{J\ of\ cubosomal\ gel}{J\ of\ the\ control\ (RV-gel)} \quad \text{----------(4)}$$

At the end of the study, after 24h, the amount of RV deposited within the skin was investigated. Briefly, the cut sec-

tion of the skin was homogenized (RQT-127A, Remi, India) with methanol and extracted for RV. The final aliquot obtained was filtered (0.45 μm) and evaluated for RV content using HPLC [43].

2.6. Stability study

In the short-term stability study, the cubosome nanoformulations were placed at room temperature away from light for 3 months and were then analyzed after 3 months by evaluating the mean PS, PDI, ZP, and % EE. Sample analysis was carried out in triplicates and the results obtained were the average of three sample analysis [23].

2.7. *In vivo* evaluation of RC-Gel

Swiss male albino mice (25–30 g) were used for skin penetration, skin irritation, and toxicity and local bioavailability measurement. The animals were housed in the cages at the room temperature of 25 ± 3°C and relative humidity of 30–70%, under 12h light/dark cycle.

2.7.1. Skin Irritancy and Toxicity Study

A skin irritancy test was carried out to assess cubosomal gel compatibility with Swiss albino mice skin (25–30 g). Two groups were made with three mice each. The first and second groups received applications of the RC-Gel and marketed gel (Flonida 5%), respectively. This test was performed to verify the skin compatibility of the cubosomal gel. Topical dose (equivalent to 20 μg of RV) was applied to the left ear of the mouse using medical spatula with right ear as control. Observation was done every 7 days to check for erythema occurrence, which indicates cutaneous vascular dilatation. The average score obtained from the scoring scale of each day and finally, the data interpretation was done as per Uttley and Van Abbe (1973) scoring method [43, 44].

Acute and sub-acute toxicity were evaluated as per the method specified by Draize, Woodard, Calvery (1944) [45, 46]. The first group was kept as sham control (no treatment), whereas the second group served as positive control (20% sodium lauryl sulfate (SLS) solution). The third and fourth group has been applied with RC-Gel and marketed gel locally, respectively. Daily application was made on the same place of mice and for the development of erythema and edema; grading was done for the toxicity study at 1, 24, 48, and 72 h, on the scale of 0–4. The application of gel was continued for 28 days, after which the mice were sacrificed, and the applied skin part was collected. Finally, it was processed for the histopathological examination to check the toxicity of the developed RC-Gel formulation [47].

2.7.2. In vivo Local Bioavailability Measurement Study

Swiss male albino mice (25–35 g) were used for local bioavailability measurement study, wherein two groups with six mice each were used. The first and second groups received topical applications of RC-Gel and simple RV-Gel, respectively. The gel was applied once on the shaved dorsal skin area (1cm^2). After 1 day of treatment, the mice were sacrificed and blood was collected [48]. Plasma was collected from the blood and further processed to estimate the drug plasma concentration using the developed HPLC method [27]. The amount of drug present on the surface of the treated skin was evaluated by washing it with ethanol (50%) [49]. Finally, the amount of drug that had penetrated into the skin was also determined using the same procedure used for the *ex vivo* diffusion study.

2.8. Statistical analysis

The optimization of the RCs was accomplished using Design-Expert® software (Stat-Ease Inc., USA).

3. RESULTS AND DISCUSSION

3.1. Development of HPLC method for RV

HPLC study was demonstrated for RV and the retention time was observed to be 3.30 min at 306 nm. The results of regression analysis for a calibration curve showed a linear relation (y = 77001x + 2858) over the concentration range of 250–800 ng/mL for RV. The determination coefficient (R^2) value was observed to be > 0.999. The HPLC chromatograms for RV and RC are as shown in supplementary Fig. (2).

3.2. Preparation, Optimization and Characterization of RC

RC was prepared using top down approach employing high-speed homogenizer and probe sonicator. Since it is observed that lipid and stabilizer concentration are the two most important factors governing the performance properties of cubosome, viz., PS, and % EE. A 3^2 full factorial design was employed to yield an optimized formulation [50]. The factor combination and performance properties of cubosome formulation batches are listed in Table **2**.

The results obtained in the regression analysis for dependent variables are summarized in supplementary Table **1**. Based on the results, the quadratic model was observed as best-fit model. The quadratic model gave high values of multiple determination coefficients (R^2). The PRESS values for the quadratic model were small compared to the other polynomial models. For both response variables, the predicted R^2 was in reasonable agreement with the adjusted R^2 indicating that the difference was less than 0.2.

Adequate precision, which measures the signal-to-noise ratio, was observed to be 30.344 and 11.203 for PS and % EE, respectively, which was >4 considered desirable (Supplementary Table **1**).

3.2.1. Particle Size Analysis

Nanoparticle size is one of the most important factors affecting not only transdermal drug delivery but also cellular uptake and biodistribution. Particles < 300 nm can transfer the entrapped drug into the deep layers of the skin [51]. The mean PS of formulated RC ranged between 89 nm and154 nm (Table **2**). Equation 6 shows the effect of independent variables on the particle size of RC.

Table 2. Observed responses from 3^2 factorial design of RC formulation batches.

Formulation Batch	Independent variables				Dependent variables		PDI	ZP (mV)
	X1	X2	X1 (%w/w)	X2 (%w/w)	Y1 (nm)	Y2 (%)		
RC1	-1	-1	3	0.5	125 ±4.22	62.39 ±0.57	0.11 ±0.05	-18.57 ±1.35
RC2	-1	0	3	1	101 ±5.36	69.30 ±0.84	0.19 ±0.07	-20.33 ±0.70
RC3	-1	+1	3	1.5	89 ±3.28	81.40 ±0.96	0.23 ±0.09	-18.65±0.74
RC4	0	-1	5	0.5	126 ±6.84	74.47 ±1.27	0.25 ±0.07	-28.10 ±0.50
RC5	0	0	5	1	113 ±2.36	85.07 ±0.91	0.18 ±0.12	-27.40 ±1.40
RC6	0	+1	5	1.5	98 ±7.19	81.31 ±0.63	0.22 ±0.11	-27.03 ±1.95
RC7	+1	-1	7	0.5	154 ±6.51	43.22 ±0.72	0.20 ±0.10	-40.27±1.56
RC8	+1	0	7	1	139 ±8.85	44.38±0.54	0.16 ±0.04	-28.40±0.61
RC9	+1	+1	7	1.5	127 ±7.10	52.07±0.80	0.26 ±0.12	-21.50 ±1.51

mean ± SD (n=3), RC- Resveratrol loaded cubosome, X1 – Glyceryl Monooleate [GMO] (% w/w), X2 – Pluronic F127 (%w/w), Y2 - Entrapment efficiency (%), Y1 - Particle size (nm), ZP- Zeta potential (mV), PDI – Polydispersibility index.

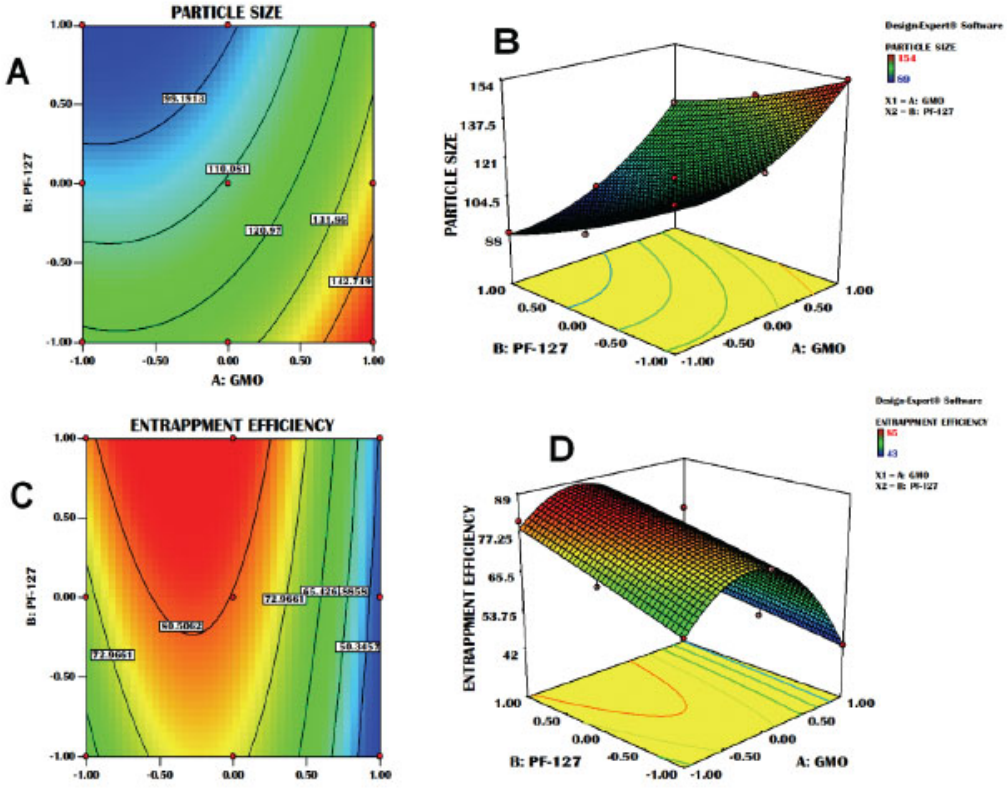

Fig. (1). 2D-contour (**A, C**), 3D-Response surface (**B, D**) displaying the effect of Glyceryl monooleate (GMO) and Pluronic F-127 (PF-127) on particle size, and EE of Resveratrol loaded cubosome (RC). GMO concentration was directly proportional to particle size whereas inversely proportional to % EE. The PF-127 concentrations have a reverse effect on the particle size and % EE, that of GMO.

$$PS = +110.89 + 17.50\ X_1 - 15.17\ X_2 + 2.25\ X_1 X_2 + 10.17\ X_1^2 + 2.17 X_2^2 \text{------- (6)}$$

Where PS is particle size, X_1 and X_2 is GMO and PF-127 concentration (%w/w), respectively.

The effect of GMO (X_1) and PF-127 (X_2) on the particle size is illustrated in Fig. 1A and 1B.

The results indicate that the GMO concentration was directly proportional to the particle size whereas PF-127 concentration was inversely correlated with it. As the PF-127 concentration decreased in the formulations, cubosomes with larger particle size were formed. This happens because lesser amount of stabilizer causes reduced interfacial stability and leads to nanoparticles aggregation [52].

3.2.2. Analysis of entrapment efficiency (EE)

EE is an important parameter used to determine drug delivery capability of cubosome nanoformulation. The EE for all cubosome nanoparticles was found to be in the range of 43.22 - 85.07% as shown in Table **2** and Fig. **1C** and **1D**. Equation 7 shows the effect of independent variables on the EE of RC.

$$EE = +80.22 - 12.33\ X_1 + 5.67\ X_2 - 2.25\ X_1 X_2 - 21.33\ X_1^2 - 0.33 X_2^2 \ldots\ldots\ldots\ldots (7)$$

Where EE is Entrapment efficiency, X_1 and X_2 are GMO and PF-127 concentration (% w/w) respectively.

The effect of GMO (X_1) and PF-127 (X_2) on the EE is illustrated in Fig. 1C and 1D. The results indicate that the PF-127 concentration was directly proportional to the % EE whereas GMO concentration was inversely proportional to it.

The results demonstrated that EE rises with an increase in PF-127 concentrations. This might be due to the presence of PF-127 over the cubosome structures which can retain some amount of RV by which EE can be increased.

3.2.3. Selection of Optimized Cubosome Nanoformulation

Based on the results obtained for dependent variables, RC5 batch having the concentrations of GMO (5% w/w) and PF-127 (1% w/w) was selected for further evaluation studies, as it had maximum EE (85.07%) with small particle size (113 nm).

3.3. Characterization of Cubosomes

3.3.1. PDI and Zeta Potential

The PDI of all prepared RC nanoparticles ranged between 0.11 and 0.26, indicating narrow homogeneous particle size distribution (Table **2**).

ZP was studied to determine the charge on cubosome nanoparticle surface which can affect the physical stability and skin permeation of cubosome nanoformulation. The high ZP values provide long-term physical stability to cubosome nanoformulation, as it prevents similarly charged particles aggregation due to the electric repulsion [53].

The ZP values of RC ranged from -18.57 to -40.27 mV (Table 2). The negative charge may be because of the GMO containing free fatty acid [54]. In addition to that, the interaction between hydroxyl ions of PF-127 with the water caused more negative charge to the cubosome nanoparticles [55]. As the literature reports more permeability for negative charged particles, hence cubosome nanoparticles can easily permeate through the skin by transdermal application [56].

3.3.2. FTIR spectrum analysis

The surface structure of the RC nanoparticles was investigated by FTIR analysis. The infrared spectrum of RV, GMO, PF-127, and RC are shown in Supplementary Fig. (**3**). The FTIR peak values of RV were displayed at wavenumbers 3300, 1512, and 1456 cm^{-1}, for –OH, and C=C functional groups. The FTIR spectra of the RC exhibited all but negligible distinguishing peaks of Resveratrol (RV) and the major characteristic peaks of GMO, and PF-127, representing the absence of any interaction between the RV and other excipients, which suggests their compatibility with each other.

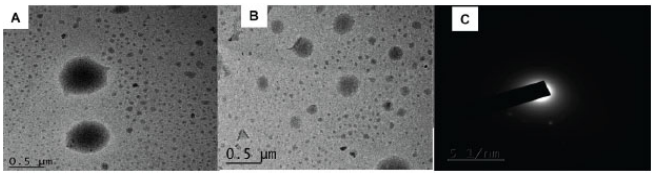

Fig. (2). High resolution-transmission electron microscopy (HR-TEM) imaging (**A and B**), and random selected area electron diffraction (SAED) pattern (**C**) of Resveratrol loaded cubosome (RC) nanoparticles.

3.3.3. TEM Analysis

The cubosome particles appeared to be cubic and uniform with smooth surface and less curvature (Figs. **2A** and **B**). The scattered particles were in the nano range and well separated from each other. The brightness around the cubic border structure indicates self-assembled lipid bilayer structure. The SAED showed brightness surrounding the centrally placed lid, indicating the crystalline nature of the cubosome nanoparticles (Fig. **2C**).

3.3.4. DSC Analysis

DSC is a rapid and reliable method for estimating drug-excipients interactions and revealing the polymorphic modifications. The DSC curves of pure RV, GMO, PF-127 and optimized-RC are shown in Fig. (**3**).

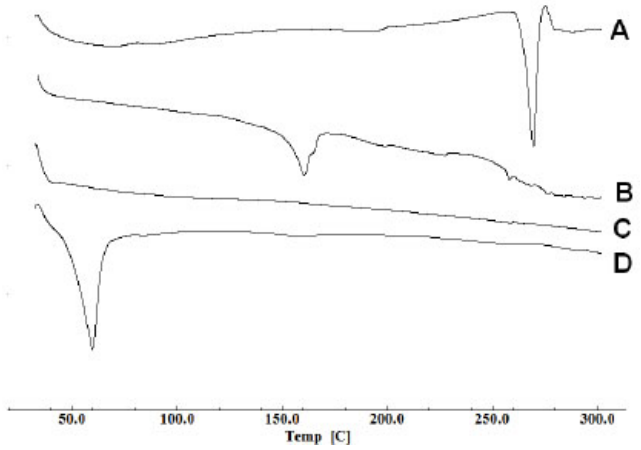

Fig. (3). DSC thermogram of Resveratrol [RV] (**A**), Resveratrol loaded cubosome [RC] (**B**), Glyceryl monooleate [GMO] (**C**), and Pluronic F-127 [PF-127] (**D**).

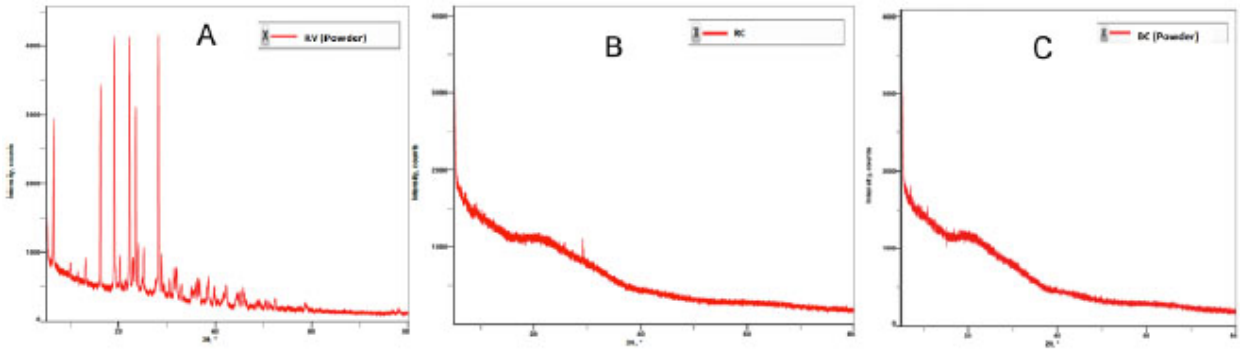

Fig. (4). The crystallanity and physical state of the resveratrol loaded cubosome (RC) was determined and confirmed by X-Ray Diffraction (XRD) spectras of (**A**) Resveratrol [RV], (**B**) Resveratrol loaded cubosome [RC], and (**C**) Blank Cubosome [BC] (**C**).

The DSC thermogram of RC (B) demonstrated that RV was completely entrapped inside the cubosome nanoparticles, as the sharp endothermic peak of RV (A) disappeared.

The DSC thermogram of RV (Fig. **3A**) exhibited a sharp endothermic peak at 269.39 °C, which corresponds to its melting point, and indicates the crystalline nature for RV. The lipid GMO emphasizes the temperature based phase transition which shows endothermic peak at 33.21 °C (Fig. **3C**), whereas the stabilizer PF-127 (Fig. **3D**) exhibited endothermic peak at 59.81 °C as it melted. Mannitol which was a cryoprotectant to obtain the freeze-dried powder of RC showed a sharp endothermic peak at 176.70 °C (Fig. **3B**).

In the DSC thermogram of optimized-RC (Fig. 3B), the endothermic peak was detected at 160.58 °C indicated for mannitol which was slightly shifted correspond to its melting point, because of bicontinuous layer formed inside the cubosome structure. In the same DSC thermogram of optimized-RC, the RV sharp peak had completely disappeared, suggesting its transformation to the non-crystalline state. This result suggests that the RV was molecularly entrapped in the cubosome nanoparticles.

3.3.5. XRD Study

XRD was performed to verify the physical state of RC in comparison to BC and pure RV (Fig. **4**).

The pure RV diffractogram demonstrated distinctive sharp crystal peaks at diffraction angles (2θ) of 16.34, 19.14, 22.31, and 28.24, suggesting its crystalline characteristic. However, these high-intensity peaks of RV disappeared completely in the diffractogram of RC. Moreover, the diffractogram obtained of RC has negligible difference when compared to that of BC. These results are similar to the DSC finding which suggests that the RV was in non-crystalline state and molecularly entrapped in the cubosome nanoparticles.

3.3.6. pH Value Measurement and Rheological Behavior for RC

The pH of the cubosome nanoformulation was analyzed in order to evaluate any probable skin irritation which could arise because of the change in the pH of skin upon *in vivo* application. The pH values and viscosities of cubosome formulation batches are listed in Table **3**.

Table 3. pH values and viscosities of RC nanoformulations.

Formulation Code	pH	Viscosity (cP)
RC1	5.57 ±0.07	3.59 ±0.09
RC2	5.95 ±0.05	3.82 ±0.04
RC3	6.14 ±0.04	3.91 ±0.03
RC4	6.87 ±0.06	7.98 ±0.04
RC5	6.50 ±0.09	8.02 ±0.04
RC6	6.67 ±0.06	8.19 ±0.08
RC7	6.72 ±0.04	15.24 ±0.06
RC8	6.90 ±0.07	17.01 ±0.09
RC9	6.94 ±0.03	17.33 ±0.07

Values represent mean ± SD (n=3); Resveratrol loaded cubosome (RC)

The pH values for all RC batches were found to be within the nonirritant acceptable pH range of 5.57 to 6.94 [57, 58].

The cubosome formulations had shown the viscosity values in the ranges of 3.59 to 17.33 cP. Increasing the amount of GMO and PF-127 in the RC nanoformulations led to the formation of more liquid crystal-like material particles that increased cubosome viscosity.

3.3.7. Drug Release Study

Fig. 5 indicates the release profile of RV from the optimized batch of RC nanoformulation (RC5) in comparison with RV solution in phosphate buffer (pH 6.8) containing Tween 80.

The drug release of RV followed biphasic release pattern with a diffusion controlled release mechanism.

Fast and complete RV release from aqueous solution was obtained in 12 h. Generally, the bicontinuous cubosome nanoformulations show a biphasic burst release with a release mechanism of diffusion from the cubic-phase matrix structure [59]. The RV drug release from the cubosome nanoparticles was biphasic, with an initial burst release of 20.52% ± 1.86 in 1 h, followed by sustained prolonged drug

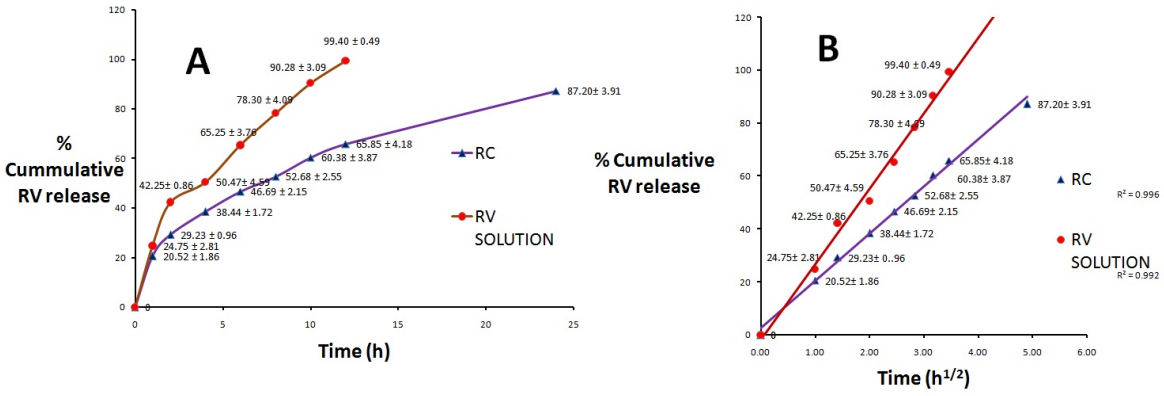

Fig. (5). (**A**) *In vitro* drug release profiles of Resveratrol [RV] from resveratrol loaded cubosome (RC) and aqueous resveratrol solution (RV solution) (mean±SD, n=6). (**B**) Graph showing linear relationship between % cumulative RV release from cubosomes (RC) and aqueous solution (RV solution) vs. square root of time.

release observed up to 24 h (Fig. **5A**). On the other hand, after 1 h, RV slow release was prolonged for 24 h may be due to the bicontinuous structure of cubosome system that can assist as a rate-controlling membrane matrix structure, with decreased RV release [59]. RV, as a lipophilic drug, has a strong interaction with the lipophilic part of the cubosome led to sustained release.

To indicate the diffusion-controlled release pattern of RV, the release data were plotted against square root of the time (Fig. **5B**). A linear relationship was found for both free RV aqueous solutions and RC with determination coefficients of 0.992 and 0.996, respectively, suggesting that the diffusion is the predominant pattern of drug release [59]. After fitting the results of dissolution study of RC with the different release kinetic models, the higuchi model had shown the best fitting with the highest R^2 of 0.996. Such a model could describe the biphasic release pattern with initial burst release followed by sustained release, with a controlled release mechanism of diffusion.

3.4. Formulation of RC-Gel

The cubosomal gel was formulated from the optimized batch (RC5) of cubosome dispersion (equivalent to 0.1% w/v of RV) by directly dispersing Carbopol (1% w/v) as gel former. Methyl paraben (0.05%) was incorporated as a preservative in RC-Gel. Visual appearance, spreadability, and clarity of prepared cubosomal gel were observed for the presence of any foreign particles. The developed RC-Gel was observed to have the same physical characteristics as that of cubosomal nanodispersion. Low viscosity and dispersion like properties of cubosomes in turn lead to poor patient compliance for a number of reasons, such as short residence time of cubosome at the site of application, difficulty in applying an effective dose, loss during application, leading to poor drug retention. Hence, to overcome these problems, optimized-RC nanoformulation was formulated as a bioadhesive gel by proper mixing with a gelling agent to form pharmaceutically acceptable RC-Gel. Simple RV-Gel was formulated in the same way by dispersing RV into Carbopol dispersion (1% w/v).

3.5. Characterization of Cubosomal Gel (RC-Gel)

Different parameters of the RV-Gel and RC-Gel were assessed, and the results are mentioned in supplementary Table 2. Both the prepared gels were found to be white, viscous creamy formulations with a smooth and homogenous appearance, and the pH was noted to be 6.93 and 4.15 for the RC-Gel and RV-Gel, respectively. RV-Gel has a slightly acidic pH compared to RC-Gel, due to the Carbopol content which can decrease the pH of the RV-Gel, whereas, in addition to Carbopol, the GMO and PF-127 may stabilize the pH of RC-Gel. The viscosity of the gel formulation was determined by using Brookfield viscometer, which was found to be 136 and 100 cP for RV- and RC-Gel, respectively. The drug content of the RC-Gel was 97.33% which showed that the RC nanoparticles were uniformly and properly distributed in the gel formulation.

3.5.1. Ex vivo Skin Permeation and Retention Studies

The *ex vivo* skin permeation and retention of RV across the shaved mouse skin was performed using a Franz diffusion cell apparatus. The RC-Gel was compared with RV-Gel for the cumulative amount of drug permeation (24 h), permeability coefficient, transdermal flux, amount of drug deposited and enhancement ratio, and the results are depicted in Table **4**.

The results demonstrate that cumulative amount of RV permeated from RC-Gel and RV-Gel was 152.26 and 30.66 µg/cm^2 respectively. Permeation flux was observed to be 3.58 µg/cm^2/h for RC-Gel whereas for the RV-Gel it was 0.72 µg/cm^2/h. Furthermore, the permeability coefficient and enhancement ratio for RC-Gel (9.66×10^{-3} and 4.97, respectively) were found to be higher than that of RV-Gel (1.94×10^{-3} and 1.0, respectively). The amount of RV deposited in the skin was 11.90 µg/cm^2 for RC-Gel which was considerably higher than that of RV-Gel.

Table 4. Result of *Ex vivo* skin permeation and retention study of the RC-Gel and RV-Gel.

Gel-Formulation	Cumulative amount of drug permeated ($\mu g/cm^2$)	Permeation flux ($J,\mu g/cm^2/h$)	Permeability Coefficient (Kp, cm/h)	Enhancement ratio	Quantity of drug deposited into skin ($\mu g/cm^2$)
RC-Gel	152.26 ± 1.12	3.58 ± 0.03	9.66×10^{-3}	4.97	11.90 ± 0.56
RV-Gel	30.66 ± 1.22	0.72 ± 0.03	1.94×10^{-3}	1.00	8.04 ± 0.15

mean ± SD (n=3);
Resveratrol loaded cubosomal gel (RC-Gel); Resveratrol Gel (RV-Gel).

These results confirm the enhanced skin permeation of RV from the cubosomal gel due to the physicochemical properties of the cubosomes (particle size, surface charge) and synergistic effect of both GMO and PF-127. The nanosized and negatively-charged cubosome nanoparticles enhance the permeation of RV through the skin. GMO can disturb the characteristic skin structure through lipophilic interaction with the skin lipids [60]. The PF-127 is a non-ionic surfactant, serving as penetration enhancer by skin sebum emulsification, by which thermodynamic coefficient of the drugs can be improved [61].

The sustained RV diffusion release was achieved through the skin due to the formation of a depot by cubosome nanoparticles in the lipid portion of stratum corneum. This may be due to the similarity between the structure of cubosome nanoparticles and the stratum corneum [62].

3.6. Stability Study

The optimized cubosome dispersion samples were studied for stability, following storage for 3 months at room temperature. They were characterized for the PS, PDI, ZP, EE, and % drug release. The results are summarized in supplementary Table 3. There were insignificant changes in the results as compared to freshly prepared formulation (0 month). The GMO maintains the integrity of the cubosome and PF-127 stabilizes this nanoformulation due to which cubosomes can be considered as thermodynamically stable, suggesting that cubosome formulations were stable at room temperature storage conditions.

3.7. *In vivo* Evaluation of RV Loaded Cubosomes

3.7.1. Skin Irritancy and Toxicity Study

The skin irritancy test was performed for RC-Gel and marketed gel as per by Uttley and Van Abbe test [44]. It was observed that the mean score of skin irritancy for the RC-Gel and marketed gel was 6.43 and 7.14, respectively (Table **5**).

Table 5. Scores of skin irritancy study for RC-gel and Marketed gel as per Uttley and Van Abbe method

Formulation	Score after (day)							Mean score values
	1	2	3	4	5	6	7	
RC-Gel	6	7	6	8	6	6	6	6.43
Marketed gel	6	6	6	8	8	8	8	7.14

(n=3); Resveratrol loaded cubosomal gel (RC-Gel)

The study demonstrated non-irritant property of the developed cubosomal gel, as the values were between 0 and 9, probably due to RV entrapped inside the cubosome nanoparticles. Upon its release from the nanoparticles, it will cause irritation to the skin.

The Draize test was used to perform acute and 28-days sub-acute skin toxicity study of RC-gel and marketed gel (Table **6**).

Table 6. Score obtained after application of formulation for the skin irritation study (Draize method).

Formulation	Erythema				Edema			
	1h	24h	48h	72h	1h	24h	48h	72h
Normal control	0	0	0	0	0	0	0	0
RC-GEL	0	0	0.67	0.67	0	0	0	0
Marketed gel	0	0	0.67	0.67	0	0	0	0
20% SLS	0	0.67	2	2.33	0	1.67	2.33	3

(n=3); Resveratrol loaded cubosomal gel (RC-Gel); Sodium Lauryl Sulphate (SLS)
Scores are labeled as 0 = no erythema, 1 = very slight erythema (light pink), 2 = well defined erythema (dark pink), 3 = moderate to severe erythema (light red), 4 = severe erythema (extreme redness). Scores are similarly labeled for edema.

The grading pattern 0-4 was used in this skin irritation test based on the development of erythema and edema [45]. The scoring was done as follows:

0–0.9: non-irritant and safe for human skin

1–1.9: mild irritant and need of preventive measures

2–3: irritant and not safe for topical application

There was no sign of erythema and edema after treatment with cubosomal gel in the acute toxicity study. Marketed gel showed negligible erythema with absence of edema. SLS (20% w/v), a positive control in this study, caused reddening of skin and high irritation with moderate to severe erythema and edema. In sub-acute toxicity study, repeated applications of the above formulations for up to 28 days showed similar results.

Also, the skin toxicity of formulated RC-Gel and marketed gel were estimated by performing a histopathological analysis of the treated skin after 28 days of application [49]. Fig. (**6A–D**) shows the histological images of skins of normal control group, RC- Gel, marketed gel, and SLS (20% w/v) as a positive control, respectively.

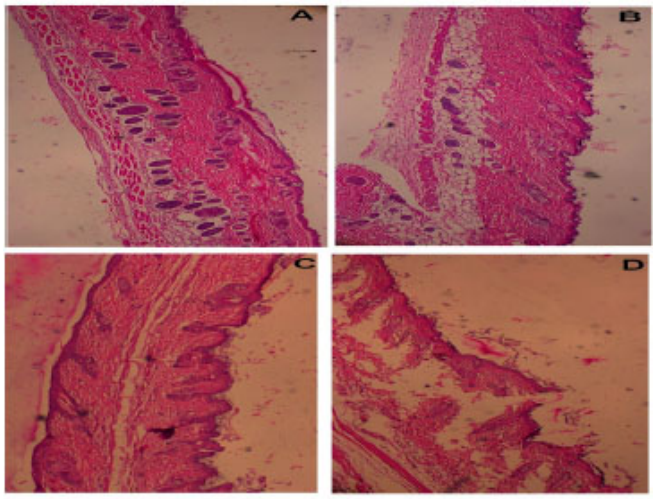

Fig. (6). (**A-D**) shows the histopathological photos of hematoxylin and eosin stained cross sections of mice skin after 28 days of application of different formulations (Magnification- 4X).

(**A**) Normal control group mice skin showing the normal structure and epidermal layer of skin. (**B**) Mice skin treated with RC- Gel, and (**C**) marketed gel demonstrated no structural differences in the mice skin as compared to normal mice skin. (**D**) Mice skin on treatment with SLS (20% w/v) as a positive control displayed structural damage and rupture of the epidermal layers of the skin. The results suggested that developed topical cubosomal gel was found to be non-irritant, non-toxic to mice skin.

It was seen that SLS (20% w/v) caused complete damage of the epidermal layer of the skin, and necrosis, which indicated the skin irritation potential of SLS (20% w/v). RC-Gel treated skin showed a continuous epidermal layer with negligible skin irritation potential, because of entrapment of RV in the cubosome nanoparticles. Marketed gel showed similar to cubosomal gel in comparison to normal skin. From the acute, sub-acute, and histopathological studies, it can be concluded that the formulated RC- Gel was safe for topical application.

3.7.2. In vivo Local Bioavailability Measurement Study

The applicability of developed RC- Gel for better skin permeation and deposition was evaluated *in vivo* using male Swiss albino mice. The local bioavailability was evaluated by calculating the amount of RV deposited (penetrated), remaining on the skin surface (not penetrated), and entering the systemic circulation. The results of skin localization are provided in Supplementary Table 4. The fraction of applied dose that penetrated skin and which formed a depot (skin localization index) for RC- Gel was found to be 61.03%, whereas for the local application of RV-Gel it was only 23.87%. The fraction of applied doses that had not penetrated through but remained on the skin surface was 38.97 and 76.13% for RC- Gel and RV-Gel, respectively. After analyzing the blood plasma concentration, it was found that no drug (from both formulations) was available in the systemic circulation which may be because of the negligible systemic availability. From the results of local bioavailability, it was confirmed that RC-Gel demonstrated good skin permeation and deposition and formed a depot as compared to RV-Gel. The structure of the cubosome in cubosomal gel may help maximize drug localization and penetration, as the cubic structure provides maximum surface area for targeting locally and increases the therapeutic activity of RV for treating melanoma conditions.

CONCLUSION

In the present research work, an attempt was made to improve the efficacy of RV by using a novel cubosome nanoformulation for topical application. The optimized cubosome nanoformulation (RC5) with GMO: PF-127 ratio (5:1) showed desirable particle size of 113 nm with 85.07% EE. The optimized RC was transferred to cubosomal gel which showed an increased level of RV permeation and deposition capacity. The XRD and DSC studies demonstrated successful RV encapsulation in the cubosome nanoparticles. TEM revealed that cubosome nanoparticles have a cubic shape with crystalline properties. *In vitro* drug release for RC showed a biphasic burst release with a release mechanism of diffusion controlled over 24 h. From the skin irritancy and toxicity study, RC-Gel was proved to be nonirritant in nature. *In vivo* local bioavailability study also demonstrated enhanced skin localization capability of RC-Gel as compared to RV-Gel. Further studies using suitable *in vitro* and *in vivo* models are required to prove the efficacy of this cubosome formulation for melanoma treatment.

ETHICS APPROVAL AND CONSENT TO PARTICIPATE

The animal studies protocol was reviewed and approved by the Committee for the Purpose of Control and Supervision of Experiments on Animals (CPCSEA) and the Institutional Animal Ethics Committee (IAEC), KLE College of Pharmacy, Belagavi, India (Ethical approval Letter No.: KLECOP/CPCSEA-Reg. No. 221/Po/Re/S/2000/CPCSEA/Res.26-13/10/2018).

HUMAN AND ANIMAL RIGHTS

No Humans were used for studies that are base of this research. All animal study procedures were performed in accordance with the National Institute of Health (NIH) guidelines for the care and use of laboratory animals. All animal experiments were conducted in strict accordance with Animal Research: Reporting of *In Vivo* Experiments (ARRIVE) guidelines.

CONSENT FOR PUBLICATION

Not applicable.

CONFLICT OF INTEREST

The authors declare no conflict of interest between them.

ACKNOWLEDGMENTS

We gratefully acknowledge Sami Labs, Bangalore, India and Mohini Organics, Mumbai, India for supplying the gift samples of RV and GMO, respectively. We would like to acknowledge STIC Cochin University, Kochi, India for performing the HR-TEM analysis of sample. We would also like to extend our acknowledgement to Dr. Ramesh Chavan, Department of Pathology, Jawaharlal Nehru Medical College, KAHER, Belagavi, for giving facility to carry out the histopathology studies. We would also like to acknowledge Healthminds Consulting Pvt Ltd for performing grammatical correction of manuscript. We would like to thank KLE Academy of Higher Education and Research (KAHER), Belagavi for providing financial support to carry out the research.

REFERENCES

[1] Gladfelter, P.; Darwish, N.H.E.; Mousa, S.A. Current status and future direction in the management of malignant melanoma. *Melanoma Res.,* **2017**, *27*(5), 403-410. http://dx.doi.org/10.1097/CMR.0000000000000379 PMID: 28800028

[2] Garbe, C.; Peris, K.; Hauschild, A.; Saiag, P.; Middleton, M.; Spatz, A.; Grob, J-J.; Malvehy, J.; Newton-Bishop, J.; Stratigos, A.; Pehamberger, H.; Eggermont, A. Diagnosis and treatment of melanoma: European consensus-based interdisciplinary guideline. *Eur. J. Cancer,* **2010**, *46*(2), 270-283. http://dx.doi.org/10.1016/j.ejca.2009.10.032 PMID: 19959353

[3] Braithwaite, D. *Demb, J.; Henderson, L. M. American Cancer Society: Cancer Facts and Figures 2016*; GA Am. Cancer Soc.: Atlanta, **2016**.

[4] Batra, P.; Sharma, A. K. Anti-Cancer Potential of Flavonoids: Recent Trends and Future Perspectives *3 Biotech,* **2013**, *3*(6), 439-459.

[5] Kuttan, G.; Pratheeshkumar, P.; Manu, K.A.; Kuttan, R. Inhibition of tumor progression by naturally occurring terpenoids. *Pharm. Biol.,* **2011**, *49*(10), 995-1007. http://dx.doi.org/10.3109/13880209.2011.559476 PMID: 21936626

[6] Steinmetz, K.A.; Potter, J.D. Vegetables, fruit, and cancer. II. Mechanisms. *Cancer Causes Control,* **1991**, *2*(6), 427-442. http://dx.doi.org/10.1007/BF00054304 PMID: 1764568

[7] Kurangi, B.K.; Jalalpure, S.S. Review of Selected Herbal Phytoconstituents for Potential Melanoma Treatment. Indian J. Health. *Sci. Biomed. Res.,* **2018**, *11*(1), 3-11.

[8] Gatouillat, G.; Balasse, E.; Joseph-Pietras, D.; Morjani, H.; Madoulet, C. Resveratrol induces cell-cycle disruption and apoptosis in chemoresistant B16 melanoma. *J. Cell. Biochem.,* **2010**, *110*(4), 893-902. http://dx.doi.org/10.1002/jcb.22601 PMID: 20564188

[9] Osmond, G.W.; Augustine, C.K.; Zipfel, P.A.; Padussis, J.; Tyler, D.S. Enhancing melanoma treatment with resveratrol. *J. Surg. Res.,* **2012**, *172*(1), 109-115. http://dx.doi.org/10.1016/j.jss.2010.07.033 PMID: 20855085

[10] Fang, Y.; Bradley, M.J.; Cook, K.M.; Herrick, E.J.; Nicholl, M.B. A potential role for resveratrol as a radiation sensitizer for melanoma treatment. *J. Surg. Res.,* **2013**, *183*(2), 645-653. http://dx.doi.org/10.1016/j.jss.2013.02.037 PMID: 23522452

[11] Niles, R.M.; McFarland, M.; Weimer, M.B.; Redkar, A.; Fu, Y.M.; Meadows, G.G. Resveratrol is a potent inducer of apoptosis in human melanoma cells. *Cancer Lett.,* **2003**, *190*(2), 157-163. http://dx.doi.org/10.1016/S0304-3835(02)00676-6 PMID: 12565170

[12] Asensi, M.; Medina, I.; Ortega, A.; Carretero, J.; Baño, M.C.; Obrador, E.; Estrela, J.M. Inhibition of cancer growth by resveratrol is related to its low bioavailability. *Free Radic. Biol. Med.,* **2002**, *33*(3), 387-398. http://dx.doi.org/10.1016/S0891-5849(02)00911-5 PMID: 12126761

[13] Karami, Z.; Hamidi, M. Cubosomes: remarkable drug delivery potential. *Drug Discov. Today,* **2016**, *21*(5), 789-801. http://dx.doi.org/10.1016/j.drudis.2016.01.004 PMID: 26780385

[14] Malmsten, M. Soft drug delivery systems. *Soft Matter,* **2006**, *2*(9), 760-769. http://dx.doi.org/10.1039/b608348j PMID: 32680216

[15] Ibrahim, H.K.; El-Leithy, I.S.; Makky, A.A. Mucoadhesive nanoparticles as carrier systems for prolonged ocular delivery of gatifloxacin/prednisolone bitherapy. *Mol. Pharm.,* **2010**, *7*(2), 576-585. http://dx.doi.org/10.1021/mp900279c PMID: 20163167

[16] Larsson, K. Cubic Lipid-Water Phases: Structures and Biomembrane Aspects. *J. Phys. Chem.,* **1989**, *93*(21), 7304-7314. http://dx.doi.org/10.1021/j100358a010

[17] Tavano, L.; Muzzalupo, R.; Picci, N.; de Cindio, B. Co-encapsulation of lipophilic antioxidants into niosomal carriers: percutaneous permeation studies for cosmeceutical applications. *Colloids Surf. B Biointerfaces,* **2014**, *114*, 144-149. http://dx.doi.org/10.1016/j.colsurfb.2013.09.055 PMID: 24176892

[18] Teskac, K.; Kristl, J. Teskaˇ. The evidence for solid lipid nanoparticles mediated cell uptake of resveratrol. *Int. J. Pharm.,* **2010**, *390*(1), 61-69. http://dx.doi.org/10.1016/j.ijpharm.2009.10.011 PMID: 19833178

[19] Sanna, V.; Roggio, A.M.; Siliani, S.; Piccinini, M.; Marceddu, S.; Mariani, A.; Sechi, M. Development of novel cationic chitosan-and anionic alginate-coated poly(D,L-lactide-co-glycolide) nanoparticles for controlled release and light protection of resveratrol. *Int. J. Nanomedicine,* **2012**, *7*, 5501-5516. http://dx.doi.org/10.2147/IJN.S36684 PMID: 23093904

[20] Carlotti, M.E.; Sapino, S.; Ugazio, E.; Gallarate, M.; Morel, S. Resveratrol in Solid Lipid Nanoparticles. *J. Dispers. Sci. Technol.,* **2012**, *33*(4), 465-471. http://dx.doi.org/10.1080/01932691.2010.548274

[21] Abdel-Bar, H.M.; El Basset Sanad, R.A. Endocytic pathways of optimized resveratrol cubosomes capturing into human hepatoma cells. *Biomed. Pharmacother.,* **2017**, *93*, 561-569. http://dx.doi.org/10.1016/j.biopha.2017.06.093 PMID: 28686970

[22] Badie, H.; Abbas, H. Novel small self-assembled resveratrol-bearing cubosomes and hexosomes: preparation, charachterization, and ex vivo permeation. *Drug Dev. Ind. Pharm.,* **2018**, *44*(12), 2013-2025. http://dx.doi.org/10.1080/03639045.2018.1508220 PMID: 30095009

[23] Elnaggar, Y.S.R.; Etman, S.M.; Abdelmonsif, D.A.; Abdallah, O.Y. Novel piperine-loaded Tween-integrated monoolein cubosomes as brain-targeted oral nanomedicine in Alzheimer's disease: pharmaceutical, biological, and toxicological studies. *Int. J. Nanomedicine,* **2015**, *10*, 5459-5473. http://dx.doi.org/10.2147/IJN.S87336 PMID: 26346130

[24] Ahirrao, M.; Shrotriya, S. In vitro and in vivo evaluation of cubosomal in situ nasal gel containing resveratrol for brain targeting. *Drug Dev. Ind. Pharm.,* **2017**, *43*(10), 1686-1693. http://dx.doi.org/10.1080/03639045.2017.1338721 PMID: 28574732

[25] Esposito, E.; Mariani, P.; Ravani, L.; Contado, C.; Volta, M.; Bido, S.; Drechsler, M.; Mazzoni, S.; Menegatti, E.; Morari, M.; Cortesi, R. Nanoparticulate lipid dispersions for bromocriptine delivery: characterization and in vivo study. *Eur. J. Pharm. Biopharm.,* **2012**, *80*(2), 306-314. http://dx.doi.org/10.1016/j.ejpb.2011.10.015 PMID: 22061262

[26] Dhamecha, D.; Movsas, R.; Sano, U.; Menon, J.U. Applications of alginate microspheres in therapeutics delivery and cell culture: Past, present and future. *Int. J. Pharm.,* **2019**, *569*(August)118627 http://dx.doi.org/10.1016/j.ijpharm.2019.118627 PMID: 31421199

[27] Kurangi, B.; Jalalpure, S.; Jagwani, S. A validated stability-indicating HPLC method for simultaneous estimation of resveratrol and piperine in cubosome and human plasma. *J. Chromatogr. B Analyt. Technol. Biomed. Life Sci.,* **2019**, *1122-1123*(May), 39-48. http://dx.doi.org/10.1016/j.jchromb.2019.05.017 PMID: 31150952

[28] Dhamecha, D.; Jalalpure, S.; Jadhav, K.; Sajjan, D. Green Synthesis of Gold Nanoparticles Using Pterocarpus Marsupium: Charac-

terization and Biocompatibility Studies. *Particul. Sci. Technol.,* **2016**, *34*(2), 156-164. http://dx.doi.org/10.1080/02726351.2015.1054972

[29] Dhamecha, D.; Jalalpure, S.; Jadhav, K. Doxorubicin Functionalized Gold Nanoparticles: Characterization and Activity against Human Cancer Cell Lines. *Process Biochem.,* **2015**, *50*(12), 2298-2306. http://dx.doi.org/10.1016/j.procbio.2015.10.007

[30] Jin, X.; Zhang, Z.H.; Li, S.L.; Sun, E.; Tan, X.B.; Song, J.; Jia, X.B. A nanostructured liquid crystalline formulation of 20(S)-protopanaxadiol with improved oral absorption. *Fitoterapia,* **2013**, *84*(1), 64-71. http://dx.doi.org/10.1016/j.fitote.2012.09.013 PMID: 23006538

[31] Morsi, N.M.; Abdelbary, G.A.; Ahmed, M.A. Silver sulfadiazine based cubosome hydrogels for topical treatment of burns: development and in vitro/in vivo characterization. *Eur. J. Pharm. Biopharm.,* **2014**, *86*(2), 178-189. http://dx.doi.org/10.1016/j.ejpb.2013.04.018 PMID: 23688805

[32] Fule, R.; Dhamecha, D.; Maniruzzaman, M.; Khale, A.; Amin, P. Development of hot melt co-formulated antimalarial solid dispersion system in fixed dose form (ARLUMELT): Evaluating amorphous state and in vivo performance. *Int. J. Pharm.,* **2015**, *496*(1), 137-156. http://dx.doi.org/10.1016/j.ijpharm.2015.09.069 PMID: 26471056

[33] Salah, S.; Mahmoud, A.A.; Kamel, A.O. Etodolac transdermal cubosomes for the treatment of rheumatoid arthritis: ex vivo permeation and in vivo pharmacokinetic studies. *Drug Deliv.,* **2017**, *24*(1), 846-856. http://dx.doi.org/10.1080/10717544.2017.1326539 PMID: 28535740

[34] Jadhav, K.; Hr, R.; Deshpande, S.; Jagwani, S.; Dhamecha, D.; Jalalpure, S.; Subburayan, K.; Baheti, D. Phytosynthesis of gold nanoparticles: Characterization, biocompatibility, and evaluation of its osteoinductive potential for application in implant dentistry. *Mater. Sci. Eng. C,* **2018**, *93*, 664-670. http://dx.doi.org/10.1016/j.msec.2018.08.028 PMID: 30274099

[35] Luo, Q.; Lin, T.; Zhang, C.Y.; Zhu, T.; Wang, L.; Ji, Z.; Jia, B.; Ge, T.; Peng, D.; Chen, W. A novel glyceryl monoolein-bearing cubosomes for gambogenic acid: Preparation, cytotoxicity and intracellular uptake. *Int. J. Pharm.,* **2015**, *493*(1-2), 30-39. http://dx.doi.org/10.1016/j.ijpharm.2015.07.036 PMID: 26209071

[36] Qian, S.; Wong, Y.C.; Zuo, Z. Development, characterization and application of in situ gel systems for intranasal delivery of tacrine. *Int. J. Pharm.,* **2014**, *468*(1-2), 272-282. http://dx.doi.org/10.1016/j.ijpharm.2014.04.015 PMID: 24709220

[37] Nasr, M.; Ghorab, M.K.; Abdelazem, A. In vitro and in vivo evaluation of cubosomes containing 5-fluorouracil for liver targeting. *Acta Pharm. Sin. B,* **2015**, *5*(1), 79-88. http://dx.doi.org/10.1016/j.apsb.2014.12.001 PMID: 26579429

[38] Peram, M.R.; Jalalpure, S.; Kumbar, V.; Patil, S.; Joshi, S.; Bhat, K.; Diwan, P. Factorial design based curcumin ethosomal nanocarriers for the skin cancer delivery: *in vitro* evaluation. *J. Liposome Res.,* **2019**, *29*(3), 291-311. http://dx.doi.org/10.1080/08982104.2018.1556292 PMID: 30526186

[39] Mitkari, B.V.; Korde, S.A.; Mahadik, K.R.; Kokare, C.R. Formulation and Evaluation of Topical Liposomal Gel for Fluconazole. *Indian J Pharm Educ Res,* **2010**, *44*(4), 324-333.

[40] Shelke, S.; Shahi, S.; Jadhav, K.; Dhamecha, D.; Tiwari, R.; Patil, H. Thermoreversible nanoethosomal gel for the intranasal delivery of Eletriptan hydrobromide. *J. Mater. Sci. Mater. Med.,* **2016**, *27*(6), 103. http://dx.doi.org/10.1007/s10856-016-5713-6 PMID: 27091045

[41] Esposito, E.; Ravani, L.; Mariani, P.; Contado, C.; Drechsler, M.; Puglia, C.; Cortesi, R. Curcumin containing monoolein aqueous dispersions: a preformulative study. *Mater. Sci. Eng. C,* **2013**, *33*(8), 4923-4934. http://dx.doi.org/10.1016/j.msec.2013.08.017 PMID: 24094206

[42] Ahad, A.; Al-Saleh, A.A.; Al-Mohizea, A.M.; Al-Jenoobi, F.I.; Raish, M.; Yassin, A.E.B.; Alam, M.A. Pharmacodynamic study of eprosartan mesylate-loaded transfersomes Carbopol® gel under Dermaroller® on rats with methyl prednisolone acetate-induced hypertension. *Biomed. Pharmacother.,* **2017**, *89*, 177-184. http://dx.doi.org/10.1016/j.biopha.2017.01.164 PMID: 28237913

[43] Khan, M.A.; Pandit, J.; Sultana, Y.; Sultana, S.; Ali, A.; Aqil, M.; Chauhan, M. Novel carbopol-based transfersomal gel of 5-fluorouracil for skin cancer treatment: in vitro characterization and in vivo study. *Drug Deliv.,* **2015**, *22*(6), 795-802. http://dx.doi.org/10.3109/10717544.2014.902146 PMID: 24735246

[44] Uttley, M.; Van Abbe, N.J. Primary Irritation of the Skin: Mouse Ear Test and Human Patch Test Procedures. *J. Soc. Cosmet. Chem.,* **1973**, *24*(4), 217-227.

[45] Draize, J.H.; Woodard, G.; Calvery, H.O. Methods for the Study of Irritation and Toxicity of Substances Applied Topically to the Skin and Mucous Membranes. *J. Pharmacol. Exp. Ther.,* **1944**, *82*(3), 377-390.

[46] Sahu, P.; Kashaw, S.K.; Sau, S.; Kushwah, V.; Jain, S.; Agrawal, R.K.; Iyer, A.K. pH Responsive 5-Fluorouracil Loaded Biocompatible Nanogels For Topical Chemotherapy of Aggressive Melanoma. *Colloids Surf. B Biointerfaces,* **2019**, *174*, 232-245. http://dx.doi.org/10.1016/j.colsurfb.2018.11.018 PMID: 30465998

[47] Singh, H.P.; Tiwary, A.K.; Jain, S. Preparation and in vitro, in vivo characterization of elastic liposomes encapsulating cyclodextrin-colchicine complexes for topical delivery of colchicine. *Yakugaku Zasshi,* **2010**, *130*(3), 397-407. PMID: 20190524

[48] Italia, J.L.; Singh, D.; Ravi Kumar, M.N. High-performance liquid chromatographic analysis of amphotericin B in rat plasma using α-naphthol as an internal standard. *Anal. Chim. Acta,* **2009**, *634*(1), 110-114. http://dx.doi.org/10.1016/j.aca.2008.12.006 PMID: 19154818

[49] Kaur, L.; Jain, S.K.; Manhas, R.K.; Sharma, D. Nanoethosomal formulation for skin targeting of amphotericin B: an in vitro and in vivo assessment. *J. Liposome Res.,* **2015**, *25*(4), 294-307. http://dx.doi.org/10.3109/08982104.2014.995670 PMID: 25547800

[50] Kurangi, B.; Shah, R.; Kemkar, V.; Honarao, U.; Mahajan, S. Formulation, Evaluation and Optimization of Time and Enzyme Dependent Polymers Matrix Based Tablet for Colon Targeted Drug Delivery. *IJPRS,* **2014**, *3*(1), 524-534.

[51] Zhai, Y.; Xu, R.; Wang, Y.; Liu, J.; Wang, Z.; Zhai, G. Ethosomes for skin delivery of ropivacaine: preparation, characterization and ex vivo penetration properties. *J. Liposome Res.,* **2015**, *25*(4), 316-324. http://dx.doi.org/10.3109/08982104.2014.999686 PMID: 25625544

[52] Mainardes, R.M.; Evangelista, R.C. PLGA nanoparticles containing praziquantel: effect of formulation variables on size distribution. *Int. J. Pharm.,* **2005**, *290*(1-2), 137-144. http://dx.doi.org/10.1016/j.ijpharm.2004.11.027 PMID: 15664139

[53] Pal, S.L.; Jana, U.; Manna, P.K.; Mohanta, G.P.; Manavalan, R. Nanoparticle: An Overview of Preparation and Characterization. *J. Appl. Pharm. Sci.,* **2011**, *1*(6), 228-234.

[54] Hundekar, Y.R.; Saboji, J.K.; Patil, S.M.; Nanjwade, B.K. Preparation and Evaluation of Diclofenac Sodium Cubosomes for Percutaneous Administration. *World J. Pharm. Pharm. Sci.,* **2014**, *3*(5), 523-539.

[55] Rizwan, S.B.; Hanley, T.; Boyd, B.J.; Rades, T.; Hook, S. Liquid crystalline systems of phytantriol and glyceryl monooleate containing a hydrophilic protein: Characterisation, swelling and release kinetics. *J. Pharm. Sci.,* **2009**, *98*(11), 4191-4204. http://dx.doi.org/10.1002/jps.21724 PMID: 19340889

[56] Kohli, A.K.; Alpar, H.O. Potential use of nanoparticles for transcutaneous vaccine delivery: effect of particle size and charge. *Int. J. Pharm.,* **2004**, *275*(1-2), 13-17. http://dx.doi.org/10.1016/j.ijpharm.2003.10.038 PMID: 15081134

[57] Barry, B.W. BW, B. Dermatological Formulations: Percutaneous Absorption. *J. Pharm. Sci.,* **1983**, *73*(4), 573.

[58] Hadgraft, J. Skin, the final frontier. *Int. J. Pharm.,* **2001**, *224*(1-2), 1-18. http://dx.doi.org/10.1016/S0378-5173(01)00731-1 PMID: 11512545

[59] Freag, M.S.; Elnaggar, Y.S.R.; Abdelmonsif, D.A.; Abdallah, O.Y. Stealth, biocompatible monoolein-based lyotropic liquid crystalline nanoparticles for enhanced aloe-emodin delivery to breast

cancer cells: in vitro and in vivo studies. *Int. J. Nanomedicine,* **2016**, *11*, 4799-4818. http://dx.doi.org/10.2147/IJN.S111736 PMID: 27703348

[60] Kwon, T.K.; Kim, J-C. Preparation and in Vitro Skin Permeation of Cubosomes Containing Hinokitiol. *J. Dispers. Sci. Technol.,* **2010**, *31*(7), 1004-1009.

[61] Smith, E.W.; Maibach, H.I. *Percutaneous Penetration Enhancers*; CRC Press, **1995**.

[62] Norlén, L.; Al-Amoudi, A. Stratum corneum keratin structure, function, and formation: the cubic rod-packing and membrane templating model. *J. Invest. Dermatol.,* **2004**, *123*(4), 715-732. http://dx.doi.org/10.1111/j.0022-202X.2004.23213.x PMID: 15373777

Original Article

A Validated Stability-indicating RP-HPLC Method for Piperine Estimation in Black Pepper, Marketed Formulation and Nanoparticles

Bhaskar Kurangi[1,2], Sunil Jalalpure[1,2]*

[1]Dr. Prabhakar Kore Basic Science Research Center, KLE Academy of Higher Education and Research, Nehru Nagar, Belagavi, Karnataka, INDIA.
[2]KLE College of Pharmacy Belagavi, KLE Academy of Higher Education and Research, Nehru Nagar, Belagavi, Karnataka, INDIA.

ABSTRACT

Aim: The aim of the study was to develop and validate a simple stability indicating reverse-phase High Performance Liquid Chromatography (RP-HPLC) method for quantitative analysis of piperine in Ayurvedic marketed formulation, black pepper and cubosome nanoformulation. **Methods:** The method was established by using Luna C_{18} HPLC column using a mobile phase consisting of acetonitrile: 0.01% ortho phosphoric acid (60:40, v/v; pH 3), delivered isocratically with flow rate of 1 mL/min and detected at 340 nm. The validation of chromatographic parameters and stress testing were performed in accordance with International Conference on Harmonization (ICH) guidelines. **Results:** The developed method was observed to be specific, linear ($r^2 > 0.999$) over the selected range of concentration 0.5 to 20 μg/mL, precise (percentage relative standard deviation < 2%), with the detection and quantification limit as 0.015 and 0.044 μg/mL respectively. The relevancy of the developed method was analyzed on the piperine entrapped cubosome nanoformulation, which was formulated by fragmentation technique. The entrapment efficiency of piperine for prepared cubosome was observed to be 87.01 %. The method was implemented for the estimation of piperine in black pepper. The concentration of piperine in marketed formulation was found to be similar with the labeled concentration. The analyte peak was found to be complete resolved without any interference of additives and degrading products. **Conclusion**: The validated method was observed to be specific, sensitive and sufficient for the routine analysis of food products, marketed formulations and nanoparticles containing piperine.

Key words: RP-HPLC, Piperine, Cubosome, Stress degradation, Ayurvedic marketed formulations.

INTRODUCTION

Black pepper is widely used as spice and well known for its pungent taste and aroma. It is categorized as Generally Recognized as Safe (GRAS) by the US Food and Drug Administration (FDA) which contains piperine as an active alkaloid constituent. Piperine found in *Piper nigrum* and *Piper longum*, belonging to *Piperaceae* family, which can be used as potential therapeutic agent for targeting various diseases. Piperine exerts wide range of pharmacological activities like antioxidant, anti-arthritic, anti-inflammatory and anti-depressant. Piperine has also been reported for anticancer activity which can be exerted through its immunomodulation characteristics.[1] Many research for piperine have been performed in combination with other phytochemicals, which have led to increased their bioavailability, prophylactic and therapeutic responses.[2,3]

Since, human recognizing the use of herbal medicines and homemade remedies, these are widely practiced for the treatment of different diseases and recently there is inclination to use herbal formulations are on increasing demand. This increase in

Submission Date: 28-04-2020;
Revision Date: 22-06-2020;
Accepted Date: 07-09-2020

DOI: 10.5530/ijper.54.3s.168

Correspondence:
Dr. Sunil Jalalpure
Professor, KLE College of Pharmacy Belagavi and Dr. Prabhakar Kore Basic Science Research Center, KLE Academy of Higher Education and Research, Nehru Nagar, Belagavi-590010 Karnataka, INDIA.
Phone: +91 9448964057
E-mail: jalalpuresunil@rediffmail.com

www.ijper.org

demand for herbal medicines or ayurvedic formulations unavoidably led to the issue of obtaining and maintaining their quality. Hence forth, there has been increased care for the quality control of herbal related or ayurvedic formulations. In the current investigation, an attempt has been performed for the analysis of Ayurvedic marketed formulations with special reference to quantitative estimation of piperine in Trikatu Churna, Ajamodadi Churna and Chitrakadi Gutika.

To date, very few analytical methods are available for the quantification of piperine in these Ayurvedic formulations; however these do not provide an easy estimation. Many more analytical techniques have been reported for the estimation of piperine in black pepper, herbal formulation, plasma samples and nanoformulations.[4-11] However, the reported HPLC techniques have several drawbacks like high flow rates,[6,9] expensive,[8,9] less sensitive,[10] multiple wavelengths,[9] lack of stability studies.[7,8,11] Hence, the current investigation was aimed with to establish HPLC method for the accurate Piperine estimation from Ayurvedic marketed formulations.

Owing to intense first-pass metabolism, pH-mediated metabolism of piperine to piperidine and sensitive nature of it during formulation and storage leads to photoisomerization, leads to difficulty in the administration of piperine and reduced its activity.[12,13] Hence, to overcome these limitations an approach with lipid based nanoformulation has been investigated. In this regard the present investigation also highlights on the formulation of piperine loaded cubosome followed by the application of the established method for piperine quantification in the formulated nanoparticles.

The present research was aimed with to establish a simple, rapid and stability showing RP-HPLC method to estimate piperine in nanoparticles, black pepper and Ayurvedic marketed formulations. Subsequently, stress degradation study under different forced or stress conditions were investigated to validate the established RP-HPLC method in the selection of experimental conditions and formulation design and analysis.

MATERIALS AND METHODS

Materials

Piperine (95%) and Glyceryl monooleate (GMO) were received as free samples from Ms. Sami Labs Ltd., Bangaluru, India and Mohini Organics Pvt. Ltd. Mumbai, India, respectively. Black pepper, Trikatu churna, Ajmodadi churna and Chitrakadi gutika were procured from the Local Ayurvedic Pharmacy, Belagavi, India. Pluronic F-127 (PF-127) was purchased from Sigma Aldrich, USA. HPLC-grade acetonitrile (ACN), methanol and orthophosphoric acid (OPA) were procured from Merck, Mumbai, India and Fisher Scientific Mumbai, India. Deionized water obtained after filtration through Millipore Direct-Q®-3 equipment (Molsheim, France) was used for the analysis.

Instrument and experimental conditions

HPLC system (LC-20AD prominence equipment, Shimadzu, Japan) consisting of SPD-M20A PDA detector, LC- 20AD pump, a SIL-20AC HT auto sampler and CBM-20A communication bus module, operated through Shimadzu LC solution software (version 1.25). Luna C18 (150 × 4.6 mm i.d., 5µm) column provided with guard column (4 x 3.0 mm i.d.) of Phenomenex, USA and 30°C of column temperature were used for separation. The mobile phase consists of ACN: 0.01% OPA [60:40 v/v; pH 3] and pumped at a flow rate of 1 mL/min. The solvents were degassed and filtered through Millex HV® polyvinylidene fluoride membrane filters (0.45 µm; Millipore, Bedford, USA). Sample injection volume was kept 10 µL and detection of piperine was done at 340 nm.

Preparation of calibration standards

A methanolic stock solution (1 mg/mL) of piperine was prepared and used for calibration standard preparations of piperine in the series of concentrations of 0.5 - 20 µg/mL, by diluting stock with mobile phase. All solutions were kept in light resistant volumetric flasks to prevent possible photoisomerization.

Validation of developed method

Validation of developed method was done by using system suitability, linearity and limit of detection (LOD), limit of quantification (LOQ), precision, accuracy and stability as per ICH guidelines.[14]

Preparation of Cubosome nanoparticles

Piperine entrapped cubosome nanoparticles were formulated by using top-down method. The fragmentation techniques were used to formulate cubosomes using high speed homogenization followed by probe sonication method.[15] Briefly, Piperine (30 mg) and a previously optimized (refer to an upcoming paper) Pluronic F-127 (PF-127, 0.3 gm) and Glyceryl monooleate (GMO, 1.5 gm) were liquefied in separate container on a magnetic stirrer at 65°C. Piperine was added in melted GMO and was mixed with liquefied PF-127 solution. This mixture was then incorporated to water (preheated) with constant stirring. Homogenization (IKA T25, Germany) was performed for 15 min with 15,000 rpm to form a fine dispersion and thereafter, probe sonicated (5 min; RivoTEK, Mumbai) to form

cubosomal nanoformulation. After 24 hr of equilibrium, cubosome was further characterized for particle size, PDI and zeta potential by DLS (Zetasizer Nano ZS, UK). Entrapment efficiency of cubosome was determined by centrifuging (Eppendorf laboratory centrifuge, 5424R, Germany) the formulation for 15 min with 1500 rpm. The supernatant obtained after centrifugation process was processed for analyzing entrapment efficiency using HPLC. For the determination of loading capacity, weighed accurately the cubosomes nanoparticles were dispersed in methanol and vortexed for 10 min. The drug content was then analyzed using HPLC. The morphology of cubosome was observed by high resolution TEM (Jeol/JEM, 2100).

Method applicability for estimation of piperine in Black pepper and ayurvedic marketed products

Black pepper and ayurvedic marketed products containing piperine (Trikatu Churna, Ajamodadi Churna and Chitrakadi Gutika) were used for estimation of piperine content using developed HPLC method. Black pepper and Chitrakadigutika were powdered using mortar and pestle to obtain fine powder. The powdered black pepper and other ayurvedic marketed products weighed accurately and dissolved in methanol to obtain 1mg/ml stock solution. The light resistant volumetric flasks holding above samples were sonicated for 10 min and filtered using a 0.45 µm syringe filter. The sample was finally diluted with mobile phase and estimated for piperine content using HPLC.

Stress degradation Assay

It is generally advisable to control the degradation conditions to prevent it from maximum amount of degradation; hence 2 hr is mostly preferred for the (mild-strong) stress degradation studies. In the present study, stress degradation assays were performed for 2 hr as per ICH recommended stress conditions. For every stress degradation assay sample preparation were performed as a) Normal drug solution (0 h) and b) drug solutions subjected for degradation for 2 hr. Acid-base degradation studies were performed by treating piperine drug solution (1 mL) with 1 M HCl (1 mL) and 1 M NaOH (1 mL) solutions, individually in a separate light resistant volumetric flask. Sealing of the flasks were done followed by heating (80°C) for the duration of 2 h. Before HPLC evaluation, both the sample solutions were neutralized. In oxidative degradation study, drug solution (1 mL) was treated with hydrogen peroxide (30% H_2O_2; 1 mL), whereas in thermal degradation drug solution (1 mL) was treated with methanol (2 mL). Sealing of the flasks containing oxidative and thermal degradation samples were performed, followed by heating (80°C) for the duration of 2 h. In photodegradation study, drug solution (1 mL) was diluted with mobile phase in transparent volumetric flask up to 10 mL, sealed and kept outside under the sunlight for 2 hr. For all above degradation studies, the sample solutions were appropriately diluted with mobile phase, filtered and processed for HPLC system.[16-18]

Statistical analysis

All the results of validation and stress degradation studies were carried out in triplicates or six times and data were expressed as mean ± SD. Microsoft excel was used to calculate mean, standard deviation, % relative standard deviation (%RSD), slope and correlation coefficient of the experimental data. ANOVA analysis was performed for the calibration curve of piperine by GraphPad Prism software (GraphPad Software Inc., CA, USA).

RESULTS AND DISCUSSION

Method development

In the current investigation, a stability indicating RP-HPLC method was successfully established for piperine estimation in cubosome, black pepper and Ayurvedic marketed formulations. The established HPLC method was also employed to evaluate the stress degradation behavior of piperine under various stress environments. The developed method was selected on the basis of different chromatographic parameters namely mobile phase composition, flow rate and column oven temperature to get sharp and intense peaks. The sharpness and peak intensity was decided on the basis of peak height, peak area, peak width and tailing if any present. In addition to that, they obtained peak is considered good if there is absence of peak broadening, shoulder peak and peak splitting. Firstly, the results obtained from the mobile phase consisting ACN: water have shown less intense peak with poor resolution. When ACN was replaced with the methanol, some additional peaks were obtained with considerable increased resolution; less sharpness and tailing were observed for piperine peak. Therefore, for further method development, ACN and buffer such as OPA (0.1% v/v) were considered in the mobile phase mixture. It was observed from the results the concentration of OPA has affected the peak characteristic and other parameters. OPA (0.1% v/v) had given the broad peak with poor resolution, hence to improve the peak characteristics; concentration of OPA was reduced to 0.01% v/v. The mobile phase comprising ACN and

0.01% OPA (60:40 v/v; pH 3) provided sharp, intense and good resolved peak with 4.67 min of retention time (Figure 1A). The increased flow rate caused tailing, whereas reduced flow rate given broadness and longer retention time, hence flow rate with 1 mL/min was observed to be most suitable with all peak characteristics. Changes made in the oven temperature (20-40°C) had also shown considerable effect on the peak characteristics and retention time. A sharp, intense peak with less retention time was achieved by optimized oven temperature of 30°C.

Method validation

System suitability

Suitability of the HPLC system confirms the feasibility and acceptability of the developed HPLC method. The results of different system suitability parameters namely peak area, retention time (tR), tailing factor and plate count were observed to be in acceptable range (Table 1). The sharp and intense peak was obtained for piperine as shown in Figure 1A.

The data resulted from the parameters of system suitability study demonstrated the method was suitable to perform further analysis of piperine in different formulations.

Linearity

Linearity of the developed method is the linear relation between the peak areas and their correspondence concentrations. The regression analysis data demonstrated that the developed method was linear with the different series of concentrations (0.5-20 µg/mL) of piperine, which were estimated at 340 nm with correlation coefficient $R^2 > 0.999$ and suggesting acceptable linearity (Table 2; Figure 2). ANOVA analysis for piperine also proved that the regression model is statistically significant which predicts the outcome variable ($P < 0.05$) (Table 3).

Limit of quantification (LOQ) and Limit of detection (LOD)

LOD and LOQ are the analytes is the lowest detectable and quantifiable concentration which gives signal to noise ratio of 3:1 and 10:1 respectively. At 340 nm, the detection and quantification limit were observed to be 0.015 and 0.044 µg/mL for piperine indicating the developed HPLC technique was sensitive to determine piperine concentration in cubosome nanoparticles and marketed products (Table 2).

Precision

The precision is the measure of closeness of agreement between the numbers of measurements obtained from numbers of samples of the same sample under the provided steps.[19] Both inter-day (on three succeeding days) and intra-day (on the same day) analysis were performed at different concentrations (low, medium and high) and results are shown in Table 4. The values for percent RSD in intra-day precision and inter-day precision ranged between 1.20-1.78 % and 0.92-1.84 % respectively, which were < 2%, indicating both precision assays satisfies acceptance criteria and demonstrated the precise characteristic of the developed method.

Accuracy

Accuracy of developed HPLC method was indicated by the closeness value or percent difference between experimental and true value.[20] Known concentrations of piperine were spiked to their preanalyzed sample (2 µg/mL) at variable levels of concentrations (50, 100 and 150 %). The mean percent recoveries were in the range of 99.04 to 101.93% for piperine (Table 5), which indicates that the developed method was applicable for extensive scale of sample investigation.

Robustness

Robustness is the capability of the developed method to remain unaltered by slight intentional changes in chromatographic parameters. The robustness of the developed HPLC technique was analyzed on the basis parameters like percent RSD and retention time obtained, after introducing intentional variations in the mobile phase flow rate (±0.1 mL/min), OPA concentration (±0.09%), mobile phase ratio (±2%) and oven temperature (±5°C). It was demonstrated that the percent RSD (<1) values and system suitability parameters were remain to be not affected (Table 6), confirming the developed HPLC method is robust.

Cubosome characterization

In the present study, blank and piperine-loaded cubosome were successfully formulated by homogenizer method. The particle size, PDI and zeta potential for blank cubosome were 101 nm, 0.14 and -12.1 mV respectively, whereas for piperine-loaded cubosome those were 114 nm, 0.16 and -29.8 mV respectively (Table 7). The low

Table 1: System suitability test parameters.

Parameter	Piperine		Acceptance criteria
	Mean	SD	
Retention time (tR, min)	4.67	0.006	-
Peak area	549279	976	-
Plate count	6523	122	> 2000
Tailing Factor	1.13	0.01	≤ 2
Assymetry factor	1.12	0.01	≤ 2

Table 2: Linearity parameters data.

Concentration range (µg/mL)	Slope	Intercept	Regression coefficient (R^2)	Limit of Detection (µg/mL)	Limit of Quantification (µg/mL)
0.5-20	65943	25272	0.999	0.015	0.044

Table 3: Results of ANOVA analysis for calibration curve of Piperine

Model	SS	df	MS	F	R^2	*P* value
Treatment (between columns)	16221	2	8111	2.995e+007	1.000	< 0.0001
Individual (between rows)	3.699e+012	5	7.399e+011			
Residual (random)	247036	10	24704			
Total	3.699e+012	17				

SS- Sum of squares; df- degree of freedom; MS- Mean square; F- Fischer statistics value; R^2 – Regression coefficient; P value- Probability value

PDI values represented homogeneous nature with uniformly dispersed particles in the cubosome.[21] Zeta potential is an important factor in evaluating nanoparticle stability,[22] which demonstrated from the results that the negative charge on the cubosome nanoparticles was exerted, may be due to GMO containing free fatty acids. It was observed from the obtained chromatogram of cubosome that there were absence of interfering peaks of excipients used in the cubosome formulation with the parent peak of piperine, which was sharp and intense (Figure 1B). In the analysis of percent EE of cubosome, the concentration of piperine entrapped in the cubosome was evaluated by the developed analytical method, which was observed to be 86.31 %. The percent drug loading capacity was found to be 1.15 % (Table 6). The low drug loading value indicates that the piperine is preferably located in the aqueous phase rather than in lipid structures.

The morphology of the cubosome nanoparticles was investigated by the HR-TEM analysis. These cubosome particles appeared to be cubic, uniform, smooth surface with less curvature (Figure 3). The scattered particles are in the nano range and well separated from each other. The brightness around the cubic border structure indicates self-assembled lipid bilayer structure.

Analysis in black pepper and Ayurvedic marketed products

The established analytical method was considered in the determination of piperine content in black pepper and commercial available Ayurvedic marketed products.

The percent piperine content in Black pepper, Trikatu Churna, Ajamodadi Churna and Chitrakadi Gutika were found to be 98.16, 98.59, 99.20 and 98.83 % respectively, which was within the range of acceptable as per the labeled claim. The absence of interfering peaks observed for the HPLC chromatograms of black pepper and other marketed formulations indicated that other drugs and ingredients used in the marketed formulations did not interfere with the parent peak of piperine which demonstrated that this developed analytical method is applicable for routine evaluation of piperine in quality control laboratories (Figure 4).

Table 4: Intra-day and inter-day precision of piperine.

Piperine concentration (µg/mL)	Intra-day RSD (%)	Inter-day RSD (%)		
		1st Day	2nd Day	3rd Day
1	1.55	0.92	1.70	0.96
2	1.20	1.49	1.55	1.73
5	1.78	1.81	1.84	1.43

(*n*=3); RSD-Relative Standard Deviation.

Table 5: Evaluation of accuracy based on percent Recovery of piperine.

Level of added piperine (%)	Recovery (%)	RSD (%)
50	99.04	1.71
100	101.93	0.72
150	100.47	1.57

(*n*=3); RSD-Relative Standard Deviation.

Stress degradation assays

The data obtained from the stress degradation assays are presented in Table 8. The method applicability was proved from the obtained HPLC chromatograms where adequate separation was seen between drug peak and their degrading peaks (Figure 5).

It was observed from the acid degradation that the percent degradation of piperine was 51.64 %, which

Table 6: Results of Robustness assay.

Parameters	Variation made	tR ± S.D.	RSD (%)	T.F.± S.D.	RSD (%)	Plate count ± S.D.	RSD (%)
Composition of Mobile phase (ACN:0.01% OPA)	60:40	4.67 ± 0.006	0.12	1.13 ± 0.01	0.88	6523 ± 122	1.87
	58:42	4.65 ± 0.006	0.12	1.29 ± 0.009	0.69	6802 ± 98	1.44
	62:38	4.73 ± 0.010	0.21	1.35 ± 0.008	0.59	6020 ± 102	1.69
Concentration of OPA	0.01%	4.67 ± 0.006	0.12	1.13 ± 0.01	0.88	6523 ± 122	1.87
	0.10%	4.69 ±0.010	0.21	1.02 ± 0.006	0.58	6902 ± 64	0.92
Flow rate	1 mL /min	4.67 ± 0.006	0.12	1.13 ± 0.01	0.88	6523 ± 122	1.87
	0.9 mL /min	4.89 ±0.010	0.20	1.20 ±0.010	0.83	7010 ± 52	0.74
	1.1 mL /min	4.32 ±0.015	0.35	0.98 ± 0.009	0.91	6008 ± 60	0.99
Column oven Temperature	30°C	4.67 ± 0.006	0.12	1.13 ± 0.01	0.88	6523 ± 122	1.87
	35°C	4.60 ± 0.010	0.22	1.10 ± 0.008	0.72	6320 ± 65	1.02

tR- Retention time; T.F.- Tailing factor; S.D. – Standard deviation; RSD - Relative Standard Deviation.

Table 7: Cubosome Nanoparticles Characterization.

Cubosome preparation	Diameter (nm)	Polydispersibility index	ZP (mV)	Entrapment Efficiency (%)	Drug loading (%)
BC	101 ± 9.06	0.14 ± 0.02	-12.1 ± 2.69	--	--
PC	114 ± 4.22	0.16 ± 0.10	-29.8 ± 1.20	86.31±0.67	1.15 ±0.11

n=3; Mean ± Standard Deviation (SD), ZP- Zeta potential, BC- Blank cubosome, PC- Piperine entrapped cubosome

shown two small insignificant degraded peaks in acid degradation environment. In alkaline degradation study, piperine was less prone to degrade at lower percentage (37.11 %) with one small degrading peak. It was observed from the acid and alkaline degradation studies that, piperine was more stable over the alkaline stress condition as compared to acid stress condition, as piperine more favorable in alkaline condition and suggesting good stability of the developed method. The HPLC chromatogram obtained under thermal degradation study suggesting heating at 80°C for 2 hr does not affected stability of piperine, as the peak appeared exactly similar to normal peaks, absence of degrading peaks and negligible percent degradation. This might be because of high melting temperature of piperine, which doesn't affect their stability. In oxidative degradation study, at the retention time 2.38 min a peroxide peak was seen with percent degradation for piperine was 32.65 %. In photodegradation study (sunlight 2 h), piperine was almost 74.84 % was degraded. It was observed from the HPLC chromatogram the parent peak was diminishing and the degrading peaks were more intensely appeared. Dilute piperine solution more prone to photodegradation which has given two distinguishable degradation peaks. This might be because of piperine converts to their degrading product piperidine.

Table 8: Results for stress degradation assay.

Stress degradation study	% Drug degradation
Acidic (1 M HCl)	51.64 ± 1.24
Basic (1 M NaOH)	37.11 ± 1.71
Thermal	2.05 ± 1.08
Oxidative	32.65 ± 1.65
Photolytic (Sunlight)	74.84 ± 1.03

n=3; Mean ± Standard Deviation (SD)

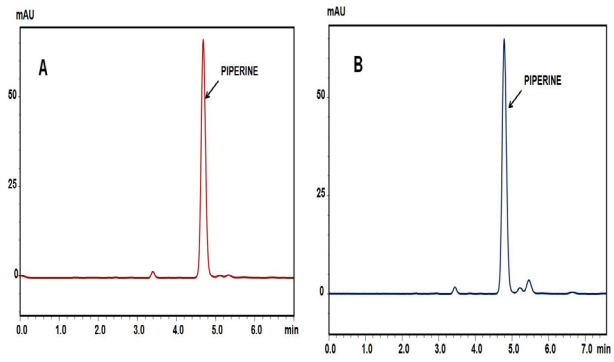

Figure 1: HPLC chromatograms for piperine (A) and piperine entrapped in cubosome nanoparticles (B) at λ_{max} 340 nm.

Under all stress degradation conditions, drugs peak integrity was maintained with nothing effect on the retention time.

Table 9: Comparison between previously published HPLC methods.						
Sr. No.	**Mobile phase And flow rate**	**Wavelength (nm)**	**Column**	**Limitations**	**Application**	**Ref.**
Piperine						
1	Methanol and water (50 : 50) Flow rate: 2ml/min	280 and 345	A stainless-steel μ Bondapak CN column	High flow rate and less sensitive	Rapid analysis of piperine in pepper and non-volatile ether extracts.	6
2	25mM KH_2PO_4 (pH 4.5)–acetonitrile (35:65) Flow rate: 1ml/min	340	C_{18}	Lack of stability study analysis in plasma	Analysis of piperine in rat plasma and methods applicability in pharmacokinetic study	7
Piperine and other drugs						
5	0.1% ortho phosphoric acid aqueous solution and acetonitrile (45:55, v/v) Flow rate: 1.2ml/min	262	C_{18}	Absence of stability study, expensive	Simultaneous estimation of curcumin and piperine with adequate separation and applied for estimation in nanoparticles	8
6	Acetonitrile : methanol : trifluoroacetic Acid : water (17.6 : 35.3 : 0.1 : 47.0, v/v/v/v) Flow rate : 1.2 ml/min	curcumin-415nm, piperine-335nm , b-17-estradiol acetate-280nm (internal standard)	Chromolith1 Speed ROD RP-18	Multiple wavelength used for detection, expensive due to high flow rate	Simultaneous estimation of Piperine and Curcumin in Plasma (human) and also applied for Clinical Pharmacological evaluation	9
7	Acetonitrile:Water (60 : 40, v/v) Flow rate : 1ml/min	240	C_{18}	Less sensitive method to detect lower concentration	Simultaneous estimation of piperine and guggulsterones in Unani dosage as well as in a nanoemulsion	10
8	25 mM Potassium dihydrogen phosphate (pH 4.5): Acetonitrile (50 : 50, v/v) Flow rate: 1ml/min	340 and 231	C_{18}	Absence of stability study	Simultaneous estimation of piperine and ketoconazole in rat plasma and culture of hepatocyte	11

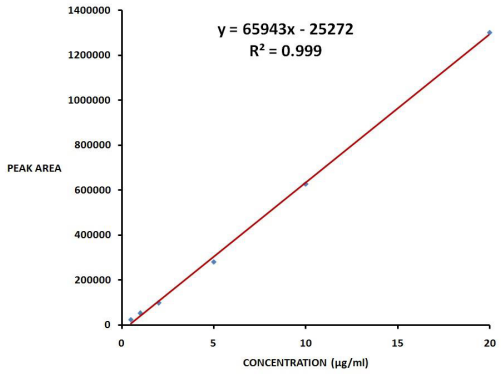

Figure 2: Linearity curve for Piperine.

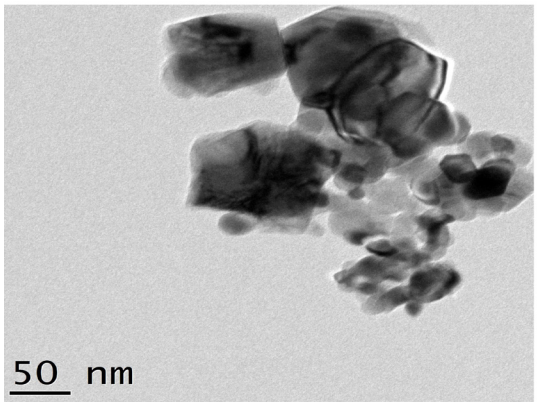

Figure 3: High resolution-transmission electronic microscopy (HR-TEM) of cubosome nanoparticles.

Comparison with previously published HPLC methods

Comparative evaluation of previously published methods and the current developed HPLC method was performed on the basis of mobile phase ratios, mobile phase flow rate, wavelength, column, stability study, limitations and applicability of the HPLC methods. The comparison data were represented in the Table 9. To date, there is no single HPLC method available which can be used for multiple analyses like estimation of piperine in nanoformulation, black pepper and marketed products and also to evaluate the degradation behavior of piperine using same parameters of developed HPLC method. The present method containing the mobile

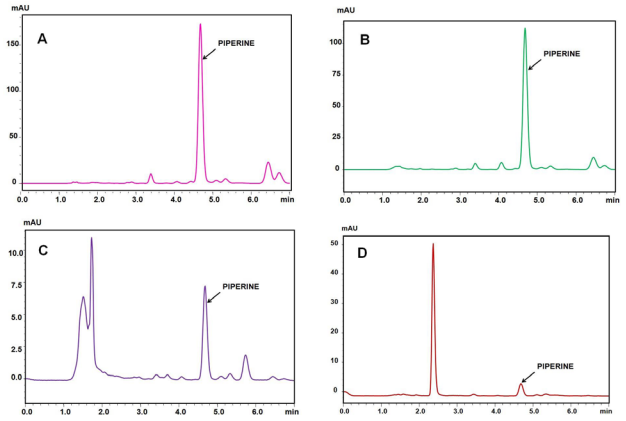

Figure 4: HPLC chromatograms for piperine obtained in the Black pepper (A), TrikatuChurna (B), AjamodadiChurna (C) and ChitrakadiGutika (D).

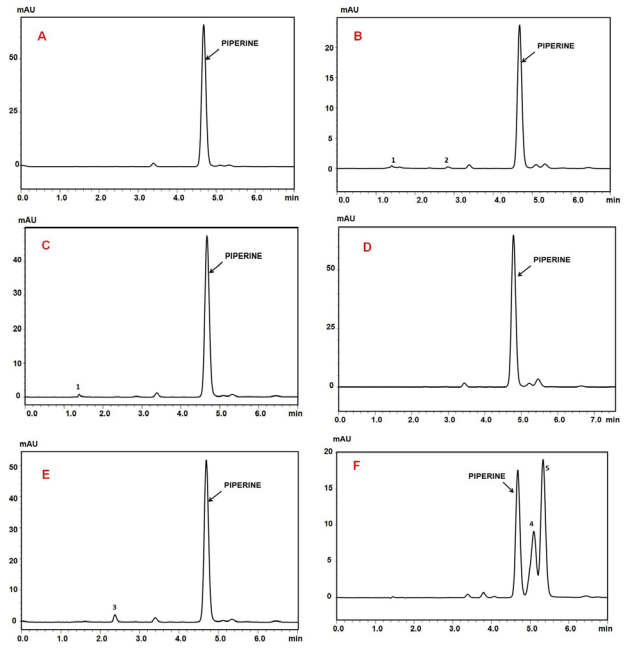

Figure 5: HPLC chromatograms of piperine (10 μg/mL) obtained in the stress degradation assays using Normal (A), Acidic (B), Basic (C), Thermal (D), Oxidation (E) and sunlight (F) stress conditions.

phase composition of ACN: 0.01% OPA (60:40 v/v; pH 3),1mL/min of flow rate with 340 nm as detection wavelength is found to be more sensitive, economic and stable when compared to other published literature.

CONCLUSION

A simple, specific, sensitive and stability indicating RP-HPLC method was successfully developed and evaluated for piperine estimation in cubosome nanoformulation, black pepper and ayurvedic marketed products. This developed RP-HPLC method allows easy quantification of piperine as compared to previously developed methods. The validation of established method was done as per ICH guidelines, which were within the acceptable limits. The established method demonstrates accurate and easy estimation of piperine in cubosome, black pepper and ayurvedic marketed products indicating reliable and sensitive nature of method. The results of stress degradation study suggested that piperine was considerably stable against acidic, alkaline and high thermal conditions. However, piperine was susceptible to degradation against oxidative and photolytic stress conditions. Hence, this simple, stability indicating RP-HPLC method is helpful for further routine quality control analysis. This method could thus be used for regular *in vitro* and *in vivo* estimation of piperine.

ACKNOWLEDGEMENT

We are thankful to KAHER, Belagavi for financial support to carry out the research work. We acknowledge Sami Labs Ltd., Bengaluru and Mohini Organics, Mumbai for supplying the gift samples.

CONFLICT OF INTEREST

The authors hereby declare that they don't have conflict of interest.

ABBREVIATIONS

ACN: Acetonitrile; **ICH:** International Conference on Harmonization; **RP-HPLC:** Reverse-Phase High Performance Liquid Chromatography; **i.d.:** internal diameter; **LOD:** Limit of detection; **LOQ:** Limit of Quantification; **GMO:** Glyceryl monooleate; **PF-127:** Pluronic F-127; **OPA:** Orthophosphoric acid; **DLS:** Dynamic light scattering **LC:** Liquid Chromatography; **RSD:** Relative standard deviation; **UV:** Ultraviolet; **PDA:** Prominence Diode Array; **RSD:** Relative Standard Deviation; **PDI:** Polydispersibility index; **EE:** Entrapment Efficiency; **HCl:** Hydrochloric acid; **NaOH:** Sodium hydroxide.

REFERENCES

1. Sunila ES, Kuttan G. Immunomodulatory and antitumor activity of *Piper longum* Linn. and piperine. J Ethnopharmacol. 2004;90(2-3):339-46. https://doi.10.1016/j.jep.2003.10.016.
2. Bhardwaj RK, Glaeser H, Becquemont L, Klotz U, Gupta SK, Fromm MF. Piperine, a major constituent of black pepper, inhibits human P-glycoprotein and CYP3A4. J Pharmacol Exp Ther, ASPET. 2002;302(2):645-50. https://doi.org/10.1124/jpet.102.034728
3. Kurangi BK, Jalalpure SS. Review of selected herbal phytoconstituents for potential melanoma treatment. Indian J Heal Sci Biomed Res. 2018;11(1):3. https://doi.org/10.4103/kleuhsj.kleuhsj_319_17.

4. Jasoliya J, Jani A. Method development and validation of RP-HPLC method for simultaneous estimation of resveratrol and piperine in combined capsule dosage form. World J Pharm Pharm Sci. 2014;3(5):1096-107.
5. Kurangi B, Jalalpure S, Jagwani S. A validated stability-indicating HPLC method for simultaneous estimation of resveratrol and piperine in cubosome and human plasma. J Chromatogr B Anal Technol Biomed Life Sci. 2019;1122-3. https://doi.org/10.1016/j.jchromb.2019.05.017
6. Rathnawathie M, Buckle KA. Determination of piperine in pepper (*Piper nigrum*) using high-performance liquid chromatography. J Chromatogr, 1983; 264:3(1) 320.
7. Bajada S, Singlab AK, Bedia KL. Liquid chromatographic method for determination of piperine in rat plasma: Application to pharmacokinetics. J Chromatogr B. 2002;776:245-49.
8. Moorthi C, Kumar CS, Mohan S, Krishnan K, Kathiresan K. Application of validated RP-HPLC-PDA method for the simultaneous estimation of curcumin and piperine in Eudragit E 100 nanoparticles. J Pharm Res. 2013;7(3):224-9. http://dx.doi.org/10.1016/j.jopr.2013.03.006.
9. Sethi P, Dua VK, Mohanty S, Mishra K, Jain R, Edwards G, *et al.* Journal of Liquid Chromatography and Related Technologies Development and Validation of a Reversed Phase HPLC Method for Simultaneous Determination of Curcumin and Piperine in Human Plasma for Application in Clinical Pharmacological Studies. J Liq Chromatogr. Relat Technol. 2009;32(20):2961-74. https://doi.org/10.1080/10826070903320178.
10. Kamal YT, Musthaba SM, Singh M, Parveen R, Ahmad S, Baboota S, *et al.* Development and validation of HPLC method for simultaneous estimation of piperine and guggulsterones in compound Unani formulation (tablets) and a nanoreservoir system. Biomed Chromatogr. 2011. https://doi.org/10.1002/bmc.2676.
11. Bajad S, Johri RK, Singh K, Singh J, Bedi KL. Simple high-performance liquid chromatography method for the simultaneous determination of ketoconazole and piperine in rat plasma and hepatocyte culture. J Chromatogr A. 2002;949(1-2):43-7.
12. Bhat BG, Chandrasekhara N. Studies on the metabolism of piperine: Absorption, tissue distribution and excretion of urinary conjugates in rats. Toxicology. 1986;40(1):83-92.
13. Hashimoto K, Yaoi T, Koshiba H, Yoshida T, Maoka T, Fujiwara Y, *et al.* Photochemical isomerization of piperine, a pungent constituent in pepper. Food Sci Technol Int. 1996; 2(1): 24-29.
14. Validation of analytical procedure: Methodology International Conference on Harmonization. "ICH Harmonised tripartite guideline - Validation of analytical procedures: Text and methodology Q2(R1). 2005.
15. Ahirrao M, Shrotriya S. *In vitro* and *in vivo* evaluation of cubosomal *in situ* nasal gel containing resveratrol for brain targeting. Drug Dev Ind Pharm. 2017;43(10):1686-93. http://dx.doi.org/10.1080/03639045.2017.1338721
16. Kumar S, Lather V, Pandita D. Stability indicating simplified HPLC method for simultaneous analysis of resveratrol and quercetin in nanoparticles and human plasma. Food Chem. 2016;197:959-64. http://dx.doi.org/10.1016/j.foodchem.2015.11.078
17. Pangeni R, Sharma S. Design expert-supported development and validation of stability indicating high-performance liquid chromatography (HPLC) method for determination of resveratrol in bulk drug and pharmaceutical formulation. Int J Pharm Sci Res. 2015;6:5115-25. https://doi.org/10.13040/IJPSR.0975-8232.6(12).5115-25.
18. Peram MR, Jalalpure S, Joshi SA, Palkar MB. A Single Robust RP-HPLC Analytical Method for Quantification of Curcuminoids in Commercial Turmeric Products, Ayurvedic Medicines and Nanovesicular Systems. J Liq Chromatogr Relat Technol. 2017; 40(10):487-98. https://doi.org/10.1080/10826076.2017.1329742.
19. Jagwani S, Jalalpure S, Dhamecha D, Hua GS, Jadhav K. Development and Validation of Reverse-Phase High-Performance Liquid Chromatographic Method for Determination of Resveratrol in Human and Rat Plasma for Preclinical and Clinical Studies. Indian J of Pharmaceutical Education and Research. 2020;54(1):187-93. https://doi.org/10.5530/ijper.54.1.22
20. Jagwani S, Jalalpure S. A Stability Indicating Reversed Phase HPLC Method for Estimation of trans -Resveratrol in Oral Capsules and Nanoliposomes. TACL. 2019;9(5):711-26.
21. Dhamecha D, Jalalpure S, Jadhav K. Doxorubicin functionalized gold nanoparticles: Characterization and activity against human cancer cell lines. Process Biochem. 2015;50(12): 2298-306.
22. Jadhav K, Deore S, Dhamecha D, Rajeshwari H R, Jagwani S, Jalalpure S, *et al.* Phytosynthesis of Silver Nanoparticles: Characterization, Biocompatibility Studies and Anticancer Activity. ACS Biomater-Sci Eng. 2018;4(3):892-9. https://doi.org/10.1021/acsbiomaterials.7b00707

PICTORIAL ABSTRACT

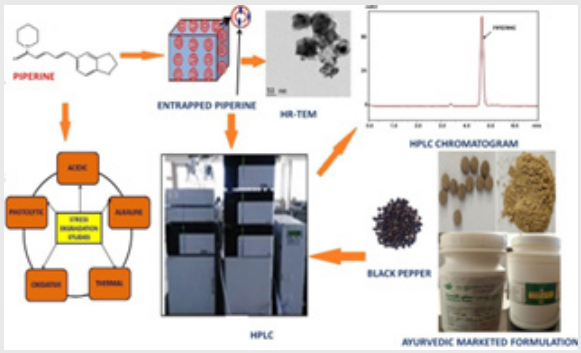

SUMMARY

RP-HPLC method was successfully developed and validated for piperine and successfully evaluated for its quantitative estimation in cubosome nanoparticles, black pepper and ayurvedic marketed products. The stability of the developed HPLC method was indicated by the stress degradation studies. The HPLC analysis was done by using Phenomenex C_{18} column using optimized mobile phase comprised of ACN: OPA (60:40, v/v), 1mL/min of flow rate with 340 nm as detection wavelength. The developed method was sensitive, accurate, precise and economical to detect piperine in cubosome nanoformulation and commercial marketed products.

About Authors

Mr. Bhaskar Kurangi, is a Ph.D scholar at KLE College of Pharmacy, Belagavi, and working at Dr. Prabhakar Kore Basic Science Research Center, KLE Academy of Higher Education and Research, Belagavi. His current research interest are development and evaluation of novel drug delivery systems, Analytical method development, Nanoparticulate drug delivery and its application to target cancers

Dr. Sunil Jalalpure is presently working as a Principal at KLE College of Pharmacy, Belagavi, K.L.E Academy of Higher Education and Research, Belagavi. His areas of research interests include isolation/ characterization of active principles from medicinal plants and their pharmacological screening for various biological activities and training the research students in Pharmacognosy, Phytochemistry and Biotechnological aspects with modern tools and techniques. He is recently involved in nanoparticle drug delivery system of herbal actives and green nanotechnology.

Cite this article: Kurangi B, Jalalpure S. A Validated Stability-indicating RP-HPLC Method for Piperine Estimation in Black Pepper, Marketed Formulation and Nanoparticles. Indian J of Pharmaceutical Education and Research. 2020;54(3s):s677-s686.

Review Article

Access this article online

Quick Response Code:

Website:
www.ijournalhs.org

DOI:
10.4103/kleuhsj.kleuhsj_319_17

Review of selected herbal phytoconstituents for potential melanoma treatment

Bhaskar Kallappa Kurangi[1], Sunil Satyappa Jalalpure[1,2]

Abstract:

Malignant melanoma is the most aggressive form of skin cancer, with a high mortality rate. The current chemotherapies have a relatively low success rate due to the development of multidrug resistance and side effects. Hence, there is need of discovering new compounds that are safe and more effective against melanoma to improve the efficiency and to lower the treatment cost for cancer care. Melanoma chemoprevention with natural herbal phytoconstituents is an emerging strategy to prevent, cure, or treat melanoma. This review summarizes the latest research in melanoma chemoprevention and treatment using the herbal phytoconstituents. Relevant mechanisms involved in the pharmacological effects of these phytochemical are discussed. Phytoconstituents that are discussed in this review are carotenoids, flavonoids, some polyphenols, piperine alkaloid, and sulforaphane having high anticancer potential mostly to be used for the treatment of melanoma.

Keywords:

Anticancer, chemoprevention, melanoma, phytoconstituents

Introduction

Melanoma

Melanoma is the most fatal kind of skin cancer which is a malignant tumor that originates from melanocytes and especially involves the skin [Figure 1]. Apart from the skin, melanomas can also found in the eyes and meninges and on various mucosal surfaces. Usually, melanomas are pigmented and amelanotic. Even the small tumors can have a tendency to metastasize and thus lead to an unfavorable prognosis. The death rate associated with melanoma is 90% which can be related with cutaneous tumors.[1,2] Melanoma incidence is going to be increased worldwide in the White populations with excessive sun exposure. In the USA, about 76,380 new cases of melanoma were diagnosed in 2016.[3] Approximately 132,000 cases of melanoma and over 2 million cases of nonmelanoma are diagnosed worldwide every year. The diagnosis for skin cancer throughout the world is one in every three cancers.[4] Worldwide, about 55,000 deaths were estimated in 2012.[5]

Ultraviolet irradiation is the most important exogenous factor for melanoma, particularly intermittent sun exposure.[6] Malignant melanoma is most common among the White-skinned peoples than Black, Asian, or Hispanic population. The White-skinned people have approximately 10 times greater risk of developing melanoma.[7] However, in the plantar malignant melanoma, it was found that melanoma incidence is equal in both the White and Black population.[8] In India, malignant melanoma is not common and its incidence rate is <0.5%.[9]

The current clinical approach and therapy selected for cutaneous melanoma are surgery, chemotherapy or immunotherapy, and/or the combination of the two. Unfortunately, attempts made for improving the survival by surgically removing lymph

[1]Dr. Prabhakar Kore Basic Science Research Center, KLE Academy of Higher Education and Research, [2]Department of Pharmacognosy and Phytochemistry, KLE University's College of Pharmacy, KLE Academy of Higher Education and Research, Belagavi, Karnataka, India

Address for correspondence:
Dr. Sunil Satyappa Jalalpure, KLE University's College of Pharmacy, KLE Academy of Higher Education and Research, Nehru Nagar, Belagavi - 590 010, Karnataka, India.
E-mail: jalalpuresunil@rediffmail.com

How to cite this article: Kurangi BK, Jalalpure SS. Review of selected herbal phytoconstituents for potential melanoma treatment. Indian J Health Sci Biomed Res 2018;11:3-11.

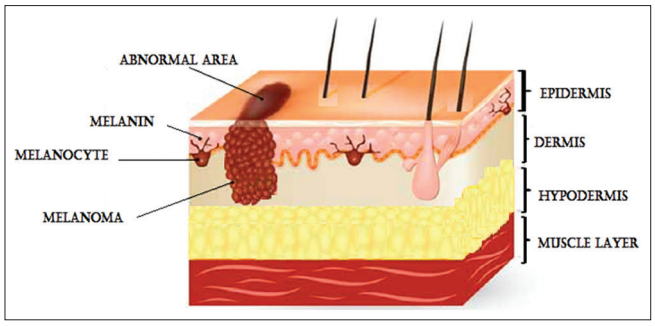

Figure 1: Melanoma tumor development in the skin

nodes can result in no overall survival benefits.[10] Other than surgery, there are two major alternatives for the management of melanoma such as chemotherapy and immunotherapy. Although the current chemotherapies have their advantages, they are either not effective enough or cause serious side effects and toxicity. In the randomized experiments to date for melanoma, it has been reported that no single drug or combination of therapies is superior to existing drugs.[11] Therefore, there is need for herbal drugs which can offer improved efficacy over existing chemotherapy, in melanoma therapy.

Need of natural herbal products

Development of multidrug resistance and severe adverse effects is the main problem that exists with chemotherapeutic agents. Some of the methods by which melanoma cells can develop resistant to chemotherapeutic agents are drug efflux systems, amplification of drug targets, or changes in drug kinetics.[12-14] To overcome drug resistance, different strategies have been attempted, such as use of nanoparticles, liposomes, and micellar drug delivery vehicles, with some reported successes.[14] The adverse effects, side effects, and multidrug resistance of cancer chemotherapy can be treated symptomatically, but in some instances, some secondary treatments may be very toxic, which is unacceptable to some cancer patients.[15-17]

Because of the drawbacks associated with conventional cancer chemotherapies, interest has been grown for natural therapies. Different phytochemical compounds obtained from the extracts of plant roots, bulbs, barks, leaves, stems, and others have shown promising potential as anticancer drugs or for serving as lead compounds in the synthesis of new drugs. The main limiting factor for natural products and traditional medicines is the different preparation method. Apart from that chemical composition, dosage determination, dose adjustment, and suitable route of administration are also important factors for the herbal medicines. Although much research on the compounds of natural origin is required to produce new drug products for which research, specifically aimed at naturally derived medicines to optimize dosages for the intended route of administration and to design the most effective dosage forms, has become essential.[18]

Phytoconstituents Showing Activity for Melanoma

Phytoconstituents exerts different types of immunomodulatory, anti-inflammatory, and antioxidant properties, but generally, they have the highest potential of exerting chemopreventive action in melanoma.[19] Number of research has been done to find out the correlation between antioxidant properties and anticancer activity of these phytoconstituents. No strong evidence has been found related with such a correlation still, but the antioxidant potential of a phytoconstituent is being regarded as an indication for potential anticancer activity.[20,21] Phytoconstituents such as carotenoids, flavonoids, and terpenoids having high anticancer potential can be used for the treatment of melanoma [Figure 2].[22-24]

Flavonoids

Flavonoids are pigmentary compounds which exist in plants. Structurally, flavonoids contain two benzene rings which are connected through a linear carbon chain and an aromatic chromophore.[25] Flavonoids include flavones, flavanones, isoflavones, anthocyanins, and flavan-3-ols (catechins). Figure 3 describes the chemical structures of some flavonoids which exhibit anticancer activities.

Epigallocatechin-3-gallate

The catechin epigallocatechin-3-gallate (EGCG) is one of the main flavonoid compounds found in green tea which has been received enormous pharmacological attention because of its potential benefits to health. EGCG possess anti-inflammatory, antioxidant, antimutagenic, and anticarcinogenic properties.[26-28]

It has been reported that EGCG has the capacity to induce apoptosis and cell cycle arrest in melanoma cells, either alone or in combination with vorinostat *in vitro*.[29,30] For the melanoma treatment, a combination strategy with interferon has shown synergistic antiproliferative effects in both *in vitro* and *in vivo* studies.[31] Different mechanisms by which EGCG has shown effects include upregulation of Bcl-2-associated X protein, downregulation of apoptosis-inhibiting proteins, cell survival-promoting proteins, a pro-apoptosis protein, activation of caspases-3, -7, and -9, and through the induction of tumor suppressor proteins.[32,33] EGCG showed pro-apoptotic activity, selective toward melanoma cells and not toward the normal melanocytes.[33] Development of EGCG into a practical therapeutic agent may require an interdisciplinary approach to modify EGCG

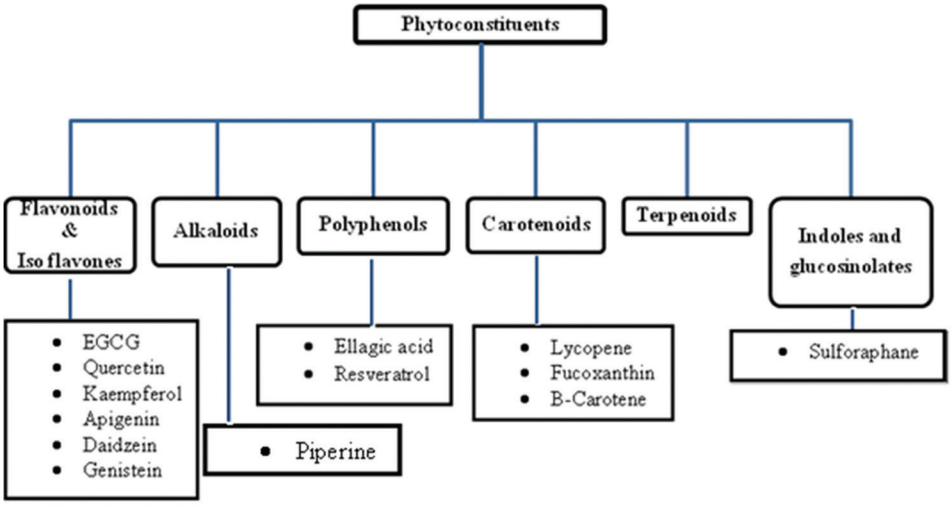

Figure 2: Classification of phytoconstituents

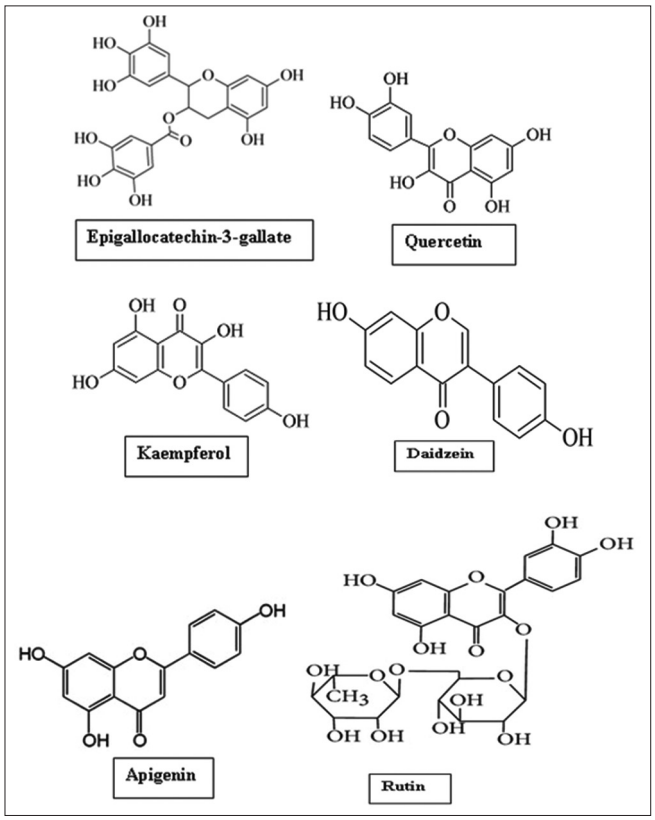

Figure 3: Chemical structures of selected flavonoids having anticancer potential

structure and increase its potency and pharmacokinetic properties.

Quercetin

Quercetin is the most abundant flavonol present in the human diet and in plants in different glycosidic forms, such as galactosides, rhamnosides, arabinosides, or glucosides.[34,35] The derivatives of quercetin accounts for 60% of the total flavonoids ingested daily and are the most abundant and important dietary flavonoids present in the human diet.[36] The quercetin derivatives are commonly found in many fruits and vegetables, such as red onions, apples, berries, parsley, olive oil, cocoa, citrus fruits, tea, and red wine.[37,38]

The mechanism by which quercetin had shown activity against melanoma at low concentrations by affecting cell viability and at higher concentrations by inducing apoptosis.[39] It was reported that in murine melanoma cells, quercetin induced apoptosis by diminishing the expression of B-cell lymphoma 2 and increasing the effectiveness of caspase-3 activity.[40] The recent study has reported that the quercetin activity for melanoma may be due to inhibitory effects on signal transducer and activator of transcription 3, which is an oncogenic protein.[41] Overall quercetin could be used to take advantage of tyrosinase activity in melanoma treatment with minimum additional side effects related with it. However, dietary intake would be suitable in the development of preventative approaches, while systems including nanoparticles or any other nanoformulation will be required to achieve the best effective quercetin concentrations for therapeutic approaches.

Kaempferol

Kaempferol, a natural flavonol compound belonging to flavonoids category, occurs mostly in a variety of plants and plant-derived food products. Kaempferol is abundantly available in tea, broccoli, beans, strawberries, and apples.[42]

Kaempferol acts in the different mechanisms for regulation of cancer cells. It has been reported that kaempferol is a potent promoter of apoptosis and also it modifies a host of cellular signaling pathways such as inhibiting cell proliferation.[43] Compared to standard

chemotherapeutic drugs, kaempferol is much less toxic to normal cells.[44] A study has shown that kaempferol blocks choroidal melanoma cell cycle progression in the G2/M phase.[45] For transdermal delivery, the kaempferol submicron emulsion systems has been developed, and it was found that because of emulsion systems, there was significant influence on the flux, the amount of drug deposition in skin and lag time.[46] The synergistic activity along with quercetin has been shown in melanogenesis inhibition. Moreover, they were considered as good blockers of enzyme activity, especially in hyperpigmentation.[47]

Daidzein

Daidzein is an isoflavone, which is a hormone-like substance found exclusively in soybeans and other legumes. It is highly soluble in alkaline environments and is part of a group of compounds, called phytoestrogens.[48]

Daidzein has shown some effective photo-protection potential in the skin by topical application.[49] Daidzein and genistein have been investigated to produce synergistic inhibitive effect on the metastatic melanoma cells (murine K1735M2).[50]

Apigenin

Apigenin is a naturally occurring product belonging to the flavonoids category which is anaglycone of several naturally occurring glycosides. Apigenin is mostly found in celery, oranges, tea, parsley, thyme, and onions.[51]

The anticancer activities of apigenin have been observed *in vitro* in the melanoma cell lines (MELs-28). The different mechanisms by which apigenin exerts action include inducing cell cycle arrest in the G2/M phase, upregulating tumor necrosis factor receptor (TNF-receptor), and the TNF-related apoptosis-inducing ligand receptor apoptotic pathway.[33] The combinations of all these actions result into chemoprotective effects of apigenin. Subsequent studies on apigenin has shown antimelanoma effects, which includes inhibition metastasis of melanoma.[52,53] Along with quercetin, there is inhibition of melanoma growth and invasive and metastatic melanoma.[52]

Rutin

Rutin is the glycoside which is the combination of quercetin flavonol and the rutinose disaccharide. It occurs in a wide variety of plants such as passion flower, buckwheat, tea, and apple. It is one of the vital nutritional components of food stuff.[54]

It has demonstrated a number of pharmacological activities, including antioxidant, cytoprotective, vasoprotective, anticarcinogenic, neuroprotective, and cardioprotective activities.[55,56] One study has reported that rutin inhibited the growth and tumor weight of B16 melanoma as well as melanin content in C57BL/6 mice.[57]

Carotenoids

Carotenoids are a class of >750 naturally occurring fat-soluble pigments commonly found in plants, algae, and photosynthetic bacteria.[58] The carotenoids containing the structure such as distinctive conjugated double bond which acts as a light-absorbing chromophore and that imparts yellow, orange, or red color to vegetables, oranges, and other food products.[59] Carotenoids are divided into two classes, such as xanthophylls and carotenes. Figure 4 describes the chemical structures of some carotenoids which exhibit anticancer activities, especially against melanoma.

Lycopene

The red color to fruits and vegetables is imparted by a natural pigment which is lycopene. Lycopene is found in watermelons, pink grapefruits, apricots, and pink guavas. It is found in particularly high amounts in tomatoes and tomato products.[59]

Lycopene is one of the most effective carotenes for oxidative stress reduction. It should be considered as an excellent additive to the diets of patients which are at high risk for melanoma.[60] Studies have shown that lycopene inhibits platelet-derived growth factor-BB, which in turn reduces melanoma cell-induced fibroblast migration and signaling transduction. Hence, this explains that lucopene bears the antitumor properties.[61]

Fucoxanthin

Fucoxanthin is an orange-colored pigment, together with chlorophylls a, c and β-carotene which are to be found in chromophyta, brown seaweeds, and diatoms.[62]

Fucoxanthin exerts anticancer effects such as reduced tumor incidences, cell cycle arrest, induction of apoptosis, inhibition of proliferation, and inhibition of metastasis.[63] The *in vitro* and *in vivo* study has shown that fucoxanthin inhibits the growth of B16F10 melanoma cells.[64] In SK-MEL-28 malignant MEL-28 study, the anticancer effect of fucoxanthin has also been reported.[65] Fucoxanthin also shown the activity against metastatic melanoma by suppressing murine melanoma cells, by downregulation of proteins involved in cell migration, cell interaction, and cell adhesion.[66]

β-Carotene

β-Carotene is an organic, abundantly found in plants and fruits. β-Carotene is a pigment which has strong red-orange color. In nature, β-carotene is a precursor to vitamin A. β-Carotene was described as an antioxidant that protected against cancer, heart disease, macular degeneration, and aging.[67-69]

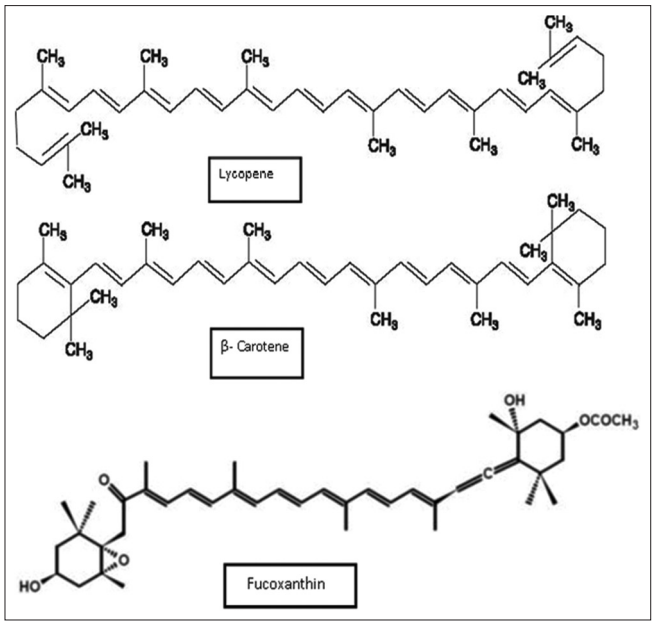

Figure 4: Chemical structures of selected carotenoids having anticancer potential

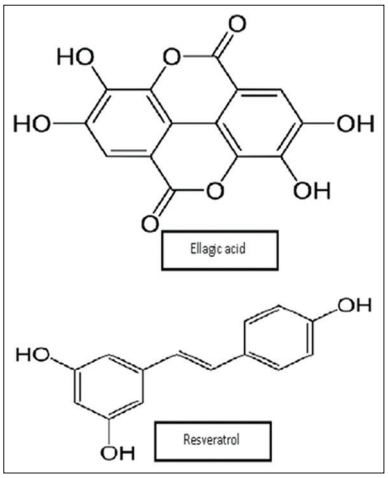

Figure 6: Chemical structures of selected polyphenols having anticancer potential

The *in vitro* study in melanoma cells reported that β-carotene is able to induce apoptosis by activating caspases-3, -8, and -9 through caspase cascade.[70] It was reported that the diet high in β-carotene may be related to a decreased melanoma risk.[71,72]

Alkaloid

Alkaloids are a group of naturally occurring nitrogenous chemical compounds found in plants, typically insoluble in water. The different organisms such as bacteria, fungi, plants, and animals are the main source of the alkaloids. Alkaloids are exerting different pharmacological actions such as antimalarial, antiasthma, anticancer, vasodilatory, antiarrhythmic, analgesic, antibacterial, and antihyperglycemic activities.[73] Berberine, cryptolepine, and vinca alkaloids have been shown activity for melanoma. In this present review, the alkaloid discussed for antimelanoma activity is piperine.[74-76]

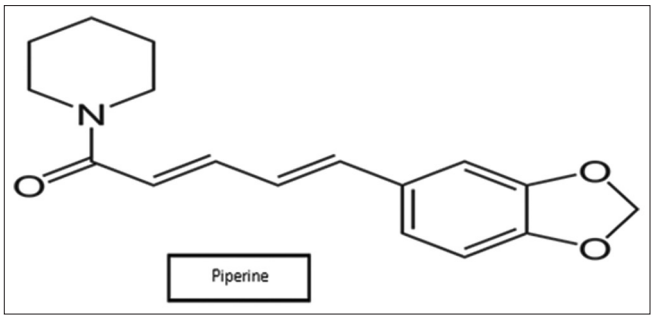

Figure 5: Chemical structure of piperine

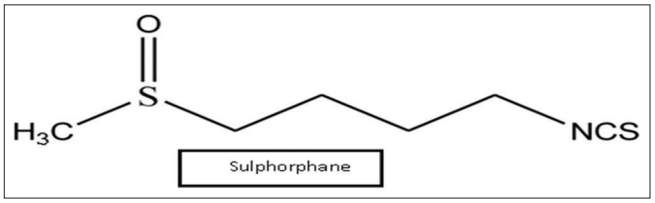

Figure 7: Chemical structure sulforaphane

Piperine

Piperine is an alkaloid found in *Piper nigrum* and *Piper longum*. It exhibits wide variety of biological actions such as anti-inflammatory, antioxidant, antiarthritic and antidepressant effects Figure 5 shows chemical structure of piperine.[77,78]

Piperine inhibits CYP3A4 and P-glycoprotein by which bioavailability of other drugs can be enhanced.[79] Curcumin has different stability problems.[80] Along with curcumin, administration of piperine increases bioavailability of curcumin.[76] Clinical trials are also being conducted to evaluate the effect of piperine in enhancing the bioavailability of other phytoconstituents. The antiproliferative effects of piperine in murine as well as in human melanoma cells were studied. The studies have reported that growth inhibitory effects of piperine were mediated by apoptosis and cell cycle arrest of both the cell lines, i.e., SK-MEL-28 and B16 F0 cells in G1 phase.[81]

Polyphenol

Polyphenols are mainly natural but also synthetic or semisynthetic, organic chemicals characterized by the presence of large multiples of phenol structural rings. There are over 8000 identified polyphenols compounds found most abundantly in whole foods such as dried spices, fruits, vegetables, red wine, and cocoa, tea, wine, and chocolates.[82] Polyphenol plays an important role in the prevention and in reduction of progression of diseases such as diabetes, cardiovascular and neurodegenerative diseases, and cancer. Figure 6 shows

the chemical structure of selected polyphenols having anticancer potential.[83]

Ellagic acid

Ellagic acid is a fused four-ring polyphenol. Ellagic acid is present in many red fruits and berries, including raspberries, strawberries, blackberries, cranberries, pomegranate, and some nuts including pecans and walnuts.

It possesses antifibrotic and antioxidant properties and also exhibits *in vitro* antitumor properties against various cancer cells.[84,85] Ellagic acid had shown apoptosis induction property in human melanoma cells.[86] Ellagic acid is thought to suppress melanogenesis by reacting with activated melanocytes and without injuring cells.[87]

Resveratrol

Resveratrol is a nutraceutical which has exciting pharmacological potential and because of this recently attracted a lot of research attention. It is a phytoalexin compound found in many plants such as grapes, peanuts, and berries. Resveratrol is a model stilbene having cardioprotection, chemoprevention, and antitumor activities.[88]

Resveratrol has been investigated as an anticancer agent. In doxorubicin-resistant murine melanoma cells, the potency of resveratrol has been demonstrated by inducing apoptosis and inhibiting the growth of melanoma tumors in mice.[89] The *in vitro* study had shown that combination with temozolomide act as an effective cytotoxic agent against melanoma cells.[90] Due to its low bioavailability, the *in vivo* anticancer effects of resveratrol are strongly limited.[91] Hence, approaches are to be done to increase its bioavailability either by bioenhancer or by nanotechnology approaches. The study had shown that resveratrol sensitizes melanoma cells to interleukin-2 immunotherapy which had caused induced cell death.[92]

Indoles and glucosinolates

Glucosinolates are a group of secondary products found in plants of the family *Cruciferae*. On enzymatic hydrolysis, they give rise to volatile, pungent, and physiologically active compounds which have antifungal, antibacterial, bioherbicidal, biopesticidal, antioxidant, antimutagenic, and anticarcinogenic activity. Recently, indole glucosinolates are attracting attention because of its properties. On hydrolysis either by chemical or enzymatic, the indole glucosinolates give the different involatile indole compounds which have anticarcinogenic activity.[93]

Sulforaphane

Sulforaphane is an isothiocyanate found especially in broccoli sprouts, Chinese kale, cabbage, and watercress. It prevents or delays preneoplastic lesions Figure 7 shows chemical structure of sulforaphane. Sulforaphane has therapeutic activity in tumor cell cultures, carcinogen-induced cancer models, and genetic animal cancer models.[94,95] The mechanisms by which sulforaphane exerts anticancer activity by suppressing various critical hallmarks of cancer, such as cell growth and proliferation, apoptosis, invasion, and migration.[96] In combination with quercetin, sulforaphane inhibits the proliferation and migration of melanoma (B16F10) cells more effectively than either compound used alone. This combined effect was predominantly due to a decrease in matrix metalloproteinases expression in the mouse tumors.[97]

The sulforaphane has shown antimetastatic activity in murine melanoma model with *in vivo* study by which it will be helpful in cancer immunotherapy.[98]

Pharmaceutical Developmental Challenges and Opportunities

Traditional use of natural herbal phytoconstituents in melanoma treatment is relatively cheap due to the availability of plants and the simple methods used in formulation development. However, commercialization of natural compounds for cancer treatment, i.e., for melanoma, may result in declining of natural resources and problems with producing a consistent quality of adulteration. Hence, most naturally derived medicinal compounds are eventually manufactured by either semisynthetically or fermentation. For commercial use, then, these are formulated into an appropriate dosage form by which cost of the products get increased. As cancer chemoprevention and treatment using natural phytoconstituents have been such an attractive approach, further efforts are fully justifiable to thoroughly understand their potencies, pharmacokinetic performances, pharmacodynamic responses, metabolisms, toxicities, drug–drug interactions, polymorphisms, and then formulations, stabilities and degradations, and dosage regimens. Lots of scientific research are to be needed to evaluate and optimize the herbal phytochemical products for safe and more effective human use. Phytochemical products should be formulated by a novel method of nanotechnology. The drawbacks related to phytoconstituents such as poor pharmacokinetic properties, targetability, and poor bioavailability of herbal phytoconstituents, for which nanotechnology should be introduced.

Conclusion

From this review, it has become clear that herbal phytoconstituents can play a major role in future melanoma treatments. This article has summarized some

selected herbal phytoconstituents such as carotenoids, flavonoids, some polyphenols, piperine alkaloid, and sulforaphane which have been studied for their possible antimelanoma activity. Antimelanoma activities of phytoconstituents can be ascribed to a distinct phytochemical or to a combination of the effects of different phytochemicals. Most of the phytoconstituents have shown both *in vitro* and *in vivo* activity for melanoma. Hence, natural phytoconstituents have been and will continue to be a promising and active source for the drug discovery in the treatment of melanoma.

Financial support and sponsorship
Nil.

Conflicts of interest
There are no conflicts of interest.

References

1. Eggermont AM, Spatz A, Robert C. Cutaneous melanoma. Lancet 2014;383:816-27.
2. Garbe C, Peris K, Hauschild A, Saiag P, Middleton M, Spatz A, *et al.* Diagnosis and treatment of melanoma: European consensus-based interdisciplinary guideline. Eur J Cancer 2010;46:270-83.
3. American Cancer Society. Cancer Facts & Figures 2016. Atlanta: American Cancer Society; 2016. p. 1-66.
4. WHO. Sunbeds, Tanning and UV Exposure. Fact Sheet No. 287. Interim Revision. WHO Media centre who.int/mediacentre/.../print.html: World Health Organization; 2010.
5. Ferlay J, Soerjomataram I, Dikshit R, Eser S, Mathers C, Rebelo M, *et al.* Cancer incidence and mortality worldwide: Sources, methods and major patterns in GLOBOCAN 2012. Int J Cancer 2015;136:E359-86.
6. Tsao H, Atkins MB, Sober AJ. Management of cutaneous melanoma. N Engl J Med 2004;351:998-1012.
7. Ries LA, Wingo PA, Miller DS, Howe HL, Weir HK, Rosenberg HM, *et al.* The annual report to the nation on the status of cancer, 1973-1997, with a special section on colorectal cancer. Cancer 2000;88:2398-424.
8. Stevens NG, Liff JM, Weiss NS. Plantar melanoma: Is the incidence of melanoma of the sole of the foot really higher in blacks than whites? Int J Cancer 1990;45:691-3.
9. Boyle P, Maisonneve P, Dore JF. Epidemiology of malignant melanoma. Br Med Bull 1995;51:523-47.
10. Thomas JM. Sentinel-node biopsy in melanoma. N Engl J Med 2007;356:418.
11. Anderson CM, Buzaid AC, Legha SS. Systemic treatments for advanced cutaneous melanoma. Oncology (Williston Park) 1995;9:1149-58.
12. Iyer AK, Singh A, Ganta S, Amiji MM. Role of integrated cancer nanomedicine in overcoming drug resistance. Adv Drug Deliv Rev 2013;65:1784-802.
13. Kunjachan S, Rychlik B, Storm G, Kiessling F, Lammers T. Multidrug resistance: Physiological principles and nanomedical solutions. Adv Drug Deliv Rev 2013;65:1852-65.
14. Markman JL, Rekechenetskiy A, Holler E, Ljubimova JY. Nanomedicine therapeutic approaches to overcome cancer drug resistance. Adv Drug Deliv Rev 2013;65:1866-79.
15. Alifrangis C, Koizia L, Rozario A, Rodney S, Harrington M, Somerville C, *et al.* The experiences of cancer patients. QJM 2011;104:1075-81.
16. Slevin ML, Stubbs L, Plant HJ, Wilson P, Gregory WM, Armes PJ, *et al.* Attitudes to chemotherapy: Comparing views of patients with cancer with those of doctors, nurses, and general public. BMJ 1990;300:1458-60.
17. Thornton M, Parry M, Gill P, Mead D, Macbeth F. Hard choices: A qualitative study of influences on the treatment decisions made by advanced lung cancer patients. Int J Palliat Nurs 2011;17:68-74.
18. Cragg GM, Newman DJ. Natural products: A continuing source of novel drug leads. Biochim Biophys Acta 2013;1830:3670-95.
19. Katiyar SK. Green tea prevents non-melanoma skin cancer by enhancing DNA repair. Arch Biochem Biophys 2011;508:152-8.
20. Wang S, Meckling KA, Marcone MF, Kakuda Y, Tsao R. Can phytochemical antioxidant rich foods act as anticancer agents? Food Res Int 2011;44:2545-54.
21. Saeidnia S, Abdollahi M. Antioxidants: Friends or foe in prevention or treatment of cancer: The debate of the century. Toxicol Appl Pharmacol 2013;271:49-63.
22. Batra P, Sharma AK. Anti-cancer potential of flavonoids: Recent trends and future perspectives. 3 Biotech 2013;3:439-59.
23. Kuttan G, Pratheeshkumar P, Manu KA, Kuttan R. Inhibition of tumor progression by naturally occurring terpenoids. Pharm Biol 2011;49:995-1007.
24. Steinmetz KA, Potter JD. Vegetables, fruit, and cancer. II. Mechanisms. Cancer Causes Control 1991;2:427-42.
25. Corcoran MP, McKay DL, Blumberg JB. Flavonoid basics: Chemistry, sources, mechanisms of action, and safety. J Nutr Gerontol Geriatr 2012;31:176-89.
26. Ahmed S, Rahman A, Hasnain A, Lalonde M, Goldberg VM, Haqqi TM, *et al.* Green tea polyphenol epigallocatechin-3-gallate inhibits the IL-1 beta-induced activity and expression of cyclooxygenase-2 and nitric oxide synthase-2 in human chondrocytes. Free Radic Biol Med 2002;33:1097-105.
27. Ichikawa D, Matsui A, Imai M, Sonoda Y, Kasahara T. Effect of various catechins on the IL-12p40 production by murine peritoneal macrophages and a macrophage cell line, J774.1. Biol Pharm Bull 2004;27:1353-8.
28. Shin HY, Kim SH, Jeong HJ, Kim SY, Shin TY, Um JY, *et al.* Epigallocatechin-3-gallate inhibits secretion of TNF-alpha, IL-6 and IL-8 through the attenuation of ERK and NF-kappaB in HMC-1 cells. Int Arch Allergy Immunol 2007;142:335-44.
29. Zhang G, Miura Y, Yagasaki K. Induction of apoptosis and cell cycle arrest in cancer cells by *in vivo* metabolites of teas. Nutr Cancer 2000;38:265-73.
30. Nihal M, Roelke CT, Wood GS. Anti-melanoma effects of vorinostat in combination with polyphenolic antioxidant (−)-epigallocatechin-3-gallate (EGCG). Pharm Res 2010;27:1103-14.
31. Nihal M, Ahsan H, Siddiqui IA, Mukhtar H, Ahmad N, Wood GS. (−)-Epigallocatechin-3-gallate (EGCG) sensitizes melanoma cells to interferon induced growth inhibition in a mouse model of human melanoma. Cell Cycle 2009;8:2057-63.
32. Chung SY, Hong W, Guang XL, Zhihong Y, Fei G, Huanyu J. Review: Cancer prevention by tea: Evidence from laboratory studies. Pharm Res 2011;64:113-22.
33. Nihal M, Ahmad N, Mukhtar H, Wood GS. Anti-proliferative and proapoptotic effects of (−)-epigallocatechin-3-gallate on human melanoma: Possible implications for the chemoprevention of melanoma. Int J Cancer 2005;114:513-21.
34. Erlund I. Review of the flavonoids quercetin, hesperetin, and naringenin: Dietary sources, bioactivities, bioavailability, and epidemiology. Nutr Res 2004;24:851-74.
35. Hollman PC, van Trijp JM, Mengelers MJ, de Vries JH, Katan MB. Bioavailability of the dietary antioxidant flavonol quercetin in man. Cancer Lett 1997;114:139-40.
36. O'Prey J, Brown J, Fleming J, Harrison PR. Effects of dietary

flavonoids on major signal transduction pathways in human epithelial cells. Biochem Pharmacol 2003;66:2075-88.
37. Harwood M, Danielewska-Nikiel B, Borzelleca JF, Flamm GW, Williams GM, Lines TC, *et al.* A critical review of the data related to the safety of quercetin and lack of evidence of *in vivo* toxicity, including lack of genotoxic/carcinogenic properties. Food Chem Toxicol 2007;45:2179-205.
38. Spagnuolo C, Russo M, Bilotto S, Tedesco I, Laratta B, Russo GL, *et al.* Dietary polyphenols in cancer prevention: The example of the flavonoid quercetin in leukemia. Ann N Y Acad Sci 2012;1259:95-103.
39. Rosner K, Röpke C, Pless V, Skovgaard GL. Late type apoptosis and apoptosis free lethal effect of quercetin in human melanoma. Biosci Biotechnol Biochem 2006;70:2169-77.
40. Zhang XM, Chen J, Xia YG, Xu Q. Apoptosis of murine melanoma B16-BL6 cells induced by quercetin targeting mitochondria, inhibiting expression of PKC-alpha and translocating PKC-delta. Cancer Chemother Pharmacol 2005;55:251-62.
41. Cao HH, Tse AK, Kwan HY, Yu H, Cheng CY, Su T, *et al.* Quercetin exerts anti-melanoma activities and inhibits STAT3 signaling. Biochem Pharmacol 2014;87:424-34.
42. Somerset SM, Johannot L. Dietary flavonoid sources in Australian adults. Nutr Cancer 2008;60:442-9.
43. Ramos S. Effects of dietary flavonoids on apoptotic pathways related to cancer chemoprevention. J Nutr Biochem 2007;18:427-42.
44. Zhang Y, Chen AY, Li M, Chen C, Yao Q. Ginkgo biloba extract kaempferol inhibits cell proliferation and induces apoptosis in pancreatic cancer cells. J Surg Res 2008;148:17-23.
45. Casagrande F, Darbon JM. Effects of structurally related flavonoids on cell cycle progression of human melanoma cells: Regulation of cyclin-dependent kinases CDK2 and CDK1. Biochem Pharmacol 2001;61:1205-15.
46. Chao Y, Huang CT, Fu LT, Huang YB, Tsai YH, Wu PC, *et al.* The effect of submicron emulsion systems on transdermal delivery of kaempferol. Chem Pharm Bull (Tokyo) 2012;60:1171-5.
47. Taherkhani N, Gheibi N. Inhibitory effects of quercetin and kaempferol as two propolis derived flavonoids on tyrosinase enzyme. Biotechnol Health Sci 2014;1:e22242.
48. Huang ZR, Hung CF, Lin YK, Fang JY. *In vitro* and *in vivo* evaluation of topical delivery and potential dermal use of soy isoflavones genistein and daidzein. Int J Pharm 2008;364:36-44.
49. Lin JY, Tournas JA, Burch JA, Monteiro-Riviere NA, Zielinski J. Topical isoflavones provide effective photoprotection to skin. Photodermatol Photoimmunol Photomed 2008;24:61-6.
50. Yong Z, Hongzhong X, Feng W, Xuya Y, Chaoyin C, Rongqing Z. Effects of genistein and daidzein on the proliferation, invasion, migration and adhesion of melanoma cells. Isinghua Sci Technol 2002;7:398-403.
51. Shukla S, Gupta S. Apigenin and cancer chemoprevention. In: Watson RR, Preedy VR, editors. Bioactive Foods in Promoting Health: Fruits and Vegetables. London, UK: Elsevier; 2010.
52. Caltagirone S, Rossi C, Poggi A, Ranelletti FO, Natali PG, Brunetti M, *et al.* Flavonoids apigenin and quercetin inhibit melanoma growth and metastatic potential. Int J Cancer 2000;87:595-600.
53. Piantelli M, Rossi C, Iezzi M, La Sorda R, Iacobelli S, Alberti S, *et al.* Flavonoids inhibit melanoma lung metastasis by impairing tumor cells endothelium interactions. J Cell Physiol 2006;207:23-9.
54. Harborne JB. Nature, distribution and function of plant flavonoids. Prog Clin Biol Res 1986;213:15-24.
55. Javed H, Khan MM, Ahmad A, Vaibhav K, Ahmad ME, Khan A, *et al.* Rutin prevents cognitive impairments by ameliorating oxidative stress and neuroinflammation in rat model of sporadic dementia of Alzheimer type. Neuroscience 2012;210:340-52.
56. Nassiri-Asl M, Mortazavi SR, Samiee-Rad F, Zangivand AA, Safdari F, Saroukhani S, *et al.* The effects of rutin on the development of pentylenetetrazole kindling and memory retrieval in rats. Epilepsy Behav 2010;18:50-3.
57. Drewa G, Schachtschabel DO, Pałgan K, Grzanka A, Sujkowska R. The influence of rutin on the weight, metastasis and melanin content of B16 melanotic melanoma in C57BL/6 mice. Neoplasma 1998;45:266-71.
58. Wang XD. Carotenoids. In: Ross CA, Caballero B, Cousins RJ, Tucker KL, Ziegler TR, editors. Modern Nutrition in Health and Disease. 11th ed. Philadelphia: Lippincott Williams & Wilkins; 2014. p. 427-39.
59. Rodriguez AD. A Guide to Carotenoid Analysis in Foods. Washington, DC, USA: ILSI Press; 2001. p. 1-64.
60. Costa A, Lindmark L, Arruda LH, Assumpção EC, Ota FS, Pereira Mde O, *et al.* Clinical, biometric and ultrasound assessment of the effects of daily use of a nutraceutical composed of lycopene, acerola extract, grape seed extract and biomarine complex in photoaged human skin. An Bras Dermatol 2012;87:52-61.
61. Wu WB, Chiang HS, Fang JY, Hung CF. Inhibitory effect of lycopene on PDGF-BB-induced signalling and migration in human dermal fibroblasts: A possible target for cancer. Biochem Soc Trans 2007;35:1377-8.
62. Beppu F, Niwano Y, Tsukui T, Hosokawa M, Miyashita K. Single and repeated oral dose toxicity study of fucoxanthin (FX), a marine carotenoid, in mice. J Toxicol Sci 2009;34:501-10.
63. Kumar SR, Hosokawa M, Miyashita K. Fucoxanthin: A marine carotenoid exerting anti-cancer effects by affecting multiple mechanisms. Mar Drugs 2013;11:5130-47.
64. Kim KN, Ahn G, Heo SJ, Kang SM, Kang MC, Yang HM, *et al.* Inhibition of tumor growth *in vitro* and *in vivo* by fucoxanthin against melanoma B16F10 cells. Environ Toxicol Pharmacol 2013;35:39-46.
65. Imbs TI, Ermakova SP, Fedoreyev SA, Anastyuk SD, Zvyagintseva TN. Isolation of fucoxanthin and highly unsaturated monogalactosyldiacylglycerol from brown alga fucus evanescens C agardh and *in vitro* investigation of their antitumor activity. Mar Biotechnol (NY) 2013;15:606-12.
66. Chung TW, Choi HJ, Lee JY, Jeong HS, Kim CH, Joo M, *et al.* Marine algal fucoxanthin inhibits the metastatic potential of cancer cells. Biochem Biophys Res Commun 2013;439:580-5.
67. Gerster H. Anticarcinogenic effect of common carotenoids. Int J Vitam Nutr Res 1993;63:93-121.
68. Kohlmeier L, Hastings SB. Epidemiologic evidence of a role of carotenoids in cardiovascular disease prevention. Am J Clin Nutr 1995;62:1370S-6S.
69. Ames BN, Shigenaga MK, Hagen TM. Oxidants, antioxidants, and the degenerative diseases of aging. Proc Natl Acad Sci U S A 1993;90:7915-22.
70. Palozza P, Serini S, Torsello A, Di Nicuolo F, Maggiano N, Ranelletti FO, *et al.* Mechanism of activation of caspase cascade during beta-carotene-induced apoptosis in human tumor cells. Nutr Cancer 2003;47:76-87.
71. Bialy TL, Rothe MJ, Grant-Kels JM. Dietary factors in the prevention and treatment of nonmelanoma skin cancer and melanoma. Dermatol Surg 2002;28:1143-52.
72. Millen AE, Tucker MA, Hartge P, Halpern A, Elder DE, Guerry D 4th, *et al.* Diet and melanoma in a case-control study. Cancer Epidemiol Biomarkers Prev 2004;13:1042-51.
73. Qiu S, Sun H, Zhang AH, Xu HY, Yan GL, Han Y, *et al.* Natural alkaloids: Basic aspects, biological roles, and future perspectives. Chin J Nat Med 2014;12:401-6.
74. Donoso JA, Himes RH. The action of two vinca alkaloids on B16 melanoma *in vitro*. Cancer Biochem Biophys 1984;7:133-45.
75. Singh T, Vaid M, Katiyar N, Sharma S, Katiyar SK. Berberine, an isoquinoline alkaloid, inhibits melanoma cancer cell migration by reducing the expressions of cyclooxygenase-2, prostaglandin E_2 and prostaglandin E_2 receptors. Carcinogenesis 2011;32:86-92.
76. Shoba G, Joy D, Joseph T, Majeed M, Rajendran R, Srinivas PS, *et al.* Influence of piperine on the pharmacokinetics of curcumin

in animals and human volunteers. Planta Med 1998;64:353-6.
77. Bang JS, Oh DH, Choi HM, Sur BJ, Lim SJ, Kim JY, *et al.* Anti-inflammatory and antiarthritic effects of piperine in human interleukin 1beta-stimulated fibroblast-like synoviocytes and in rat arthritis models. Arthritis Res Ther 2009;11:R49.
78. Wattanathorn J, Chonpathompikunlert P, Muchimapura S, Priprem A, Tankamnerdthai O. Piperine, the potential functional food for mood and cognitive disorders. Food Chem Toxicol 2008;46:3106-10.
79. Bhardwaj RK, Glaeser H, Becquemont L, Klotz U, Gupta SK, Fromm MF, *et al.* Piperine, a major constituent of black pepper, inhibits human P-glycoprotein and CYP3A4. J Pharmacol Exp Ther 2002;302:645-50.
80. Peram MR, Jalalpure SS, Palkar MB, Diwan PV. Stability studies of pure and mixture form of curcuminoids by reverse phase-HPLC method under various experimental stress conditions. Food Sci Biotechnol 2017;26:591.
81. Fofaria NM, Kim SH, Srivastava SK. Piperine causes G1 phase cell cycle arrest and apoptosis in melanoma cells through checkpoint kinase-1 activation. PLoS One 2014;9:e94298.
82. Han X, Shen T, Lou H. Dietary polyphenols and their biological significance. Int J Mol Sci 2007;8:950-88.
83. Pandey KB, Rizvi SI. Plant polyphenols as dietary antioxidants in human health and disease. Oxid Med Cell Longev 2009;2:270-8.
84. Thresiamma KC, Kuttan R. Inhibition of liver fibrosis by ellagic acid. Indian J Physiol Pharmacol 1996;40:363-6.
85. Losso JN, Bansode RR, Trappey A 2nd, Bawadi HA, Truax R. *In vitro* anti-proliferative activities of ellagic acid. J Nutr Biochem 2004;15:672-8.
86. Kim S, Liu Y, Gaber MW, Bumgardner JD, Haggard WO, Yang Y, *et al.* Development of chitosan-ellagic acid films as a local drug delivery system to induce apoptotic death of human melanoma cells. J Biomed Mater Res B Appl Biomater 2009;90:145-55.
87. Shimogaki H, Tanaka Y, Tamai H, Masuda M. *In vitro* and *in vivo* evaluation of ellagic acid on melanogenesis inhibition. Int J Cosmet Sci 2000;22:291-303.
88. Shen T, Xie CF, Wang XN, Luo HX. Stilbenoids. In: Ramawat KG, Merillon JM, editors. Natural Products. Berlin, Germany: Springer; 2013. p. 1901-49.
89. Gatouillat G, Balasse E, Joseph-Pietras D, Morjani H, Madoulet C. Resveratrol induces cell-cycle disruption and apoptosis in chemoresistant B16 melanoma. J Cell Biochem 2010;110:893-902.
90. Osmond GW, Augustine CK, Zipfel PA, Padussis J, Tyler DS. Enhancing melanoma treatment with resveratrol. J Surg Res 2012;172:109-15.
91. Asensi M, Medina I, Ortega A, Carretero J, Baño MC, Obrador E, *et al.* Inhibition of cancer growth by resveratrol is related to its low bioavailability. Free Radic Biol Med 2002;33:387-98.
92. Guan H, Singh NP, Singh UP, Nagarkatti PS, Nagarkatti M. Resveratrol prevents endothelial cells injury in high-dose interleukin-2 therapy against melanoma. PLoS One 2012;7:e35650.
93. McDanell R, McLean AE, Hanley AB, Heaney RK, Fenwick GR. Chemical and biological properties of indole glucosinolates (glucobrassicins): A review. Food Chem Toxicol 1988;26:59-70.
94. Fimognari C, Hrelia P. Sulforaphane as a promising molecule for fighting cancer. Mutat Res 2007;635:90-104.
95. Juge N, Mithen RF, Traka M. Molecular basis for chemoprevention by sulforaphane: A comprehensive review. Cell Mol Life Sci 2007;64:1105-27.
96. Arcidiacono P, Ragonese F, Stabile A, Pistilli A, Kuligina E, Rende M, *et al.* Antitumor activity and expression profiles of genes induced by sulforaphane in human melanoma cells. Eur J Nutr 2017. DOI 10.1007/s00394-017-1527-7.
97. Pradhan SJ, Mishra R, Sharma P, Kundu GC. Quercetin and sulforaphane in combination suppress the progression of melanoma through the down-regulation of matrix metalloproteinase-9. Exp Ther Med 2010;1:915-20.
98. Thejass P, Kuttan G. Modulation of cell-mediated immune response in B16F-10 melanoma-induced metastatic tumor-bearing C57BL/6 mice by sulforaphane. Immunopharmacol Immunotoxicol 2007;29:173-86.